VOLUME XXIV JULY-OCTOBER, 1945 NOS. 3-4

THE BELL SYSTEM TECHNICAL JOURNAL

DEVOTED TO THE SCIENTIFIC AND ENGINEERING ASPECTS OF ELECTRICAL COMMUNICATION

AMERICAN TELEPHONE AND TELEGRAPH COMPANY
NEW YORK

$1.00 (Double Copy) *$1.50 per Year*

THE BELL SYSTEM TECHNICAL JOURNAL

Published quarterly by the
American Telephone and Telegraph Company
195 Broadway, New York, N. Y.

SUBSCRIPTIONS

Subscriptions are accepted at $1.50 per year. Single copies are 50 cents each. The foreign postage is 35 cents per year or 9 cents per copy.

PRINTED IN U. S. A.

CORRECTIONS FOR ISSUE OF APRIL, 1945

Page 207: Abscissa for Fig. 12.29, $P = \dfrac{M}{1 - c_t/c_0}$

should be $P = \dfrac{M}{1 + c_t/c_0}$

Page 240: Equation (15.60), $W_0 = \dfrac{\beta}{\delta}\dfrac{\left[\dfrac{\alpha}{\beta} - \dfrac{\bar{\gamma}}{\bar{\delta}}\right]}{\left[\dfrac{\gamma}{\delta} + \dfrac{\bar{\gamma}}{\bar{\delta}}\right]}$

should be $W_0 = \dfrac{\beta}{\delta}\dfrac{\left[\dfrac{\alpha}{\beta} + \dfrac{\bar{\gamma}}{\bar{\delta}}\right]}{\left[\dfrac{\gamma}{\delta} + \dfrac{\bar{\gamma}}{\bar{\delta}}\right]}$

The Bell System Technical Journal

Vol. XXIV *July-October, 1945* *Nos. 3-4*

Physical Limitations in Electron Ballistics*

By J. R. PIERCE

Introduction

THE subject of this talk is "Physical Limitations in Electron Ballistics". It is pleasant to have a chance to talk about such physical limitations, because there is so little we can do about them. And, although these limitations are apt to be discouraging, a knowledge of them is very valuable, for it keeps us from spending time trying, like the inventors of perpetual motion machines, to do the impossible.

As electron ballistics is particularly subject to physical limitations, there are so many that it is impossible to discuss all of them thoroughly at this time. Also, many of the limitations are of a rather complicated nature, and to deduce them from basic principles in a quantitative way requires much thought and patience. I think the best I can do is to try to mention most of the chief limitations, as a warning to the uninitiated that rocks lie ahead in certain directions, but to concentrate attention on only a few of them. I have chosen this evening to devote particular attention to limitations that bear on the production and use of electron beams in which considerable current is required, such as those used in cathode ray tubes and high-frequency oscillators, and to mention only briefly as a sort of introduction problems pertaining more closely to low-current devices such as electron microscopes.

The Wave Nature of the Electron

One of the most important limitations in electron microscopy is the dual nature, wave and corpuscular, of the electron. Without making any attempt to justify or explain the combination of wave and particle concepts which is characteristic of modern physics, we may describe its consequence at once; very small objects don't cast distinct shadows. This cannot be explained merely in terms of the physical size of the electron and the object. When an electron beam is reflected from a surface of regularly

* A lecture given under the auspices of the Basic Science Group of the New York Section of the A.I.E.E., as a part of an Electron Ballistics Symposium, Columbia University, March 21, 1945.

spaced obstacles (the atoms in a crystal lattice, for instance) diffraction patterns are obtained, similar to those which may be obtained with waves of X-rays or light. It appears that electrons get around sufficiently small objects just as sound waves get around telephone poles, automobiles, and even houses, and if the objects are sufficiently small their effect on the electron flow will either be absent or will consist of a few ripples which are meaningless in disclosing the shape or size of the object.

The electron wave-length, which varies inversely as the momentum of the electron, may be simply expressed in terms of the energy V in electron volts. A simple non-relativistic expression which is only 5% in error at 100,000 volts (a high voltage for electron microscopes), is*

$$\lambda = \sqrt{150/V} \times 10^{-8} \text{ cm} \tag{1}$$

Thus for 30,000-volt electrons the wave-length is 7×10^{-10} cm or about 1.4×10^{-7} times the diameter of a hair and 1.2×10^{-5} times the length of a wave of yellow light.

In terms of this wave-length λ and the half angle of the cone of rays accepted by the objective, α, we can express the distance d between point objects which can just be distinguished in an electron microscope. This distance is

$$d = .61\lambda/\sin \alpha \tag{2}$$

For small values of α

$$2\alpha = 1/\text{f} \tag{3}$$

where f is the well known photographic f number, the ratio of the focal length to the lens diameter. We see that, just as with cameras, the smaller the f number the better. In electron microscopes a small f enables us to distinguish smaller objects.

Aberrations

Just as in cameras, the limitation to the f number is imposed by lens aberrations. But in electron lenses the aberrations are much more severe. Why is this so? Because with electron lenses we have less freedom of design than with optical lenses.

Consider an electric lens. The quantity analogous to the index of refraction for light is the square root of the potential with respect to the cathode. Now suppose that with a light lens we know the index of refraction at every point along the axis. Suppose, for instance, that the index of refraction is 1 everywhere along the axis except for a space L long

* The relativistic expression is

$$\lambda = (\sqrt{150/V}/\sqrt{1 + .98 \times 10^{-6}V}) \times 10^{-8} \text{ cm}$$

where it is 2, as in Fig. 1. Our lens may be converging or diverging; strong or weak. In the analogous electric case, however, the potential throughout the lens space must satisfy Laplace's equation, and this means that if it is specified along the axis it is known everywhere. We can easily see this by writing down Laplace's equation for an axially symmetrical field.

$$\frac{1}{r}\frac{\partial}{\partial r}\left(r\frac{\partial V}{\partial r}\right)+\frac{\partial^2 V}{\partial z^2}=0 \tag{4}$$

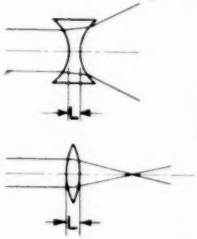

LIGHT-CONDITIONS OFF AXIS NOT FIXED BY CONDITIONS ON AXIS

ELECTRIC FIELD-FIELD OFF AXIS SPECIFIED BY POTENTIAL ON AXIS

$$V=\frac{1}{\pi}\int_0^{\pi} f(z+ir\cos\theta)\,d\theta$$

Fig. 1—Contrast between optical and electric focussing conditions.

The field near the axis may be expanded in powers of f

$$\frac{\partial V}{\partial r}=ar+\cdots \tag{5}$$

Substituting this into (4),

$$\frac{1}{r}\frac{\partial}{\partial r}(ar^2)=2a=\frac{-\partial^2 V}{\partial z^2}$$

$$\frac{\partial V}{\partial r}=\frac{-1}{2}\frac{\partial^2 V}{\partial z^2}r \tag{6}$$

As a matter of fact, the potential V (z,r) remote from the axis can be expressed in terms of the potential $V_0(z)$ on the axis as

$$V=\frac{1}{\pi}\int_0^{\pi} V_0(z+ir\cos\theta)\,d\theta \tag{7}$$

If we could introduce charges into our lens, Laplace's equation would no longer hold and we would have more freedom of design. The methods proposed for the introduction of charges comprise the use of free charges (space charge) which are largely uncontrollable, and the use of curved grids, which do more damage than good. In other words, the cures are worse than the disease.

Similar limitations apply to magnetic lenses, and in the end we find that because of the simplest form of aberration, spherical aberration, best definition is achieved in electron microscopes with f numbers of 100 or greater, while the f number of a light microscope objective corrected for spherical aberration and other defects as well may be around unity. Thus the electron microscope is severely handicapped, and this handicap is overcome only because electron waves are much less than 1/100 the length of light waves.

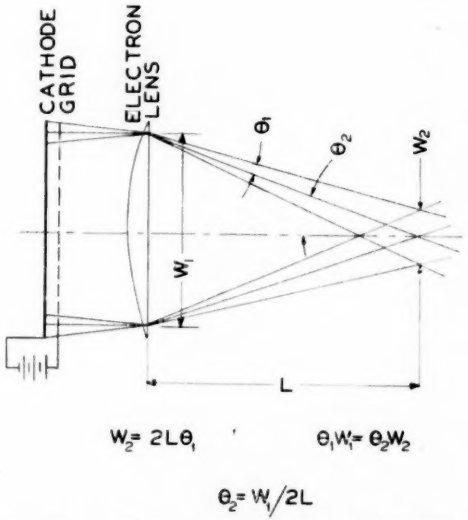

Fig. 2—Approximate relation between beam size and angular spread.

Thermal Velocities of Electrons

In many electron-optical systems, and particularly in such devices as cathode ray tubes, it is desirable to focus an electron beam into a small area, so as to produce a very small spot on a fluorescent screen, or to pass a considerable current through a small aperture. We might think at first that if our focusing system were good enough, that is, if it had very small aberrations, we could focus a current from a cathode of given area into as small a space as we desired. This, unfortunately, is not so. The obstacle is the thermal velocities of the electrons emitted by the cathode.

A simple example will show the sort of thing we should expect to take place. Figure 2 shows a plane cathode and near to it a positive grid so fine as to cause no appreciable deflections of the electrons which pass through it. Farther on we have an aberrationless electron lens designed to focus

the electron stream at a spot a distance L beyond it. The electrons will leave the cathode with some slight sidewise velocity components; so, electron paths will pass at several angles through a given point on the lens. The lens will bend these paths approximately equally, and hence we can see that at the point where the beam is narrowest it will still have some appreciable diameter W_2.

Now consider the beam at the lens. Suppose that through a given point all the paths lie within a cone of half angle θ. Then the width W_2 is approximately

$$W_2 = 2L\theta_1 \tag{8}$$

We can also see that the paths at W_2 will lie within an angle approximately

$$\theta_2 = W_1/2L \tag{9}$$

Hence we see that approximately

$$\theta_1 W_1 = \theta_2 W_2 \tag{10}$$

In other words, we can have a small spot through which electrons pass over a wide angular range, or we can have a broad beam in which all paths are nearly parallel, but we can't have a narrow spot and nearly parallel rays.

We see that the actual width of spot will depend on the thermal velocities, which are proportional to the square root of the cathode temperature, and on the forward velocity, which is proportional to the square root of the accelerating voltage. By using more involved arguments we discover that for any point in an electron stream, where the beam is wide, narrow, or intermediate, the current in an arbitrary direction chosen as the x direction can be expressed[4,*]

$$dj = \frac{4kT}{\pi m} j_0 v_x \epsilon^{(1/kT)(eV - mv^2/2)}\, dv_x\, dv_y\, dv_z \tag{11}$$

$$v = v_x^2 + v_y^2 + v_z^2$$

$$\text{when } v > \sqrt{2eV/m}; \tag{12}$$

$$\text{or } dj = 0 \tag{13}$$

$$\text{when } v < \sqrt{2eV/m} \tag{14}$$

Here j_0 is the cathode current density, V is voltage with respect to the cathode, T is the absolute temperature of the cathode in degrees Kelvin, and v_x, v_y, and v_z are the three velocity components; dj is the element

* This expression neglects the effects of electron collisions, which may actually make the current density smaller.

of current density carried by electrons which have velocity components about v_x, v_y, v_z, lying in the little range of velocity $dv_x\ dv_y\ dv_z$.

The reason for restriction (12) is that if an electron starts with zero thermal velocity from the cathode, it will attain the velocity given by the right side of (12) by falling through the potential drop V. As electrons cannot have velocities smaller than this, we have (13) and (14).

By integrating (11) with appropriate limits we obtain a more specialized but very useful expression

$$j < j_m = j_o\left(1 + \frac{11600V}{T}\right)\sin^2\theta \tag{15}$$

For usual values of voltage, unity in the parentheses is negligible, and we can say that if all the electron paths approaching a given point in an electron beam lie within a cone of half angle θ, the current density j at that point cannot be greater than a limiting value j_m which is proportional to the

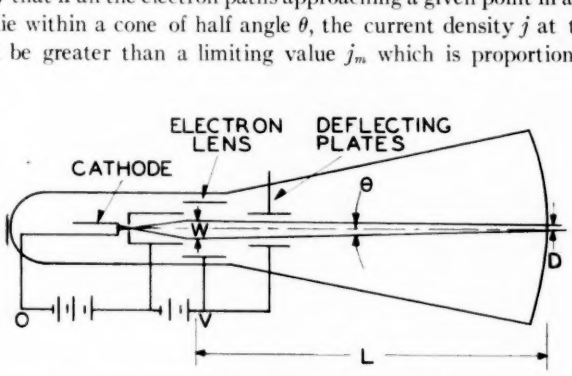

Fig. 3—Parameters important in determining spot size in a cathode ray tube.

cathode current density, to the voltage, to $\sin^2\theta$, and inversely proportional to the cathode temperature.

Let us see what this means in some practical cases. Figure 3 shows a cathode ray tube. The electron stream has a width W at the final electron lens, and is focused on a screen a distance L beyond the lens. The half angle of the cone of rays reaching the screen cannot be greater than

$$\sin\theta = \theta = W/2L \tag{16}$$

Suppose the spot must have a diameter not greater than d. Let the spot current be i. Then from (15),

$$j = \frac{4i}{\pi d^2} < j_0\left(1 + \frac{11600V}{T}\right)(W/2L)^2,$$

$$i < \frac{\pi d^2}{4}\, j_0\left(1 + \frac{11600V}{T}\right)(W/2L)^2. \tag{17}$$

Thus if for a given spot size we want to increase the spot current, and if we are limited to a given cathode current density because of cathode life, we must make V larger, W larger or L smaller.

Making W larger increases both lens and deflection aberrations. Making L smaller means that for a given linear deflection we must increase the angular deflection, and this too tends to defocus the spot. Because of these limitations, it is necessary to avail ourselves of the remaining variable and raise the operating voltage V.

Another illustration, perhaps a little more subtle, of the effect of thermal velocities, lies in the analysis of the properties of a type of vacuum tube amplifier known as the "deflection tube". In such a device, illustrated in Fig. 4, an electron stream from a cathode is accelerated and focused by a lens and deflected by a pair of deflecting electrodes so as to hit or miss an output electrode. Such a device may be used as an amplifier.

Now it is obvious that as the output electrode on which the beam is focused is moved farther away from the deflecting plates, a given deflecting voltage will produce a greater linear deflection of the beam at the output.

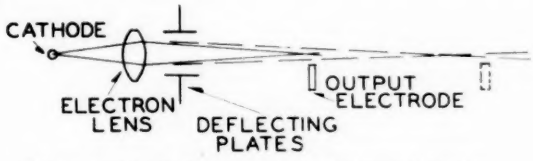

Fig. 4—Amplifying tube making use of electron deflection.

As this at first sight seems desirable; it has been seriously suggested not only that this be done, but that an elaborate electron optical system be interposed between the deflecting plates and the output electrode to amplify the deflection.

The merit of a deflection tube is roughly measured by the deflecting voltage required to move the beam from entirely missing the output electrode to entirely hitting the output electrode, and, of course, moving the output electrode farther away or putting lenses between the deflecting plates and the output electrode doesn't reduce this voltage at all. As we improve the deflection sensitivity by these means, we simply increase the spot size at the same time. Focusing our attention on the beam between the deflecting plates, we appreciate at once that the electron paths through each point will be spread over some cone of half angle θ, and that to change from a clean miss to a clean hit we must deflect the electrons through an angle of at least 2θ, regardless of what we do to the beam afterwards.

Returning for a moment to equation (15), we see that it says the current density can be less than a certain limiting value depending on θ. Yet

expression (15) was obtained by integrating a supposedly exact expression. What does this inequality mean?

The answer is that for the current to have the limiting value, electrons of *all allowable velocities* must approach *each part* of the spot from *all angles* lying within the cone of half angle θ. When the average current density in the spot is less than the limiting current density, the possibilities are

(a) Electrons are approaching each point in the beam from all angles, but along some angles only electrons which left the cathode with greater than zero velocity can reach the spot.

(b) Electrons leaving the cathode with all velocities can reach the spot, but at some portions of the spot electrons don't come in at all angles within the cone angle θ.

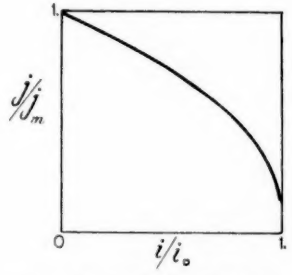

Fig. 5—Relation between nearness of approach to limiting current density and fraction of current utilized.

Thus, we can have less than the limiting current either because electrons do not reach the spot with all allowable velocities or from all allowable angles. Of course both factors may operate.

We can easily see how lens aberrations, which we know are present in all electron-optical systems, can prevent our attaining the limiting current density. There is a more fundamental limitation, however. It can be shown that even with perfect focusing, we must sort out and throw away part of the current in order to approach the limiting current density, and we can even derive a theoretical curve for the case of perfect focusing relating the fraction of the limiting current density which is attained to the fraction of the cathode current which can reach the spot. Figure 5 shows such a curve which applies for voltages higher than, say, 10 volts.

Usually, the failure to approach the limiting current density is chiefly caused by aberrations, and in ordinary cathode ray tubes the current density in the spot may be only a small fraction of the limiting value. A very close approach to the limiting current density has been achieved in a

special cathode ray tube designed by Dr. C. J. Davisson of the Bell Telephone Laboratories.

When we become thoroughly convinced that these equations expressing the effects of thermal velocities very much cramp our style in designing electron-optical devices, as good engineers we wonder if there isn't, after all, some way of getting around them. I don't think there is. The suggestion illustrated in Fig. 6 is a typical example of such an attempt. We know that in a strong magnetic field electrons tend to follow the lines of force. Why not use a very strong magnetic field with lines of force approaching the axis at a gentle angle to drag the electron stream toward the axis?

An electron off axis traveling parallel to the axis certainly will be dragged inward by such a field. The catch is that the field pulls the electron in because it makes the electron spiral around the axis. As the beam converges and the field becomes stronger, the pitch of each spiral decreases and the angular speed of each electron increases. Finally, if the field is strong enough, all the kinetic energy of the electron is converted from forward

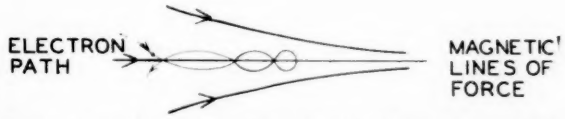

Fig. 6—Reflection of an electron by a magnetic field with strongly converging lines of force.

motion to revolution about the axis; the electron ceases to move into the field and bounces back out. It may be some small consolation to know that very high-current densities can be achieved by this means, but only because in their flat spiralling the electrons approach a spot at much wider angles with the axis than the small inclination of the lines of force.

Space Charge Limitations

In electron beam devices using reasonably large currents, the space charge of the electrons is a very serious source of trouble both in complicating design of the devices and in limiting their performance.

Let us begin our consideration right at the electron gun, the source of electron flow in many devices such as cathode ray tubes and certain high-frequency tubes. Electron guns are sometimes designed on the basis of radial space charge limited electron flow between a cathode in the form of a spherical cap of radius r_o and a concentric spherical anode a distance d from the cathode. It can be shown that by use of suitable electrodes external to the beam, radial motion can be maintained between cathode and anode along

straight lines normal to the cathode surface. A hole in the anode electrode will allow the beam to emerge from the gun. Because of the change in

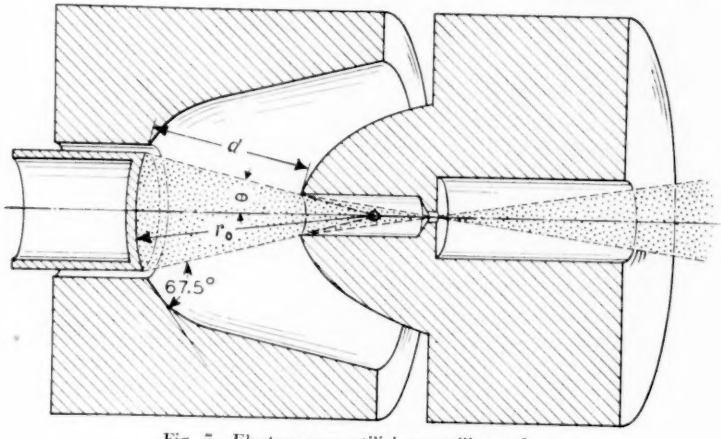

Fig. 7—Electron gun utilizing rectilinear flow.

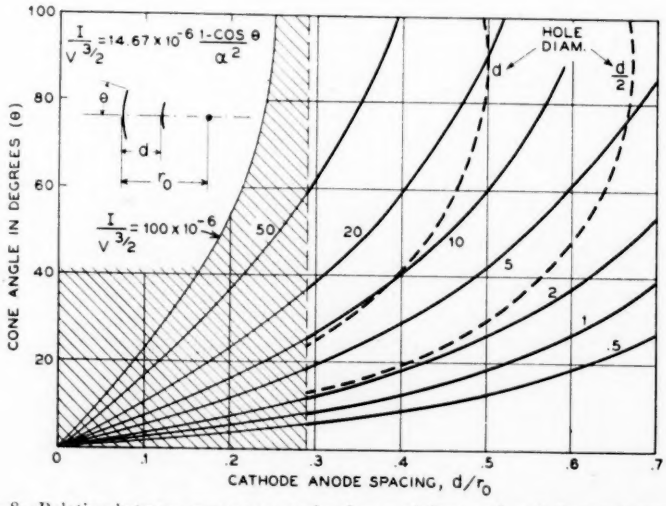

Fig. 8—Relation between perveance, angle of cone of flow, and cathode-anode spacing.

field near the hole, the hole acts as a diverging electron lens.[11] Figure 7 illustrates such a gun.[15] The curves shown in Fig. 8 relate to this sort of

electron gun. They are plots of a factor called the perveance, which is defined as

$$P = I/V^{3/2} \tag{18}$$

(that is, current divided by voltage to the 3/2 power) as a function of θ, the half angle of the cone of flow, and d/r_o, the ratio of cathode-anode spacing to cathode radius. In getting an idea of the meaning of the curves, we may note that a perveance of 10^{-6} means a current of 1 milliampere at 100 volts. It is obvious from the curves that to get very high values of perveance, that is, high current at a given voltage, θ must be large and the cathode-anode spacing must be small. Making θ large means that electrons approach the axis at steep angles; aberrations are bad and the beam tends to diverge rapidly beyond crossover. Moving the anode near to the cathode means that the hole which must be cut in the anode to allow the beam to pass through must be large, and cutting such a large hole in the anode defeats our aim of getting higher perveance; we can't pull electrons away from the cathode with an electrode which isn't there. Further, for ratios of spacing to cathode radius less than about .29, the lens action of the hole in the anode causes the emerging beam to diverge, which would make the gun unsuitable for many applications.

When we build guns for small currents at high voltages, such as cathode ray tube guns, space charge causes little trouble; when we try to obtain large currents at lower voltages, we find ourselves seriously embarrassed.

Suppose we now turn our attention to the effect of space charge in beams when the beam travels a distance many times its own width. Consider, for instance, the case of a circular disk forming a space charge limited cathode. Suppose we place opposite this a fine grid, and shoot an electron stream out into a conducting box, as illustrated in Fig. 9a. We immediately realize that there will be a potential gradient away from the charge forming the beam. In this case, the gradient will be toward the nearest conductor; that is outwards, and the electron beam will diverge.

How can we overcome such divergence? One way would be to arrange the boundary conditions in such a fashion that all the field would be directed along the beam instead of outwards; this might be done by surrounding the beam by a series of conducting rings and applying to them successively higher voltages as in 9b, the voltages which would occur in electron flow between infinite parallel planes with the same current density. Another way in which the same effect may be achieved is through use of specially shaped electrodes outside of the beam, as shown in Fig. 9c.[11] In maintaining parallel flow by these means, the electric field due to the electrons acts along the beam, and increases continually in magnitude with

distance from the cathode. We can in fact calculate the potential at any distance along the beam by the well known Child's law equation

$$I = 2.33 \times 10^{-6} AV^{3/2}/x^2$$
$$V = 5{,}690 x^{4/3} I^{2/3}/A^{2/3} \tag{19}$$

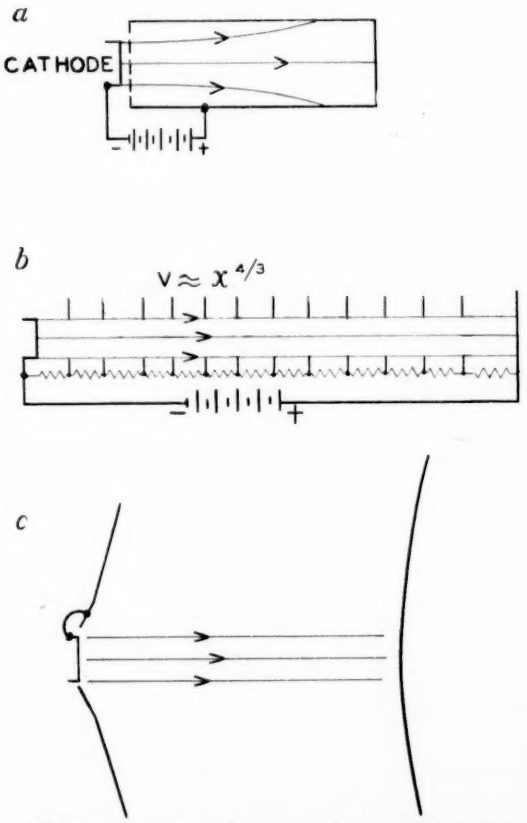

Fig. 9—Avoiding beam divergence by means of a longitudinal electric field.

Here V is the anode voltage, x the cathode-anode spacing, I the current in amperes and A the cathode area.

Suppose we take as an example

$$A = 1 \text{ cm}^2$$
$$I = .01 \text{ amp.}$$
$$x = 10 \text{ cm}$$

Then

$$V = 5{,}700 \text{ volts}$$

Thus to maintain parallel motion of the modest current of 10 milliamperes spread over an area of one square centimeter requires 5,700 volts. Moreover, the requirement of distributing this voltage smoothly along the beam would make it very difficult to put the beam to any use.

One means for mitigating the situation is to use an electron lens and direct the beam inward. Of course, the beam will eventually become parallel and then diverge again, but by this means a fairly large current can be made to travel a considerable distance. Some calculations made by Thompson and Headrick[12] cover this type of motion, with an especial emphasis on the problem in cathode ray tubes, in which the currents are moderate.

In order to confine large currents into beams, an axial magnetic field is sometimes used, as shown in Fig. 10 Here a cathode-grid combination shoots a beam of electrons into a long conducting tube. A long coil around the tube produces an axial magnetic field intended to confine the electron

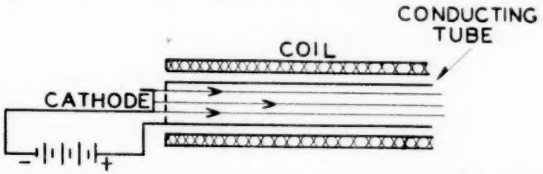

Fig. 10—Avoiding beam divergence by means of a longitudinal magnetic field.

paths in a roughly parallel beam. The radial electric field due to space charge will cause the beam to expand somewhat and to rotate about the axis. As the magnetic field is made stronger and stronger, the electrons will follow paths more and more nearly straight and parallel to the axis. For a given current and voltage, there is one sort of physical limitation in the strength of magnetic field we need to get a satisfactory beam. It is another effect that I wish to discuss.

Suppose we have a very strong magnetic field, in which the electrons travel almost in straight lines. We know, of course, that the radial electric field is still present, and this means that the potential toward the center of the beam is depressed; this in turn means that the center electrons are slowed down. This slowing down of course increases the density of electrons in the center of the beam. The result is that if for some critical voltage or speed of injection we increase current beyond a certain value, the process runs away, the potential at the center of the beam drops to zero, and another type of electron flow with a "virtual cathode" of zero electron velocity at the center of the beam is established. Thus, although the magnetic field

has overcome the diverging effect of the space charge, we still have a space charge limitation of the beam current. C. J. Calbick has calculated the value of this limiting current.[13] If the beam completely fills a conducting tube at a potential V with respect to the cathode, the limiting beam current is independent of the diameter of the beam and is

$$I = 29.3 \times 10^{-6} V^{3/2} \tag{20}$$

If the beam diameter is less than that of the conducting tube, the limiting current is lower.

But perhaps we can completely overcome the effects of space charge. Suppose we put a very little gas in the discharge space. Then positive ions will be formed. Any tendency of the electronic space charge to lower the potential and slow up the electrons will trap positive ions in the potential minimum and so raise the potential. Thus the gas enables us to get rid of the the slowing up effect of the space charge as well as its diverging effect.

Before we congratulate ourselves unduly, it might be well to make sure about the stability of an electron beam in which the electronic space charge is neutralized by heavy positive ions. Langmuir and Tonks, in their work on plasma oscillations, introduced a concept, extended later by Hahn and Ramo, which enables us to investigate this problem. The concept is that of space charge waves. It is found that in a cloud of electrons whose net space charge is neutralized by heavy, relatively immobile positive ions, small disturbances of the electron charge density produce a linear restoring force; and this, together with the mass of the electrons, makes possible a type of space charge wave which may be compared roughly with sound waves, although much of the detailed behavior of space charge waves is quite different from that of sound waves. We may express a disturbance in an electron beam in terms of these space charge waves and then examine the subsequent history of the disturbance as a function of time. This has been done[14] and the perhaps surprising result is that even when the electronic space charge is neutralized by heavy positive ions, the flow tends to collapse if the current is raised above a limiting value

$$I = 190 \times 10^{-6} V^{3/2} \tag{21}$$

It is true that this current is 6.5 times the limiting current in the absence of ions, but it is a limit nevertheless.

If this limit in the presence of ions seems unnatural, perhaps we should recall a mechanical analogy. Consider a vertical long column subjected to a load F. If we subject it to a sidewise force αF proportional to F, as shown in Fig. 11a, the behavior on increasing F will be a gradual deformation (analogous to the space charge lowering of potential in the absence of ions)

ending in collapse. However, even if, as in 11b, there is no sidewise loading and no bending during loading, we know from Euler's formula that beyond a certain loading the column will still collapse. This behavior is analogous to that of an electron beam in which the electronic space charge is neutralized by positive ions and there is no depression of potential in the beam.

This space charge limitation either in the presence or absence of ions allows the passage of quite a large current through a tube, as the table below will show:

Voltage	Current, amperes, no ions	Current, amperes, ions
1000	.927	6.01
100	.029	.190
10	.009	.060

We might therefore feel that the space charge is disposed of in a practical sense, and so it is in many cases.*

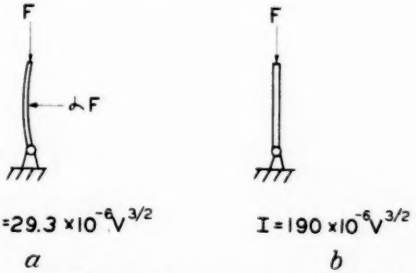

Fig. 11—Comparison of limiting stable beam currents with and without positive ions.

Power Dissipation Limitations

Having talked about various limitations imposed by wave effects, aberrations, thermal velocities and space charge on the electron flow in the beam itself, I want to close by discussing briefly a topic which seems hardly included in electron ballistics but yet is vital to any application in that field. I refer to the problems associated with power dissipation when electrons strike something and stop. This is a good deal like the problem imposed by suddenly coming down to earth while studying the sensations of a free fall. It is inevitable and may be fatal unless satisfactory provision is made for the dissipation of kinetic energy.

What I want chiefly to bring out are the consequences of scaling a given electronic device down in size. If we change the size of each part of an

* It appears that in many gas discharges, including those in which plasma oscillations are observed, the current is too high to allow persistence of the homogeneous flow upon which the plasma oscillation equations are based.

electron device in the ratio R, if we keep all voltages the same, and if we change all magnetic fields in the ratio $1/R$, electron current will remain the same (provided the cathode is still capable of giving space charge limited emission). Electron paths will remain exactly similar, though smaller; the power into the electron beam will remain the same, but what will happen to the power dissipation capabilities of the device and what will happen to the temperature?

In a device cooled by radiation alone and with cool surroundings, the radiating area varies as R^2, and since the radiation per unit area varies as T^4, the temperature will vary as $R^{-\frac{1}{2}}$.

In considering a case of cooling by conduction alone, think of a rod carrying a certain amount of power away. If all the dimensions of a rod are changed by a factor R, the length will be changed by a factor R, the cross sectional area will change by a factor R^2, and if the thermal conductivity

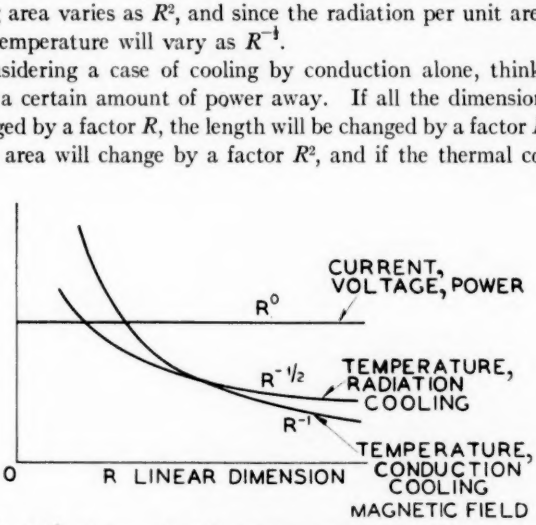

Fig. 12—Variation of magnetic field and temperature in scaling an electronic device.

remains constant the temperature will vary as R^{-1}. This is a faster rate of variation than in the case of cooling by radiation, and hence as the system is scaled to a smaller and smaller size, cooling by conduction will become negligible and radiation cooling only will remain effective and will determine the temperature.

Figure 12 gives an idea of the variation of various quantities discussed.

We want to make electronic devices smaller for a number of reasons; perhaps chiefly to reduce transit time and so to secure operation at higher frequencies. In doing this, we encounter the fundamental limitation of reduced power dissipation capabilities and increased temperature. What is the trouble? We have scaled everything. Or have we? The answer is, we have not. The electrons, atoms, and quanta are still the same size. Had we been able to scale these, we should have increased the heat conductivity and the radiating power of our device, and all would have been

well. As it is, if we make a tube for given power smaller and smaller, using the most refractory materials available we eventually reach a size of tube which will, despite our best efforts, melt, thaw, and resolve itself into a dew.

CONCLUSION

Perhaps after these somewhat gloomy words concerning physical limitations in electron ballistics, you may wonder how it is at all possible to surmount the difficulties mentioned. It certainly is not easy; all electronic devices represent compromises of one sort or another between fundamental physical limitations of electron flow on the one hand and structural complications on the other. In working with vacuum tubes one is perhaps troubled more by physical limitations, difficulties of construction, inadequacy of materials and the lack of quantitative agreement between complicated phenomena and relatively simple theories than in any other part of the electric art. It is for this reason that a friend of mine twisted an old aphorism into a new one and said, "Nature abhors a vacuum tube".

REFERENCES

Electron Microscopes

1. James Hillier and A. W. Vance: "Recent Developments in the Electron Microscope," *Proc. I.R.E.* 29, pp. 167–176, April, 1941.
2. L. Marton and R. G. E. Hutter: "The Transmission Type of Electron Microscope and Its Optics," *Proc. I.R.E.* 32, pp. 3–11, Jan. 1944.

Thermal Velocities

3. D. B. Langmuir: "Theoretical Limitations of Cathode-Ray Tubes," *Proc. I.R.E* 25, pp. 977–991, Aug., 1937.
4. J. R. Pierce: "Limiting Current Densities in Electron Beams," *Jour. App. Phys.*, 10, pp. 715–724, Oct., 1939.
5. J. R. Pierce: "After Acceleration and Deflection," *Proc. I.R.E.* 29, pp. 28–31, Jan., 1941.
6. R. R. Law: "Factors Governing the Performance of Electron Guns in Cathode-Ray Tubes," *Proc. I.R.E.* 30, pp. 103–105, Feb., 1942.
7. J. R. Pierce: "Theoretical Limitation to Transconductance in Certain Types of Vacuum Tubes," *Proc. I.R.E.* 31, pp. 657–663, Dec., 1943.

Space Charge

8. C. E. Fay, A. L. Samuel and W. Shockley: "On the Theory of Space Charge Between Parallel Plane Electrodes," *Bell Sys. Tech. Jour.* 17, pp. 49–79, 1938.
9. I. Langmuir and K. Blodgett: "Currents Limited by Space Chargeb etween Coaxial Cylinders," *Phys. Rev.* 22, pp. 347–356, 1923.
10. I. Langmuir and K. B. Blodgett: "Currents Limited by Space Charge between Concentric Spheres," *Phys. Rev.* 24, pp. 49–59, 1924.
11. J. R. Pierce: "Rectilinear Electron Flow in Beams," *Jour. of App. Phys.* 11, pp. 548–554, Aug., 1940.
12. B. J. Thompson and L. B. Headrick: "Space Charge Limitations on the Focus of Electron Beams," *Proc. I.R.E.*, 28, pp. 318–324, July, 1940.
13. C. J. Calbick: "Energy Distribution of Electrons within Dense Electron Beams," *Bull. Am. Phys. Soc.*, 19, No. 2, p. 14 (April 28, 1944).
14. J. R. Pierce: "Limiting Stable Current in Electron Beams in the Presence of Ions," *Jour. App. Phys.* 15, No. 10, pp. 721–726 (1944).
15. A. L. Samuel, "Some Notes on the Design of Electron Guns," Proc. IRE 33, pp. 233–240, April, 1945.

Electron Ballistics in High-Frequency Fields*

By A. L. SAMUEL

THIS, the final lecture of a series on Electron Ballistics, is not a summary of the material which has been previously presented but rather it is an attempt to show how the ballistic approach can be extended to the analysis of high-frequency devices. Much that might otherwise be said about ultra-high frequencies cannot be said because of secrecy requirements. However, there is considerable material which can be presented, within the limits of the necessary security regulations, which may be of interest to those who are not already well acquainted with the subject. I will, perforce, not be able to say anything specific about actual devices utilizing the principles to be discussed.

Many of the ultra-high-frequency devices which have come into use during the last few years have employed electron beams of one sort or another. These devices can be analysed in any one of a number of ways. For example, we can write the equation of space-charge flow. This approach considers the electric charge as a continuous fluid subject to Poisson's equation. The small-signal theory of Peterson and Llewellyn is an example of this type of analysis. Or if we wish we can consider the various types of wave motion which can exist in a space-charge region. The space-charge-wave analysis of Hahn and Ramo as applied to velocity-variation tubes is an example of this. In addition there is an electron-ballistic approach to the problem and it is with this method that we will be concerned in the present lecture.

Before we become involved in the details of the analysis, we should perhaps spend a few moments considering the relationship between these various methods. If we have an interaction taking place between electric fields and moving charges, we know at once from Newton's second law that the forces acting on the electrons must of necessity be equal and opposite to those acting on the fields. It is therefore a matter of small concern whether we consider the forces acting on the electrons and the effects of these forces on the electron motion or whether we consider the alteration in fields which the electron motion produces. We can, if we wish, compute the energy transfer to an electric field by the motion of an electric charge or we can compute the change in energy of the electron which accompanies this trans-

* Originally presented on April 11, 1945 as the concluding lecture of a symposium on Electron Ballistics sponsored by the Basic Science Group of the American Institute of Electrical Engineers.

fer. I was tempted to say "which results from this transfer" but this implies a cause and an effect, a notion which has no place in the present discussion. The dual aspect of any energy-transfer problem must always be kept in mind. Much needless discussion frequently arises between proponents of one point of view and those preferring the other when the only difference is one of language and both groups are really saying the same thing. The electron-ballistic approach yields a simple physical picture; it is capable of being applied to widely differing situations, but it is not well suited for a determination of the reactive contributions of an electron stream.

Basic Concepts

There are several concepts which we will find useful in our analysis. These concepts are extremely simple, so simple in fact that one is tempted to assume that they are well known. However, these concepts are so basic to the subject, and their results so far reaching that we must pause to consider them.

The first is the concept of total current, as distinguished from its components. One way of writing Kirchhoff's second law is

$$\text{Div. } J = 0 \tag{1}$$

This simply says that the total current entering or leaving any differential region in space is zero. This expression must of course be generalized by including displacement currents as proposed by Maxwell if applied to alternating currents. The current J is the total current density as here defined. An important consequence of equation (1), actually only an alternate way of stating it, is that the total current always exists in closed paths. Let us take a simple case of a two-element thermionic vacuum tube connected to a battery. Visualize the situation existing if but a single electron leaves the cathode and travels to the plate. The electron takes a finite time to cross from the cathode to the plate. During this time a current exists, the magnitude being given by the relationship

$$I = ev$$

and according to our premise this current is the same in every part of the circuit. The current begins at the instant that the electron leaves the cathode and it ceases when the electron arrives at the plate. In the apparently empty region ahead of the electron there must exist a displacement component, numerically equal to the conduction, or perhaps we should say convection component accounted for by the moving electron. An ammeter, were there one sufficiently sensitive and fast, connected in the external leads would read a current during this same interval of time.

I have chosen to talk about but a single electron to emphasize the electron-

ballistic aspect; however, the concept is much broader than this since it is not at all dependent upon a corpuscular concept of the electron. As a result of this property of the total current, the current to any electrode within a vacuum tube does not necessarily bear any relationship to the number of electrons which enter or leave it. Obviously then, currents can exist in the grid circuit of a three-element tube even though none of the electrons are actually intercepted by the grid. This current may have any phase relationship to an impressed voltage on the grid so that the grid may draw power from the external circuit, or it may deliver power to the external circuit, all without actually intercepting any electronic current. The grid-current component resulting from the electronic flow between cathode and plate may equally well bear a quadrature relationship to the impressed voltage, in which case it will either increase or decrease the apparent interelectrode capacitance. If these effects seem queer it is because one is still confusing the electronic component with the total current.

A second basic concept once stated becomes self-evident. This is to the effect that the only one thing which we can do to an electron is to change its velocity, that is, if we are to confine ourselves to the classical concept of an electron. We can change its longitudinal velocity, that is, alter its speed but not its direction other than possibly to reverse it, or we can introduce a transverse component to its velocity, that is, alter its direction as well as its speed. Thought of in this light all electronic devices in which a control is exercised over an electron stream are velocity-modulated devices. It might be argued that one could equally well say that *all we can do is to change the electron's acceleration* (*derivative of velocity*) *or its position* (*integral of velocity*). The singling out of velocity is in a sense arbitrary. It does, however, have some very interesting ramifications.

I might digress for a moment to elaborate on this idea. Since some of the newer devices have been labeled velocity-modulation tubes, there is a perfectly understandable tendency on the part of the uninitiated to assume that these tubes differ from earlier known devices, such as, for example, the space-charge-control tubes, the Barkhausen tube or the magnetron in the fact that they employ velocity modulation. The real difference lies elsewhere as we shall see in a few moments. At the same time that these newer devices were introduced, there was introduced a new way of looking at something which is very old in the art. This newer viewpoint, to my way of thinking, constitutes a far greater fundamental contribution than do the specific devices which have received so much attention. The pioneers in this new approach: Heil and Heil, Bruche and Recknagel, the Varian Brothers, Hahn and Metcalf, to mention a few, and the many other workers who lost in the race to publish their independent contributions in this field—all of these people deserve the greatest of praise for their stimulating contributions

to our thinking. My only point in all this discussion is to emphasize that the basic method of acting on the electron stream has not really been changed at all. The entire matter is summarized in the original statement that the only thing which we can do to an electron is to change its velocity.

Before going on to the next aspect of the problem there is a closely related concept which should be mentioned. This concept is that a change in the component of the velocity of an electron along one space coordinate does not introduce components of velocity in directions orthogonal to the first. For example, if an electron beam is deflected by a transverse electric field, there will be no accompanying change in the longitudinal velocity. The difficulty in the way of doing this in a practical case has nothing to do with the concept but only with the problem of producing unidirectional fields. Analyses of deflecting field problems which ignore the longitudinal components of the fringing fields are apt to be wrong. The problem of high-frequency deflecting fields has been treated in great detail in the literature and frequently with more acrimony than accuracy.

One further note should be added at this point. In an earlier lecture it was pointed out that the magnetic effects of an electromagnetic field are in general very much smaller than the electric effects. We will not stop to prove that this is still true at the frequencies which now interest us but will accept it without further discussion.

For our next concept we leave electron flow for a moment and consider the fields within a resonant cavity. You may very properly object that this has nothing to do with electron ballistics, and indeed it does not. However, we will find it necessary to discuss problems involving cavity resonators, and a failure to understand some of the properties of these circuit elements can cause a great deal of trouble. There are two conflicting approaches to this problem which I will attempt to reconcile.

The physicist when first presented with the problem of a resonant cavity is inclined to say: *This is a boundary value problem. The solution consists in writing Maxwell's equations subject to the conditions that the tangential component of E must be zero along the conducting walls. While a scalar and a magnetic vector potential can be defined, the field is not related to the former in the simple manner used in electrostatic problems.*

The engineer, on the other hand, is inclined to say: *This looks like an extension of the usual resonant circuit. A capacitance exists between the top and bottom walls of the cavity; charging currents will flow through the single turn toroidal inductance formed by the side walls. I would like to know what voltage difference exists between the top and bottom walls, and what currents exists in the side walls.*

Now, actually, I am maligning both the physicist and the engineer by my statements; nevertheless, there are these two approaches. Which is cor-

rect? Well, they both are. It is not correct to speak of an electrostatic potential within a resonant cavity; nevertheless, we may and do talk about the voltage between the top and bottom of a resonant cavity. What do we mean? Simply the maximum instantaneous line integral of the electric field taken along some specified path. In any practical device utilizing electron beams we are naturally interested in the path taken by the electrons. The fact that the line integral is different for different paths is of no great concern. We are interested in but one of these paths. We shall therefore have occasion to talk about voltages in cavities but we must always remember what is meant, and we must never for one instant forget that this voltage is not unique but that it depends upon some assumed path.

The second peculiarity of this voltage must also be emphasized. The line integral must be taken at a specified instant in time. In effect one takes a photograph of the field at some instant in time and then at one's leisure performs the integration.

Now, of course, an electron when projected through such a cavity will perform yet another type of integration. The change in squared velocity of the electron as expressed in volts will be given by the line integral of the field encountered by the electron; that is, integrated not instantaneously but with the electron velocity. This is not a simple process, because the electron velocity is continuously being changed by the field interaction and therefore the velocity with which the integration is performed depends upon the integrated value of the field up to the point in question. This has nothing to do with the concept of voltage in a resonant cavity. The cavity voltage can, however, be considered as the maximum change in squared velocity expressed in volts which an electron could receive if its entrance velocity was very large so that the transit time was small compared with the period of the cavity field.

The four basic concepts which I have chosen to recall to your mind are, by way of summary: (1) the total current is the same in all parts of a circuit, that is div. $J = 0$; (2) the only way we can act on an electron is to change its velocity; (3) the changes in the velocity component of an electron along any one rectangular coordinate have no effect on the velocity components along any other coordinate; and (4) for convenience, a voltage can be defined in a resonant circuit as the line integral of the electric field taken along some prescribed path.

Transit Angle

Since we are to deal with the interaction of electrons and high-frequency fields, we frequently find it convenient to measure electron velocity not directly but in terms of the equivalent potential difference through which an electron must fall to obtain the velocity in question, and the unit of measure

will be a volt. Instead of measuring the time required for an electron to traverse any given distance in seconds, it is also convenient to use, as a unit of time, one radian of angle at the operating frequency. We frequently refer to the transit angle of an electron rather than the transit time, although both terms are used. In fact, we may on occasion measure distances in terms of transit angle, and this usage is extended to measure dimensions transverse to the direction of travel of the electron beam. When used in this fashion, we mean that the dimension in question is such that were an electron to be projected in this direction with a velocity equal to that of the electrons in the main beam, the high-frequency field would change through the stated number of radians during the transit time.

The Five Functions in an Electronic Device

With this preliminary discussion out of the way we can now answer the question which has probably been troubling quite a few of you. If the only thing we can do to an electron is to change its velocity, then in what basic way does the velocity-modulation tube differ from the conventional negative grid tube or from the magnetron?

Well, this is an involved story. If we are to make any use at all of an electron beam we must in general perform five distinct operations or functions. First we must produce the beam. Then we must impress a signal of some sort onto the beam. From what I have just said this can be done only by varying the velocities of the electrons contained in the beam. The third operation consists in converting this variation into a usable form. It is in this way that the diverse forms of electronic devices differ to the greatest degree. We will go into this matter in more detail shortly. The fourth operation consists in abstracting energy from the beam, and the final operation consists in collecting the spent electrons. While these operations are distinct from an analytical point of view, in many actual devices they are performed more or less simultaneously and more than one operation may be performed by certain portions of the tube structure. In fact, in some devices, for example in the space-charge-control tube, the confusion is so great as to make the separation seem rather forced. This very confusion may partly explain why vacuum-tube engineers who were steeped in the art were so slow to realize the advantages of this new way of looking at things which I will call the velocity-modulation concept.

By way of mental exercise in this new way of thinking let us see how we can analyze a simple space-charge-control triode. Well, first of all we have to identify the electron gun which produces the beam. The electrons most certainly come from the cathode, but where is the first accelerating electrode? Actually there isn't any unless we think of the combined d-c field resulting from the d-c potentials on the grid and plate as assisted by

the initial emission velocities as performing this function. The next function, that of varying the electron velocities, is performed by the grid which varies the potential gradient in the vicinity of the cathode and hence the velocity of the electrons as they approach a potential minimum or virtual cathode which is formed a short distance in front of the cathode by the action of space charge. This virtual cathode performs the third function, that of conversion, by sorting out the electrons and allowing only those electrons with emission velocities greater than some specific value to pass. This, then, is one of the conversion mechanisms which we will call virtual-cathode sorting. In this example the virtual cathode occurs very close to the real cathode but this is not always the case. The fourth function, that of utilization, is performed by allowing the sorted electrons to traverse an electromagnetic field between the virtual cathode and the plate. This operation is completed by the time the electrons have reached the plate. Of course in the triode the plate then performs the final operation, that of collecting the spent electrons and dissipating the remaining energy as heat. It should be clearly realized, however, that this last function need not necessarily be performed by the same electrode which provides the output field. Indeed the so-called inductive-output tube proposed by Haeff is a space-charge-control tube in which these two operations are separated.

Conversion Mechanisms

But now to get back to a cataloguing of the different kinds of conversion mechanisms. The first general type involves sorting. The first kind which we have mentioned is by virtual-cathode sorting. A second kind of sorting might involve deflecting the electron beam in proportion to its longitudinal velocity instead of reflecting or transmitting it. Various deflection tubes have been proposed from time to time using this mechanism. We shall be forced to neglect this phase of the problem this evening because of time limitations but those of you who are interested will find the literature filled with detailed discussions. Still a third type of sorting, sometimes called anode sorting, is used in certain Barkhausen tubes when the plate is operated at or near the cathode potential so that fast electrons are collected while slow electrons are reflected and caused to retraverse a high-frequency field. There are still other types of sorting mechanisms but I will not burden you with these.

A second general type of conversion mechanism I will call bunching, to distinguish *sorting* in which electrons are separated according to their velocities from *bunching* in which electrons of differing velocities are brought together. Now it just happens that many of the older devices used sorting, while many of the newer devices use bunching but this is not universally the case. For example, the magnetron as used at high frequencies and the

cyclotron both employ a combination of sorting and bunching. A peculiar property of the motion of an electron in a magnetic field lies in the existence of the so called Larmor frequency. You will recall that the angular velocity of an electron in a magnetic field depends only upon the field-strength and not at all upon the electron's linear velocity. This time in seconds is given by

$$t = \frac{0.357 \times 10^{-6}}{H},$$

or in radians

$$\theta = 2\pi \frac{10600}{\lambda H}.$$

Electrons of widely differing velocity can thus revolve together in spoke-like bunches with the faster electrons going around larger circles than the slow ones, but just enough larger to keep them together. This, then, is one kind of bunching, which for simplicity we shall call magnetic bunching. It is used in the magnetron and in the cyclotron. We will have more to say on this subject a little later.

A second kind of bunching was used in some of the early Barkhausen tubes where the plate electrode was operated at a fairly high negative potential so that none of the electrons were able to reach it. Under such conditions a uniformly spaced stream of electrons with varying velocities is reflected as a bunched stream, the slower electrons being reflected almost at once and the faster electrons penetrating the retarding field for a greater distance and hence taking longer to return. This same type of bunching is used in a newer form of oscillator, commonly referred to as a reflex tube which was suggested by Hahn and Metcalf in 1939, and by others at about the same time. The reflex tube differs from the Barkhausen tube, not in the basic mechanisms so much as in the fact that the conversion mechanism occurs in a different region in the tube from the region devoted to velocity modulation and to energy abstraction. A second kind of bunching is then reflex bunching.

A third type of bunching was used in the diode oscillators of Muller and of Llewellyn. The mathematical research done by W. E. Benham may be mentioned as of interest in this connection. In these tubes a uniform stream of electrons becomes bunched simply through the fact that faster moving electrons overtake slower ones which precede them. In these earlier forms of tubes we again have the case where this conversion is performed simultaneously with one or more of the other processes so that it is very difficult to separate them. However, in 1935 Heil and Heil proposed a tube in which the conversion region was separated from the other regions of the

tube. This tube, the velocity-modulation tubes of Hahn and Metcalf, and the klystron tubes of the Varian Brothers, are alike in their use of transit-time bunching in a relatively-field-free drift tube. Since this separation of functions renders these devices much easier to analyze and since the structures are quite interesting in any case we will spend most of our time considering them and will, I fear, rather neglect some of the other types of tubes.

We will, of course, keep our analysis as general as possible so that the results may be applied to a variety of different devices.

Input Gap Analysis

Let us begin by a small-signal consideration of a uniform electron stream entering a region in which there is a longitudinal field defined as some function of the distance and of time. This can be the entire Llewellyn diode or it can be the input region of a klystron. We ask ourselves with what velocity will the electrons leave this region and what will be the net exchange of energy between the electrons and the field. At any point within the field a typical electron will experience an acceleration given by

$$\ddot{y} = \frac{1}{\xi} E + \eta f(y) f(t) \tag{1}$$

where η is proportional to the maximum amplitude of the h.f. field, but contains a numerical constant so that $\ddot{y}$ is expressed in centimeters per second per second. Now in the usual case $f(t)$ will be a simple sine function but $f(y)$ may assume a variety of forms. Again, by way of simplifying our work we will assume that it is also a sine function. Let us consider how we can go about solving this apparently simple equation. Unfortunately this expression can not be solved directly because the value of t at any plane (that is, the time of arrival of an electron at this plane) depends upon the interchange of energy between the electron and the field. Here we are forced back to the time-honored mathematical device of assuming a solution in the form of a series and then evaluating these coefficients. There is a large number of ways in which this can be done, and consequently a large number of different solutions which look very different but which all give comparable answers. Usually when such solutions are published, the arithmetical work is omitted leaving one with the feeling that there is something involved that is not within the ken of ordinary mortals. The fact is that the work is usually extremely tedious but actually very simple. It will be instructive to follow through one form of such an analysis in just enough detail to see the amount of work involved.

Since we are interested in the energy which is proportional to $\dot{y}^2$ we will write at once

$$(\dot{y}^2)_{y=a} = K = K_0 + \eta K_1 + \eta^2 K_2 + \eta^3 K_3 + \ldots$$

where the K's are a function of the transit time, of the field distribution and of the entrance phase, and we will proceed to evaluate these coefficients. The average energy per unit of change as expressed in volts is then simply

$\frac{\xi \bar{K}}{2}$ at the end of the field while the gain is:

$$V_{av} = (\xi/2)(\bar{K} - \bar{K}_0) = \frac{\eta \xi \bar{K}_1}{2} + \frac{\eta^2 \xi \bar{K}_2}{2} + \cdots$$

where the bar means that we are averaging over all values of the entrance phase.

It is of interest to evaluate the value of velocity $\dot{y}^2$ which individual electrons receive as a function of the entrance phase. For small signals it is usually sufficient to evaluate $\dot{y}^2$ maximized with respect to the starting phase, then

$$V_{max} = (\xi/2)(K - K_0)_{max} = \left[\frac{\eta \xi K_1}{2} + \frac{\eta^2 \xi K_2}{2} + \cdots\right] \text{max.}$$

We can further define the ratio of V_{max} to the largest value it can have as a coefficient β, sometimes called the modulation coefficient.

But now to evaluate the K's. There are many ways of doing this as I have intimated. We will proceed by writing

$$y = y_0(t) + \eta y_1(t) + \eta^2 y_2(t) + \eta_3 y_3(t) + \ldots$$

where the y's are coefficients depending upon the transit time t which in itself is a function of the applied field thus

$$t = t_0 + \eta t_1 + \eta^2 t_2 + \eta^3 t_3 + \ldots.$$

We can then expand each function of time into a series remembering that

$$f(x + d) = f(x) + \frac{f'(x)\, d}{1!} + \frac{f''(x)\, d^2}{2!} \cdots$$

or for our particular case

$$y_0(t) = y_0(t_0) + \frac{\ddot{y}_0(t_0)[\eta t_1 + \eta^2 t_2 + \eta^3 t_3 + \cdots]}{1!} + \frac{\ddot{y}_0(t_0)[\eta t_1 + \eta^2 t_2 + \eta^3 t_3 + \cdots]^2}{2!} + \cdots$$

Now we can expand $y_1(t)$, $y_2(t)$ etc. in exactly the same way. Finally we get a collection of terms which can be grouped in like powers of η thus

$$y = y_0(t_0) + \eta \text{ [terms in } \dot{y}, \ddot{y}, t_1, t_2, \text{ etc.]} + \eta^2 [\quad] \ldots$$

The coefficient of the η is in fact $\dot{y}_0(t_0)\, t_1 + y_1(t_0)$. We will not bother to write the rest. This expression can then be differentiated to get $\dot{y}$ and then

squared. However, we still have some undetermined coefficients the t_1, t_2 etc. terms. These we can evaluate by noting that we wish these values at $y = a$, where a is a fixed distance in the actual device. At this distance the t coefficients in the expression for y must have such values that the value of y does not change with the value of η. This can only be true if the individual expressions multiplying each power of η are each equal to zero. Equating these expressions to zero one can evaluate all of the t's. For example the first term yields

$$\dot{y}_0(t_0)t_1 + y_1(t_0) = 0$$

or

$$t_1 = -\frac{y_1(t_0)}{\dot{y}_0(t_0)}.$$

Introducing these values, differentiating and squaring, one finally gets an expression for $(\dot{y}^2)y = 0$ as a power series in y, the coefficients all being of a form easily evaluated for any specified field distribution. Since we have by definition called these coefficients K_0, K_1, etc. these values are then

$$K_0 = \ddot{y}_0^2$$

$$K_1 = 2(\ddot{y}_0\ddot{y} - y_0\ddot{y}_1)$$

$$K_2 = (\ddot{y}_1^2 - 2y_1\ddot{y}_1 + 2\ddot{y}_0\ddot{y}_2) - 2\ddot{y}_0 y_2 + \frac{\ddot{y}_0\ddot{y}_1^2}{\ddot{y}_0}$$

This then constitutes the formal solution of the problem. We must now particularize our problem to some specific field distribution and evaluate the y coefficients. Suppose, for example, that there is a uniform d.c. field (E of equation 1) and an alternating field which varies as some cosine function of distance. Then the latter is

$$f(y) = \cos\left(\frac{\pi y}{b} + c\right)$$

and

$$\ddot{y} = \frac{1}{\xi} E + \eta \cos(\omega t + \varphi) \cos\left(\frac{\pi y}{b} + c\right)$$

we must eliminate the y which appears in this expression and replace y by its equivalent

$$y = y_0 + \eta y_1 + \eta^2 y_2 + \ldots$$

and expanding

$$\cos\left(\frac{\pi y}{b}+c\right)=\cos\left(\frac{\pi y_0}{b}+c\right)+\frac{\frac{\pi}{b}\sin\left(\frac{\pi y_0}{b}+c\right)[\eta y_1+\eta^2 y_2+\cdots]+\cdots}{1!}$$

and as before equating like powers of η with $\ddot{y}$ defined as

$$\ddot{y}=\ddot{y}_0+\eta\,\ddot{y}_1+\eta^2\ddot{y}_2+\cdots$$

we finally arrive at

$$\ddot{y}_0=\frac{1}{\xi}E$$

$$\ddot{y}_1=\cos(\omega t+\varphi)\cos\left(\frac{\pi y_0}{b}+c\right)$$

$$\ddot{y}_2=-y_1\pi/b\cos(\omega t+\varphi)\sin\left(\frac{\pi y_0}{b}+c\right).$$

Now we need only integrate these expressions to obtain the values of the $\dot{y}$'s and the y's needed to evaluate the K's.

If we average $\dot{y}^2$ over all values of the starting phase we can write the energy contributed by the field to the electron's velocity. When this is done one finds that the odd powers of η are identically zero leaving only the even powers to be considered and for small signal analysis purposes we need only consider $\bar{K}_2$. The energy per electron expressed in volts is

$$V=2.49\times10^{-8}E^2\lambda^2 f(\theta)$$

where $f(\theta)=\omega^2\bar{K}_2$, and the power is obtained by multiplying this expression by the beam current in amperes.

The end results can be expressed as curves of $f(\theta)$ against θ as shown in Fig. 1. Three examples are shown: the uniform field case and two different harmonic distributions as indicated by the smaller plot in the lower left-hand corner. You will note that there exist regions of positive $f(\theta)$ where the net transfer of energy is from the field to the electron and regions in which the transfer is in the other direction; the former portions are of considerable interest in connection with the input gaps in velocity modulation tubes, and for that matter in the cathode grid region of the negative grid tube although this is more complicated than is here indicated, as this transfer of energy constitutes a loss to the field which loads the input circuit. The latter portions may be utilized as was done in the Muller and Llewellyn diodes to obtain sustained oscillations.

If, as I have indicated, we maximize $\dot{y}^2$ as a function of the starting phase we can evaluate the modulation coefficient. The value for the uniform field

case, as shown in Fig. 2, is simply, $\beta = \dfrac{\sin \theta/2}{\theta/2}$. For future reference we will write the loss expression for this case as

$$f(\theta) = 2\,(1 - \cos\theta) - \theta \sin\theta.$$

Drift Space Analysis

Now let us consider the conversion region in a typical velocity-variation tube. Figure 3 is a drawing of several such devices with the conversion

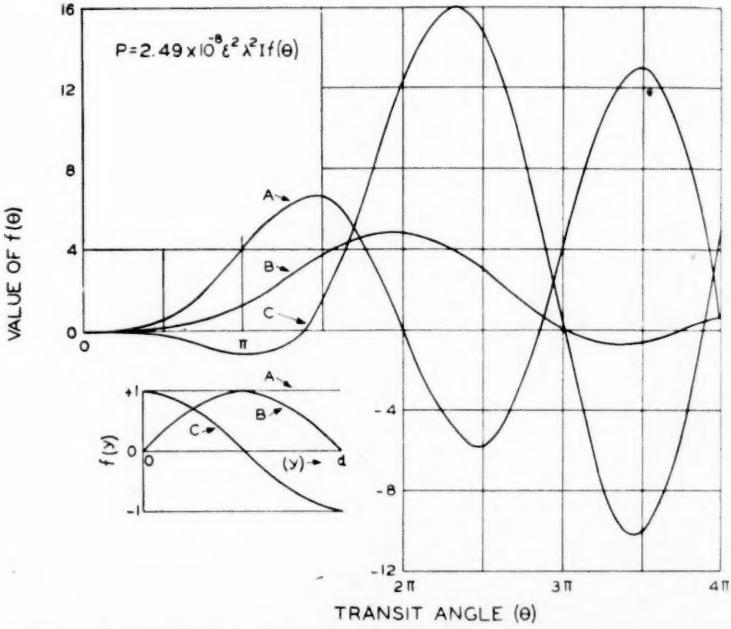

Fig. 1—The energy transfer between an initially uniform electron stream and a longitudinal electromagnetic field as a function of transit angle.

regions indicated. We will assume for the moment that the electrons enter this region with a small variation in velocity and at a perfectly uniform rate. Since the total number of electrons entering the region must be equal to the number of electrons leaving the region we may write

$$i_1\, dt_1 = i_0 dt_0$$

or

$$i_1 = i_0 \frac{dt_0}{dt_1}.$$

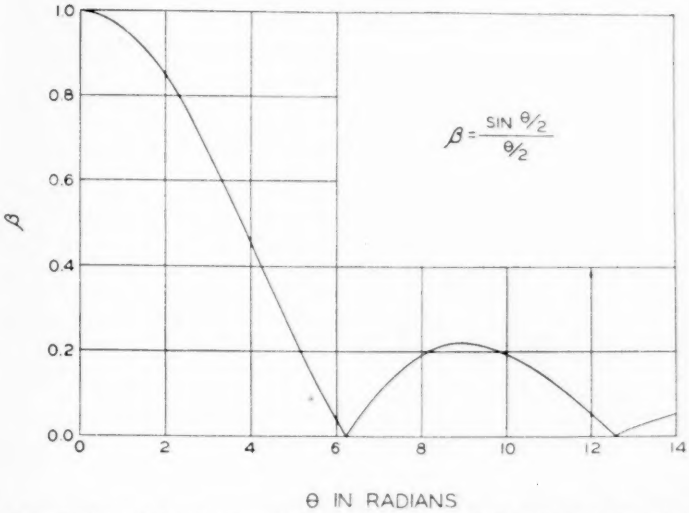

Fig. 2—The (velocity) modulation coefficient between an initially uniform electron stream and a uniform electromagnetic field as a function of transit angle.

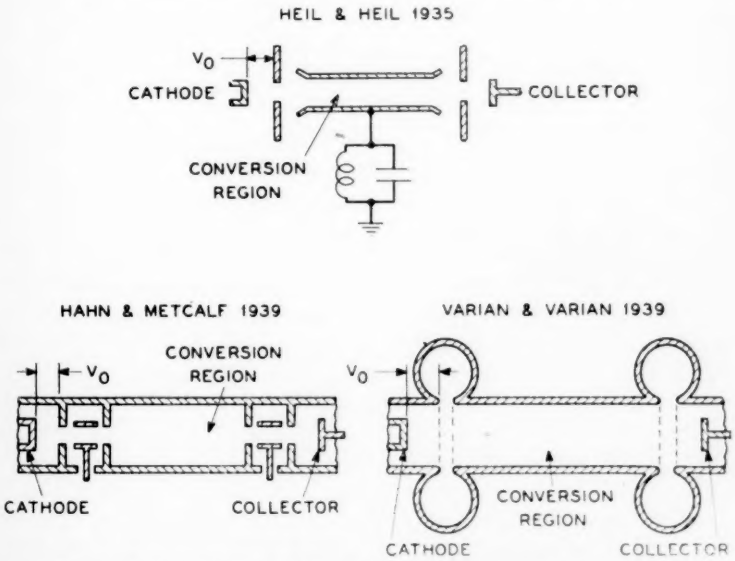

Fig. 3—Typical velocity variation devices employing transit-time bunching.

However, a relationship exists between t_1 and t_0,

$$t_1 = t_0 + \frac{\ell}{v}.$$

Where

$$v = v_0 \sqrt{1 + \alpha \sin \omega t_1},$$

$$t_1 = t_0 + \frac{\ell}{v_0 \sqrt{1 + \alpha \sin \omega t_1}}.$$

Now if $\alpha \ll 1$

$$t_1 = t_0 + \frac{\ell}{v_0}\left(1 - \frac{\alpha}{2} \sin \omega t_1 + \cdots\right)$$

and

$$\frac{dt_0}{dt_1} = 1 + \frac{\ell}{v_0} \frac{\alpha\omega}{2} \cos \omega t_1$$

and finally

$$i_1 = i_0\left(1 + \frac{\ell\alpha\omega}{v_0 \cdot 2} \cos \omega t_1\right)$$

but

$$\frac{\ell\omega}{v_0} = \theta$$

so that finally

$$i_1 = i_0\left(1 + \frac{\alpha\theta}{2} \cos \omega t_1\right).$$

This says that the velocity variation impressed on the beam at the entrance to the drift space or conversion region has resulted in a current variation at the output. For those of you who think in vacuum tube parameters it is of interest to differentiate this expression with respect to the a-c voltage and obtain the transconductance

$$G_m = \left|\frac{di_1}{dV_{a\cdot c\cdot}}\right|$$

rewriting

$$|i| = i_0\left(1 + \frac{V_{ac}\theta}{2V}\right)$$

$$\left|\frac{di_1}{dV_{ac}}\right| = \frac{\theta i_0}{2V}.$$

This result is obtained by neglecting all of the higher order terms and is therefore only a small signal theory of a very restricted sort.

Now let us consider what we have done. Well, we have followed a small interval of time through the drift tube. At the input this time dt_0 had a current i_0 associated with it; at the output the size of this unit of time is different—it is now dt_1 and the current associated with it is i_1. The physical picture corresponding to this phenomenon is that of a uniform distribution of electric charge becoming bunched with time as it traverses the drift space.

The next step in the analysis is to carry our approximation a step further and consider higher-order terms. Expanding the expression for i_1 and using our nomenclature the desired expression is

$$i_1 = i_0\left[1 + 2\left(J_1\left(\frac{\alpha\theta}{2}\right)\cos\omega t + J_2\left(2\frac{\alpha\theta}{2}\right)\cos 2\omega t + J_n\left(n\frac{\alpha\theta}{2}\right)\cos n\omega t\right)\right].$$

This equation is not exact since it neglects space charge effects but it does indicate the presence of harmonics in the beam current and it reveals certain non-linear effects which can also be illustrated by the so-called phase-focusing diagrams of Bruche and Rechnagel.

Phase-Focusing Diagrams

Bruche and Recknagel pointed out that an analogy exists between the focusing in space of a parallel light beam and the focusing in phase of the electrons in a uniform electron beam. In fact a small-signal theory can be developed entirely in terms of optical equations. We will not go into this aspect in detail but we will use their diagram (Fig. 4) to illustrate the bunching effect graphically. A uniform beam of electrons is represented by a series of parallel lines in distance and time coordinates, focus being indicated by a crossing of these lines after they have been deflected by the velocity modulation.

This general type of diagram has been popularized in this country by the Varians, and their associates under the name Applegate diagram, the only difference being an interchange of axis. Figure 5, taken from a recent paper by Dr. A. E. Harrison, illustrates this version of the Bruche and Recknagel diagram.

Now if instead of judging the current density by the density of the lines on the diagram, we make a plot of the current density as a function of time for different fixed distances from the input gap, the pictures are somewhat as shown on Fig. 6. Figure 7 represents a plot presented by Kompfner and combines in one illustration the type of presentation used by Tombs.

Phase Focusing in a Reflex Tube

It might be well to pause for a moment in our discussion of transit time bunching to consider how the phase focusing diagrams can be applied to a reflex tube. The elements of a modern reflex tube are shown in Fig. 8

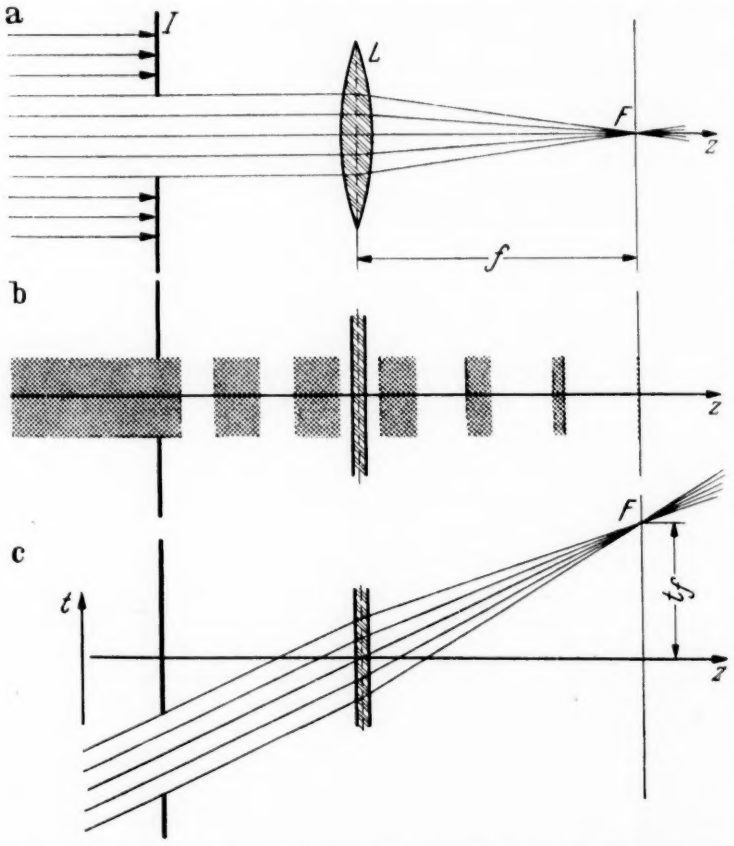

Fig. 4—The phase-focusing diagram of Bruche and Recknagel showing the analogy to optical focusing.

which was taken from a recent I.R.E. paper by Dr. J. R. Pierce. Electrons from the cathode pass through an input gap defined by two grids where they are modulated in velocity. In traveling in the retarding field produced by the repeller those electrons which passed the gap when the field was becoming progressively less accelerated, become bunched; the faster electrons

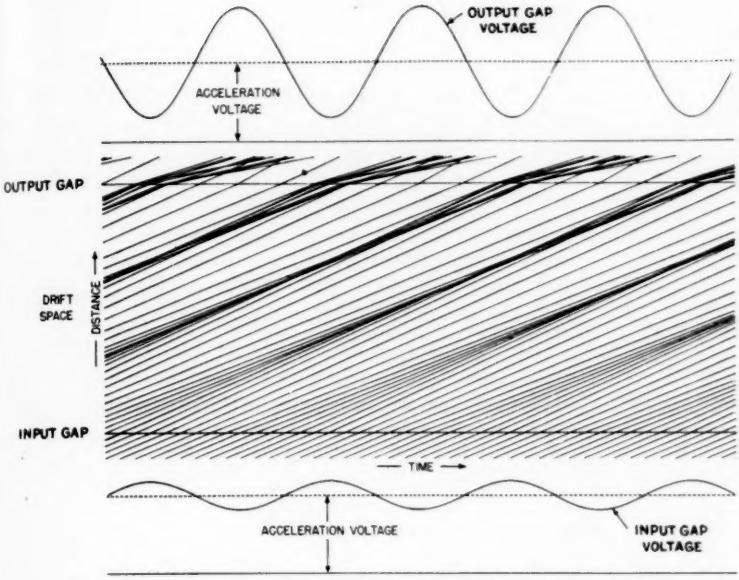

Fig. 5—Applegate's version of the phase-focusing diagram (Harrison).

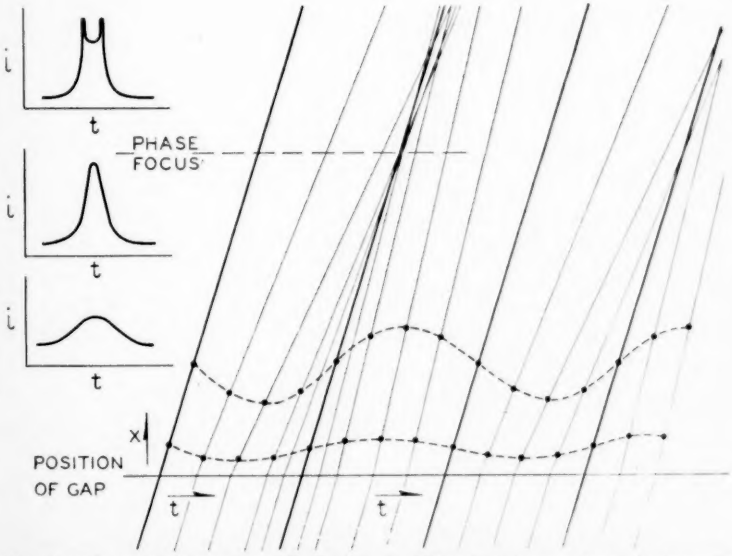

Fig. 6—The conduction-current distribution at different distances along the beam as predicted by the phase-focusing diagram.

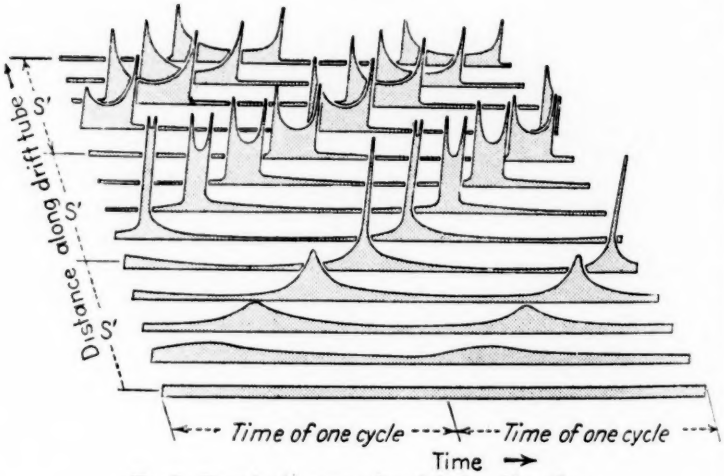

Fig. 7—Kompfner's presentation of the bunching effect.

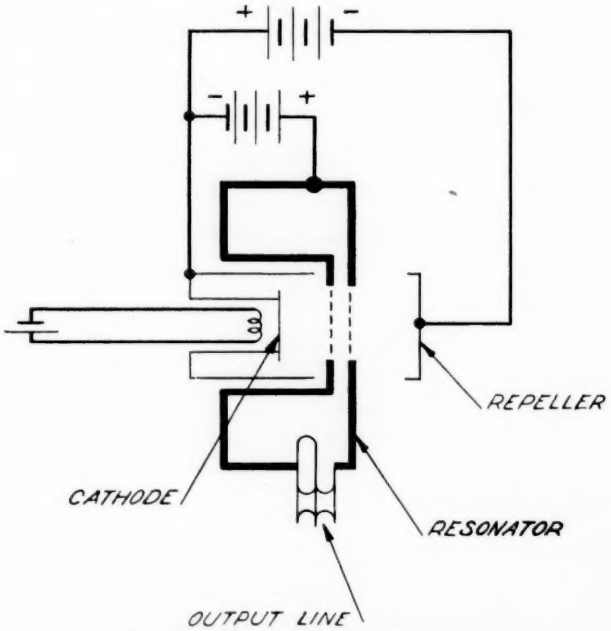

Fig. 8—The elements of a modern reflex tube (Pierce).

penetrating the field to a greater extent and waiting, as it were, for the slower electrons which follow to catch up. The electrons which pass across the gap while the field is becoming progressively more accelerating are spread out. If the retarding field is uniform it can be likened to the earth's gravitational field and the phase-focusing paths on our time-distance plot are parabolas. Figure 9, taken from Pierce's paper, illustrates this while Fig. 10 is such a plot taken from the paper by Harrison. One interesting and,

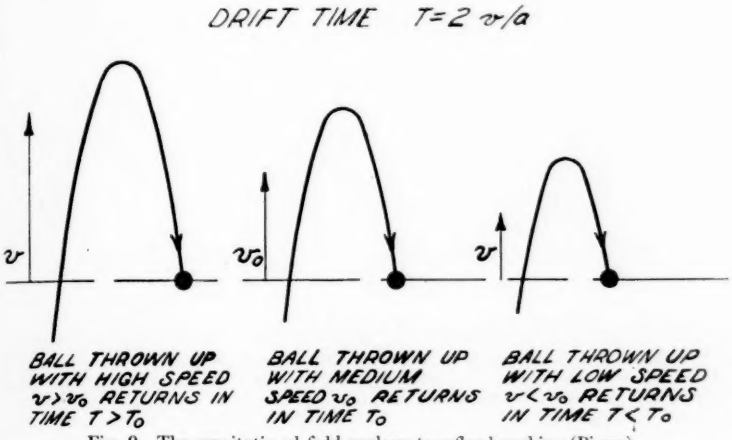

Fig. 9—The gravitational-field analogy to reflex bunching (Pierce).

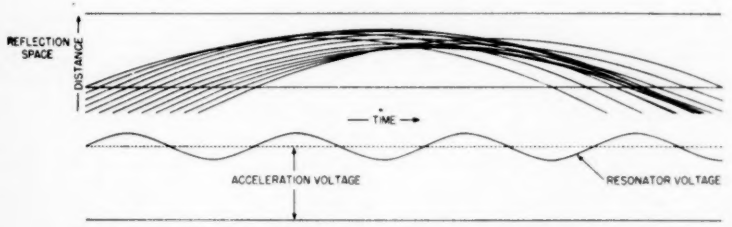

Fig. 10—The phase-focusing diagram for a reflex oscillator (Harrison).

in a way, unfortunate difference between reflection bunching and direct transit-time bunching is the fact that for reflection bunching the slow electrons catch up with the fast ones while the reverse is true for the other type. This means that if both types of bunching are present as shown in Fig. 11, (also taken from Harrison's paper) one will tend to undo the effect of the other.

Another way of combining effects of separate bunching actions is to build

a cascade transit-time-bunching amplifier in which a series of three gaps is used together with two drift spaces. The first gap velocity modulates the beam; this modulation is converted into a current modulation in the first drift space. The beam then excites the second cavity, which again velocity modulates the beam in quadrature with the original modulation. This action of course occurs in the output gap of a two-gap tube but it is not there used. Here this second and larger velocity modulation is converted to current modulation in the second drift space. The output is finally taken off the beam by the third gap. A phase-focusing diagram of this sort (again taken from Harrison's paper) is shown in Fig. 12.

Space-Charge-Wave Analysis

This phase-focusing approach is rather intriguing as one feels that one has a physical picture of what is going on. The picture is, however, very inexact except under certain highly specialized cases, as it completely ignores

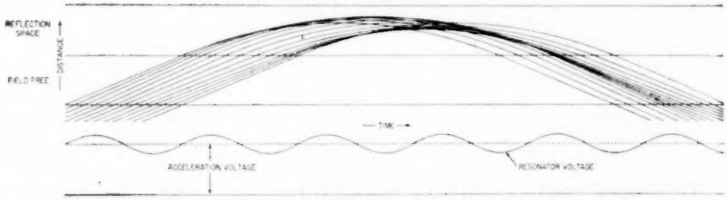

Fig. 11—Diagram showing reflex bunching combined with field-free transit-time bunching (Harrison).

space-charge effects. These space-charge effects are of two sorts: a d-c effect, if you will, and an r-f effect; that is, the presence of the electrons of the beam will alter the average velocity of the electrons at different parts of the beam, and will tend to undo the bunching action. Because of this second effect, the electrons are effectively prevented from passing each other as the graphical solution suggests. Instead, as the density of the electrons in the bunch becomes greater, the mutual repulsion forces tend to prevent a further concentration of charge. The electron bunch then tends to disperse. The action could be likened to the propagation of a sound wave in a moving column of air. While there are several approximate ways to handle this problem, Hahn was the first to propose a really satisfactory theory. Incidentally it should be noted that the Benham, Muller, Llewellyn and Peterson type of theory is capable of treating this aspect of the problem in a rigorous way and including all space-charge effects, but unfortunately these theories are limited in that they have been applied only to the parallel-plane case, and of course they are only small-signal theories.

Hahn's analysis starts by treating an infinitely long electron beam, using cylindrical co-ordinates and is limited to a small signal theory where the a-c motions are small compared to the d-c but it does not ignore the r-f effects of the space charge forces. The electron beam is thought of as a moving dielectric rod which is capable of propagating axial waves much as a dielec-

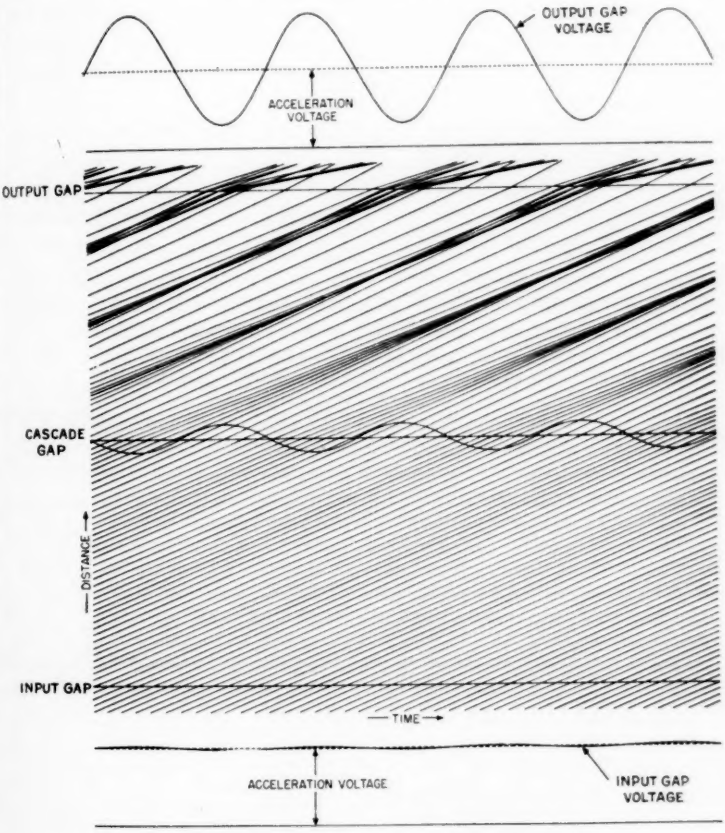

Fig. 12—Diagram for a cascade amplifier (Harrison).

tric wave guide will do. He assumes an axial magnetic field and a stream of positive ions having the same velocity axially and the same charge density. These ions are assumed to have infinite mass. The solution is much too complicated and involved to present here even in abstract. It involves the complete solution of Maxwell's equations subjected to the stated assump-

tions as restricted by the assumed boundary conditions at the edge of the beam.

It is found that two waves are possible, one traveling slightly faster than the electron beam and the second traveling slower. A point where the velocity components are in phase will correspond to the input to the beam, while points where the current components are in phase correspond to the desired positions for the output. The propagation constants for these two waves in a simplified special case where the magnetic field strength is infinite are given by Hahn, as well as expressions for the optimum drift tube length. He goes on to consider the case where the magnetic field is zero and finds that for this case the density of the charge does not vary much but instead the beam swells in and out so that instead of being lumps of charge with spaces between, the lumps appear in the outer boundary. Hahn has extended his general method of analysis to consider the modulation coefficient of gaps through which the beam must pass. His results are a great deal more general than those we have presented.

Ramo has reformulated Hahn's theory by means of retarded potentials for the most important case. This results in some simplification of the theory. He computes the more important design constants for a velocity modulated tube, such as the optimum drift tube length and the amount and phase of the transconductance. Those of you who are particularly interested are referred to the original paper. An interesting aspect brought out rather forcibly by Ramo's analysis is the existence of higher-order waves on the beam, always occurring in pairs, one faster and the other slower than the beam velocity.

The Magnetron

In what time remains I want to say just a very few words about the magnetron. This is a very complicated subject and one which cannot be adequately dealt with in an entire evening, and certainly not in the time remaining.

As you all know, the magnetron was invented and named by Dr. A. W. Hull. Habann, Zacek, Okabe and others pioneered in the use of the magnetron as an ultra-high-frequency oscillator. As envisioned today a magnetron is a two-element device, usually cylindrical with a centrally located cathode and a surrounding anode. The anode may be continuous or it may be split into a number of segments as suggested by Okabe, and these segments joined together either externally or internally by resonant circuits.

The basic ballistic problems of the magnetron, and hence the only problems which directly concern us at this time are (1) that of determining the

electron paths within the magnetron and having determined these paths (2) that of getting an understanding of the mechanism whereby electrons in traversing these paths are able to deliver energy to the connected high-frequency circuits. One might think that the first problem would be a relatively easy job. As a matter of fact the literature is surfeited with papers purporting to give the answer. Unfortunately almost all of the published work ignores the effect of space charge. A few moments' thought will suggest that space charge may be a controlling factor because of the long electron paths which are sure to result in crossed electric and magnetic fields, and indeed more detailed computations bear this out. Nevertheless the neglect of space charge greatly simplifies the problem. There are those who believe that the no-space-charge theories have no bearing on the way actual magnetrons work and that any correspondence between the predictions of such theories and the actual behavior of magnetrons is simply the result of an unfortunate coincidence. In fact Brillouin points out that the simplified form in which the Larmor theorem is applied by many, is in itself an approximation which was perfectly valid as originally applied by Larmor to the electronic orbits within the atom but which does not apply to conditions as they exist in the magnetron.

A number of recent workers have attempted to include the effects of space charge but have unfortunately largely restricted themselves to small signal theories while the magnetron is seldom operated under small signal conditions, at least not intentionally. Most theories are further restricted to a consideration either of the coaxial case where the cathode radius is small compared to the anode radius or of the plane case. Most practical structures are intermediate between these extremes.

As an example of the difficulties involved, Fig. 13, reproduced from a paper by Kilgore, shows the electron paths as computed neglecting space charge and also shows experimental proof that these paths actually exist. This illustration has been frequently reproduced and widely accepted. The experimental picture was obtained in the presence of gas, to make the electron beam path visible, and unfortunately the ionization which makes the beam visible also tends to neutralize space charge effects. The experimental arrangement departs still further from reality in that the electron emission from the cathode was restricted to a limited region so that the space charge forces were still further reduced. Now it is probably true that some magnetrons operate with electron paths as shown; still it is not true that all magnetrons operate in this way.

Contrasting with this picture which was until recently commonly accepted, Brillouin, Blewett and Ramo, and others have shown that stable distributions are possible in which a space charge of almost uniform density rotates with a uniform angular velocity about the axis. Brillouin goes so

far as to label the curves due to Kilgore as wrong, and pictures the possible electron trajectories as shown in Fig. 14.

One of the earliest papers to consider this newer picture of the electron paths in the magnetron was published by Posthumus in 1935. This was definitely a ballistic approach and hence suitable for discussing tonight.

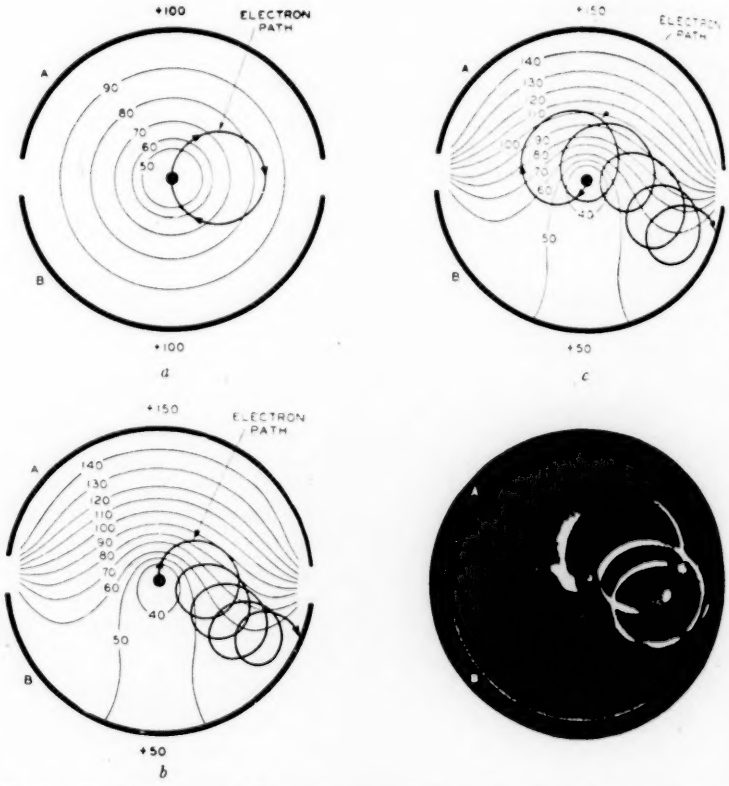

Fig. 13—Typical electron paths in a two-segment magnetron showing how electrons arrive at the plate-half of lower potential (Kilgore).

Posthumus limits his discussion to but one type of oscillation which can be obtained in the split-anode magnetron. Those of you who are familiar with the early literature on the magnetron will recall that two distinct types of oscillations were frequently described. One type usually called "electronic" was found to occur under conditions when the magnetic field was just

high enough to cut off the anode current under static conditions. This field has the value computed by Hull:

$$H = \frac{6.72\sqrt{V}}{R}$$

Hull's first computation, by the way, was made neglecting space charge, but, strangely enough, the result is not changed by space charge. These electronic oscillations were assumed to be related in frequency to the time of transit of an electron from the cathode to the anode, and at cutoff this is inversely proportional to the field strength, as expressed by the empirical relationship

$$\lambda H = 13{,}100.$$

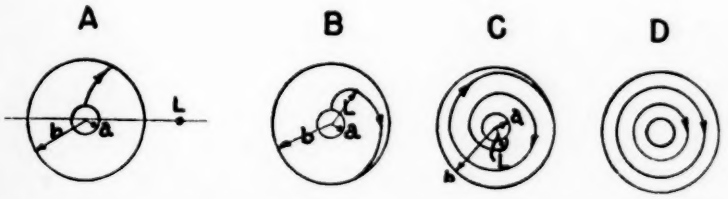

Electronic trajectories for different magnetic fields
A—small magnetic field $L \gg b$
B—moderate magnetic field $L \approx b$
C—strong magnetic field $L \ll b$
D—critical magnetic field $L = 0$

Fig. 14—Electronic trajectories for different magnetic fields varying from weak fields to the critical field shown to the right (Brillouin).

In general, it was found that best operation occurred when the magnetic field was not quite perpendicular to the electric field. The efficiency and outputs as reported for this type of oscillator were always low, in spite of the large amount of effort devoted to it by an equally large number of workers. A second type of oscillation, usually referred to as negative resistance oscillations, has also been the subject of considerable study and some practical use has been made of it at relatively low frequencies.

Contrasting with this, Posthumus described a third kind of oscillation which he called rotating field oscillations. As in the electronic oscillations the preferred frequency is determined by the magnetic field-strength and the anode potential, the frequency being inversely proportional to the magnetic field-strength. Contrasting with the electronic oscillations, the rotating

field oscillations occur with the magnetic field-strength very much above the critical cutoff value and the efficiency on occasion reached as much as 70%. While a careful reading of the literature will reveal that some of the earlier experimenters were occasionally dealing with these oscillations, Posthumus' observations represent a new departure in magnetron theory and practice and one which we might do well to investigate.

Posthumus' approach consisted in studying the electron paths in a magnetron in detail in order to find the conditions under which electrons may reach the plate with considerably less energy than that corresponding to the plate potential. He assumed a magnetron having k pairs of plates and based his calculations on the supposition of a rotating electric field with k pairs of poles. In reality there exists a simple alternating field but this can be resolved into two rotating fields rotating in opposite directions. Power engineers will recognize this as identical with the procedure used in analyzing single-phase rotating machinery. Posthumus neglected the field opposite to the static angular velocity and considered only one component. This is an approximation but a fairly plausible one which can be partially justified.

In the absence of oscillations there is a radial electric field independent of the angular position and inversely proportional to radius (for the coaxial cylindrical case). When oscillations are present there is an additional radial field which varies as some periodic function of the angle and with a period 2π, and a tangential component of the same general type. For simplicity these functions are taken to be simple harmonic functions and can therefore be split into two circular rotating fields.

Posthumus writes the two simultaneous differential equations determining the path of an electron, neglecting space charge, and inquires if a solution is possible for an elecron path which travels at approximately the same angular velocity as the rotating field but lags it by an angle α. An equally satisfactory way of looking at this is to say that we transform our coordinates from a fixed system to one rotating with the field and inquire if a solution is possible where α the angular motion is always small. He finds that such a solution is indeed possible and that for the electron motion to be stable the value of α must be such that the electrons are somewhat behind the line for which the field has its maximum retarding value. The electrons are thus in a position to lose energy to the field and to spiral out toward the anode.

Posthumus defined the value of the electron's radial velocity squared at the anode as P and the total velocity squared at the anode as Q. Normalized plots of these two parameters are shown in Fig. 15 as a function of frequency. The upper plot shows the radial velocity. Obviously for electrons to reach the plate at all they must have a positive velocity at the plate. Electrons can therefore reach the plate with any given field value, say $Z = 2$,

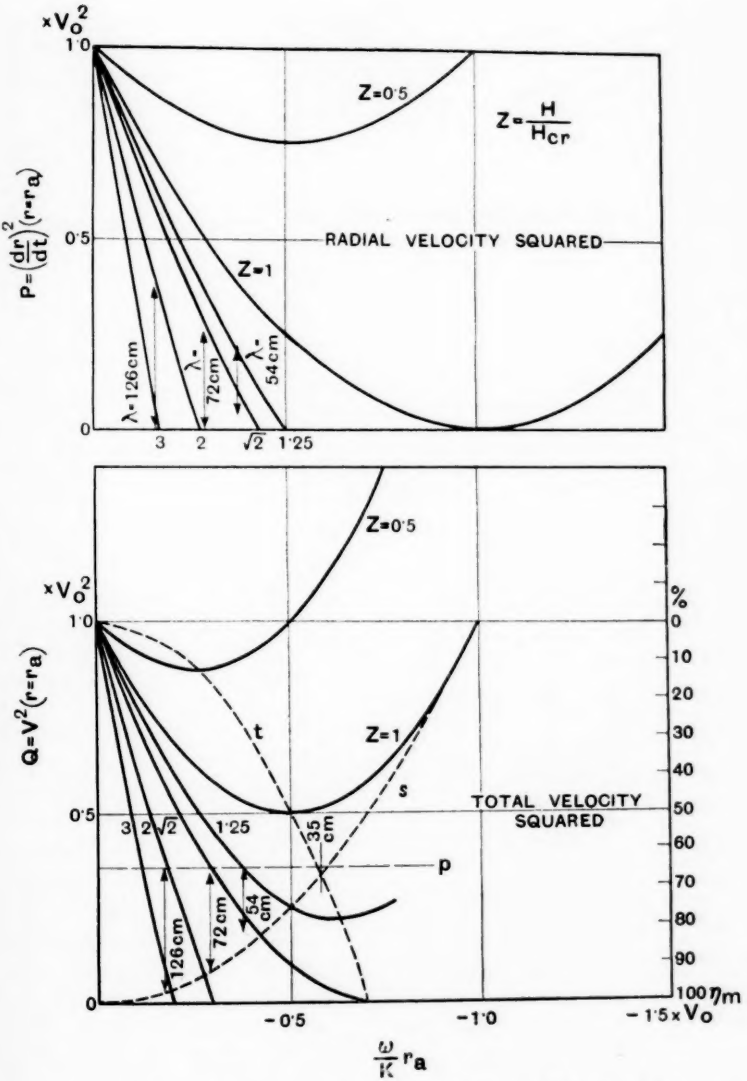

Fig. 15—Electron velocities in the magnetron according to Posthumus.

that is with a field equal to twice the cutoff value, for all frequencies less than the equivalent value defined by the intercept of the $Z = 2$ line with

the abscissa axis. The line for $P = 0$ appears on the lower curve as the dotted line s. Here the ordinate is the total velocity squared, normalized with respect to the value without oscillation. Efficiencies can therefore be put on the plot directly as shown by the right-hand scale in per cent. The line s is therefore a plot of the maximum possible efficiency. This refers to what we might call the electronic efficiency since no account is taken of circuit losses. Now in any physical device there are some circuit losses and hence a lower value of electronic efficiency for which sustained oscillations are not possible. The dotted line p is Posthumus' experimental value for this lower limit. Between the lines p and s, then, oscillations are possible at frequencies given by the abscissae and with field values shown on the solid lines. Actual data for an experimental tube are shown on the plot, oscillations occurring at the wavelengths indicated and over the ranges in field shown by the lines terminating in arrows.

One additional line t is shown on the plot connecting points on the different Z lines for which the efficiency is a maximum. The optimum design would be one based on the intersection of this line with the p line. Still other facts will appear from a detailed study of these results but we shall not be able to devote any more time to this interesting subject.

Conclusion

In concluding a talk of this sort and particularly in concluding a series of talks, it is usually appropriate to look ahead to the future and predict the trend of affairs, or perhaps to point out certain fruitful fields of research. I find this a singularly difficult thing to do. However, it is not revealing any military secrets to say that much of the progress of the last few years has been in the direction of making things work and not toward getting a clearer understanding of the underlying theory. If, for example, an illuminating approach could be devised which would make the problems associated with transverse fields, both electric and magnetic, appear as simple and straightforward as do longitudinal-electric-field problems, as a result of the velocity-modulation concept, then I believe even more striking advances could be made in the ultra-high-frequency field than those which the war years have brought forth.

Selected Bibliography

A. Papers of a Historical or Review Nature

H. Backhausen and K. Kurz, "The Shortest Waves Obtained with Vacuum Tubes", *Phys. Zeits*, vol. 21, p. 1 (1920).

E. W. B. Gill and G. H. Morrell, "Short Electric Waves Obtained by Valves", *Phil. Mag.*, vol. 44, p. 161 (1922).

A. W. Hull, "The Effect of a Uniform Magnetic Field on the Motion of Electrons between Coaxial Cylinders", *Phys. Rev.*, vol. 18, p. 31 (1921).

E. Habann, "A New Vacuum Tube Generator", *Zeits f. Hochfreq.*, vol. 24, p. 115 (1924).

A. Zacek, "A Method for the Production of Very Short Electromagnetic Waves", *Zeits f. Hockfreq.*, vol. 32, p. 172 (1928).
K. Okabe, "Production of Intense Extra-Short Electromagnetic Waves by Split-Anode Magnetron", *I.E.E. Jour.*, Japan, 1928, p. 284. See also I.R.E. Proc., vol. 17, p. 652 (1929); *I. R. E. Proc.*, vol. 18, p. 1748 (1930).
K. Kohl, "Continuous Ultra-Short Electric Waves", *Ergebnisse der exaktlen Naturwissenschaften*, vol. 9, p. 275 (1930). Bibliography of 135 titles.
M. J. Kelly and A. L. Samuel, "Vacuum Tubes as High-Frequency Oscillators", *Elec. Eng.*, vol. 53, p. 1504, Nov. 1934.
E. C. S. Megaw, "Electronic Oscillations", *Jour. I. E. E.* (London), vol. 22, p. 313, April (1933). (Bibliography of 47 titles.)
G. R. Kilgore, "Magnetron Oscillators for the Generation of Frequencies Between 300 and 600 Megacycles", *Proc. I. R. E.*, vol. 24, p. 1140, Aug. (1936).

B. Papers Dealing With Parallel Plane Electronics

W. E. Benham, "Theory of the Internal Action of Thermionic Systems at Moderately High Frequencies".
Part I, *Phil. Mag.*, vol. 5, p. 641, March (1928).
Part II, *Phil. Mag.*, vol. 11, p. 457, February (1931).
Johannes Muller, "Electron Oscillations in High Vacuum", *Hockfreq. u Elek. Akus*, vol. 41, p. 156, May (1933).
F. B. Llewellyn, "Vacuum Tube Electronics at Ultra-High Frequencies", *I. R. E. Proc.*, vol. 21, p. 1532, Nov. (1933).
C. J. Bakker and G. de Vries, "Amplification of Small Alternating Tensions by an Inductive Action of the Electrons in a Radio Valve with Negative Anode", *Physica*, vol. 1, p. 1045, Nov. (1934).
C. J. Bakker and G. de Vries, "On Vacuum Tube Electronics", *Physica*, vol. 2, p. 683, July (1935).
G. Grunberg, "On the Theory of Operation of Electron Tubes", *Tech. Phys.* (U. S. S. R.), vol. 3, No. 2, p. 181, Feb. (1936).
D. O. North, "Analysis of the Effects of Space Charge on Grid Impedance", *I. R. E. Proc.*, vol. 24, p. 108, Jan. (1936).
W. E. Benham, "A Contribution to Tube and Amplifier Theory," *Proc. I. R. E.*, vol. 26, p. 1093, Sept. (1938).
F. B. Llewellyn and L. C. Peterson, "Vacuum Tube Networks", *Proc. I. R. E.*, vol. 32, p. 144, March (1944).

C. Velocity Modulation Papers

A. Arsenjewa-Heil and O. Heil, "Electromagnetic Oscillations of High Intensity", *Zeits f. phys.*, vol. 95, p. 752, and p. 62, Nov. & Dec. (1935).
(English Translation in *Electronics*, vol. 16, p. 7, July 1943).
E. Bruche and A. Recknagel, "On the Phase Focusing of Electrons in Rapidly Fluctuating Electric Fields", *Zeits f. phys.*, vol. 108, p. 459, March (1938).
W. C. Hahn and G. F. Metcalf, "Velocity-Modulated Tubes" *I. R. E. Proc.*, vol. 27, p. 106, Feb. (1939).
R. H. Varian and S. F. Varian, "A High-Frequency Oscillator and Amplifier", *Jour. Apl. Phys.*, vol. 10, p. 321, May (1939).
W. C. Hahn, "Small Signal Theory of Velocity Modulated Electron Beams", *G-E. Rev.*, vol. 42, p. 258, June (1939).
D. L. Webster, "Cathode Ray Bunching", *Jour. Apl. Phys.*, vol. 10, p. 501, July (1939).
W. C. Hahn, "Wave Energy and Transconductance of Velocity-Modulated Electron Beams", *G-E. Rev.*, vol. 42, p. 497, Nov. (1939).
S. Ramo, "The Electronic Wave Theory of Velocity Modulation Tubes", *Proc. I. R. E.*, vol. 27, p. 757, Dec. (1939).
J. R. Pierce, "Reflex Oscillators", *Proc. I. R. E.*, vol. 33, p. 112, Feb. (1945).

D. Graphical Solutions for Velocity Modulation Tubes

E. Bruche and A. Recknagel, "On the Phase Focusing of Electrons in Rapidly Fluctuating Electric Fields", *Zeits f. Phys.*, vol. 108, p. 459, March (1939).
D. M. Tombs, "Velocity-Modulation Beams", *Wireless Eng.*, vol. 17, p. 54, Feb. (1940).

R. Kompfner, "Velocity Modulation—Results of Further Considerations", *Wireless Eng.*, vol. 17, p. 478, Nov. (1940).
A. E. Harrison, "Graphical Methods for Analysis of Velocity Modulation Bunching", *Proc. I. R. E.*, vol. 33, p. 20, Jan. (1945).

E. Magnetrons

W. E. Benham, "Electronic Theory and the Magnetron", *Proc. Phys. Soc.*, vol. 47, p. 1, Jan. (1935).
K. Posthumus, "Oscillations in a Split Anode Magnetron", *Wireless Eng.*, vol. 12, p. 126, March (1935).
L. Tonks, "Motion of Electrons in Crossed Electric and Magnetic Fields with Space Charge", *Physik Z Sowjet*, vol. 8, p. 572 (1935).
H. Awendu, H. Thoma and M. Tombs, "Paths of Electrons in Magnetrons Taking Account of Space Charge", *Zeits. f. Phys.*, vol. 97, p. 202, Oct. (1935).
W. E. Benham, "Electronic Theory and the Magnetron Oscillator", *Proc. Phys. Soc.*, vol. 47, p. 1, Jan. (1935).
M. Grechowa, "Investigation of the Curve of the Electron Path in a Magnetron", *Tech. Phys. Jour.* (U. S. S. R.), vol. 3, p. 633 (1936).
S. V. Bellustin, "Theory of the Motion of Electrons in Crossed Electric and Magnetic Fields with Space Charge", *Physik Z. Towjel*, vol. 10, p. 251 (1936).
Grunberg and Wolkenstein, "The Influence of a Homogeneous Magnetic Field on the Motion of Electrons Between Coaxial Cylindrical Electrodes", *Tech. Phys. Jour.* (U. S. S. R.), vol. 8, p. 19 (1938).
F. Herringer and F. Hulster, "Oscillations in Tubes with Magnetic Fields", *Hock freq Tech u Elek Akus*, vol. 49, p. 123 (1937).
E. B. Moullin, "Consideration of the Effect of Space Charge in the Magnetron", *Phys. Soc. Proc.*, vol. 36, p. 94, Jan. (1940).
J. P. Blewett and S. Ramo, "High-Frequency Behavior of a Space Charge", *Phys. Rev.*, vol. 57, p. 635, April (1940).
J. P. Blewett and S. Ramo, "Propagation of Electromagnetic Waves in a Space Charge Rotating in a Magnetic Field", *Jour. Appl. Phys.*, vol. 12, p. 856, Dec. (1941).
L. Brillouin, "Practical Results from Theoretical Studies of Magnetrons", *Proc. I. R. E.*, vol. 32 p. 216, April (1944).

Dynamics of Package Cushioning

By RAYMOND D. MINDLIN

Introduction

MECHANICAL damage is a common occurrence in the transportation of packaged articles. The causes of failures are generally inadequate protective cushioning, lack of ruggedness of the outer packing container, or occasional abnormal weakness of the packaged article. The first of these difficulties is the subject of this paper.

One of the major influences in reducing the incidence of mechanical failures of packaged articles in recent years has been the use of the drop test. The drop test is performed simply by raising the package to a specified height and dropping it to the floor. The package and its contents are then examined for damage. This is a go-no-go test and requires a large number of samples before a reliable estimate of quality can be made. An adequate number of tests is prohibitive when the article packaged is costly. In such cases it is important, and in any case it is useful, to supplement the drop test data with measurements and calculations. It is also possible to evolve rational procedures for designing packages, as described in the present paper, so that a particular product will survive a drop test at any specified height, with a known factor of safety and with a minimum amount of space assigned for cushioning. The drop test then becomes only a check instead of playing an integral role in a cut and try design procedure.

Assuming that the outer container is adequate, the survival of a packaged article in a drop test still depends upon a large number of factors descriptive of the mechanical properties of both the cushioning medium and the packaged item. However, the more important properties can be grouped so that they may be replaced by knowledge of only the following factors:

(1) The magnitude of the maximum acceleration that the cushioning permits the packaged item to reach.
(2) The form of the acceleration-time relation.
(3) The strengths, natural frequencies of vibration and damping of the structural elements of the packaged article.

Part I of this paper is concerned primarily with methods for predicting maximum acceleration of the packaged article with emphasis on non-linear cushioning. Part II deals primarily with the prediction of the form of the acceleration-time relation. Part III deals with the effect of acceleration on

the packaged article and gives methods for determining whether or not the strength of the packaged article will be exceeded. The strength determinations themselves are not dealt with here; but the information in Part III is essential in interpreting and applying the data obtained in strength measurements. In Part IV some consideration is given to the influence of distributed mass and elasticity.

It cannot be emphasized too strongly that the determination of the mechanical properties of the packaged article, not dealt with in this paper, is an essential preliminary to a rational design procedure for packaging. The whole purpose in designing package cushioning is to limit the forces which may act on the packaged item. If one does not know to what values to limit the forces, a rational design procedure cannot be applied.

It is interesting to observe that the methods described here for analyzing and designing package cushioning are directly applicable to the design of shock mounts intended to protect equipment from the effects of a sudden change in velocity. All of the principles, formulas and design curves given here may be used in the shock mount problem with the simple substitution of $V^2/2g$ for h, where h is the height of drop in the packaging problem, g is the acceleration of gravity and V is the velocity change in the shock mount problem.

This paper is essentially a report on a study undertaken at the Bell Telephone Laboratories, Inc., in the Electronic Apparatus Development Department. The results have been applied to the packaging of large vacuum tubes and all of the examples used to illustrate the analysis and design procedures in the paper are taken from vacuum tube applications.

Miss H. A. Lefkowitz, Member of the Technical Staff, Bell Telephone Laboratories, assisted in the mathematical studies. The oscillograms, used as illustrations, were prepared under the supervision of Mr. F. W. Stubner, Member of the Technical Staff, Bell Telephone Laboratories. Figure 3.8.2 was taken from a thesis submitted by Mr. C. Ulucay in partial fulfillment of the requirements for the degree of Master of Science in the Department of Civil Engineering at Columbia University. The calculations for Figs. 3.5.1 to 3.5.6 and Fig. 3.2.2 for $\beta_1 > 0$ were performed on the Westinghouse Mechanical Transients Analyzer under the supervision of Dr. G. D. McCann, Transmission Engineer, Westinghouse Electric and Manufacturing Company.

Assumptions

The procedures to be described for the analysis and design of package cushioning are based on applications of a few simple laws of mechanics to an idealized mechanical system representing the package and its contents.

Essentially, a package consists of

1. Elements of the packaged article which are susceptible to mechanical damage.

2a. The packaged article as a whole.

2b. A cushioning medium (excelsior, cardboard spring pads, metal springs, etc.)

3. An outer container (cardboard carton, wood packing case, etc.)

The four major components are illustrated schematically in Fig. 0.2.1. The system is further idealized by "lumping the parameters"; for example, the outer container is considered as a single mass, the cushioning is considered as a massless spring with friction losses. The result of this idealization is to lose some of the fine detail of the real distributed system such as wave propagation through the cushioning and higher modes of vibration in

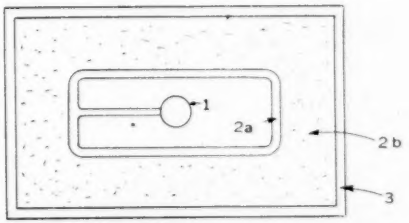

Fig. 0.2.1—Schematic representation of a package.
1. Element of packaged article
2a. Packaged article as a whole
2b. Cushioning
3. Outer container

the package structure and in the packaged article. Some consideration of these details is given in Part IV.

The idealized system is illustrated in Fig. 0.2.2. The major components of the system are as follows:

1. A structural element of the packaged item is represented by a mass (m_1) supported by a linear massless spring with or without velocity damping. The mass m_1 is assumed to be small in comparison with the mass of the whole packaged item.

2a. The whole packaged item is represented by a mass m_2.

2b. The cushioning is represented by a spring which may have a linear or non-linear load-displacement characteristic and which dissipates energy through velocity damping or dry friction. Permanent deformation of the cushioning is not considered, that is, in a repetition of the drop test it is assumed that the package has the same properties as before the first test. A properly designed package will have essen-

tially this characteristic. The mass of the cushioning is assumed to be small in comparison with m_2, except in Section 4.2.

3. The outer container is represented by the mass m_3. The impact of m_3 on the floor is assumed to be inelastic and during contact the relative displacement between m_3 and the initial position of the floor is assumed to be small in comparison with the relative displacement between m_2 and m_3. In other words, no spring action is assigned to the outer container and the floor is considered rigid.

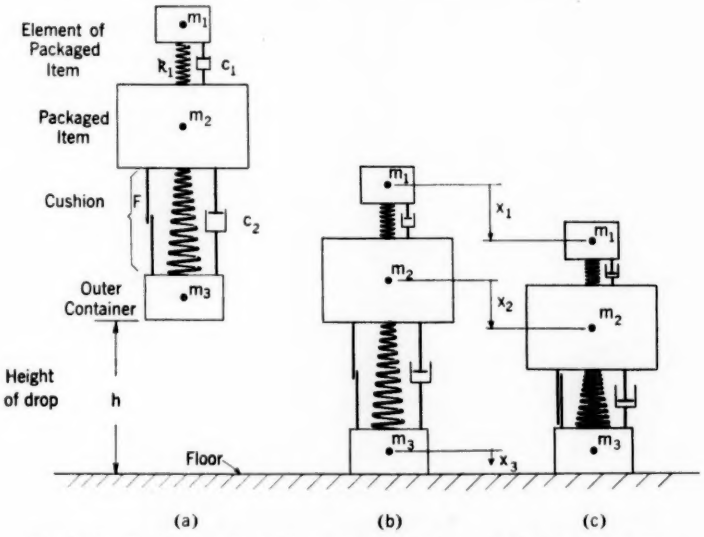

Fig. 0.2.2—Idealized mechanical system representing a package in a drop test.

PART I

MAXIMUM ACCELERATION AND DISPLACEMENT

1.1 Introduction

Most of Part I is concerned with the prediction of the maximum acceleration that the cushioning permits the packaged article (m_2) to attain. In many instances this will be all the information necessary for judging the suitability of a cushioning system. It will be all that is necessary if the shape and scale of the acceleration-time function satisfy certain criteria which are treated in detail in Parts III and IV. If these criteria are satisfied, the effect of the drop on the packaged article is found by multiplying the

dead load stresses (obtained in the usual manner) by the ratio of the maximum acceleration to the acceleration of gravity. If the criteria for the use of maximum acceleration alone are not satisfied, then Parts II and III will supply a numerical factor (the Amplification Factor) by which the maximum acceleration should be multiplied, and the remainder of the procedure is the same as before.

The determination of the maximum acceleration is founded on a knowledge of the load-displacement characteristics of the cushioning. When the cushioning system is simple enough, the load-displacement relation may be found or designed by purely analytical procedures. The tension spring package, discussed in Sections 1.7 and 1.8, is an example where such a treatment is possible. In many instances, as with distributed cushioning, the load-displacement relation is more easily found by test.

A load-displacement test is made by applying successively increasing forces, with weights or in a load testing machine, to the packaged item completely assembled in its package, and measuring the corresponding displacements. The force is applied usually by means of a rod inserted in a hole cut through the outer container and the cushioning to the packaged item. It is convenient to use a low loading rate in the test, and, in doing so, the effect of resisting forces that depend on velocity is lost. These forces are often of little importance but, in certain designs, it is necessary to consider them. This is done for velocity damping in Sections 2.5, 2.6, 3.2 and 3.5.

Most of Part I is concerned with cushioning having non-linear load-displacement characteristics. Linear cushioning is rarely encountered, but it will be treated first because of its simplicity and because it will be convenient later to express the maximum acceleration in non-linear cases in terms of the maximum acceleration in a hypothetical linear case.

1.2 Derivation of Equations of Motion

To introduce the method of analysis that will be used in Part I, the simplest possible system is considered first. The m_1 system is omitted entirely, the mass of the outer container (m_3) is neglected, and the cushioning is assumed to have no damping or friction. There remain only the mass m_2 (the mass of the packaged item alone) and the supporting spring, as shown in Fig. 1.2.1. If the spring is linear its displacement is proportional to the applied load throughout the range of use (see Fig. 1.4.1). The spring rate (k_2) of a linear spring is a constant usually expressed in terms of pounds per inch. The force (P) transmitted through a linear spring is therefore given by

$$P = k_2 x_2, \tag{1.2.1}$$

where x_2 is the displacement of m_2 measured downward from its position at first contact of the spring with the floor (see Fig. 1.2.1). For a non-linear spring P will be some other function of x_2:

$$P = P(x_2). \tag{1.2.2}$$

To write the equation of motion for the mass m_2, we consider the forces acting on it at any instant. These are (see Fig. 1.2.2(b)) the spring force P and the weight $m_2 g$, where g is the acceleration of gravity. When x_2 is positive (i.e., a downward displacement of m_2 from its position at first contact of the spring with the floor) the spring exerts an upward force P

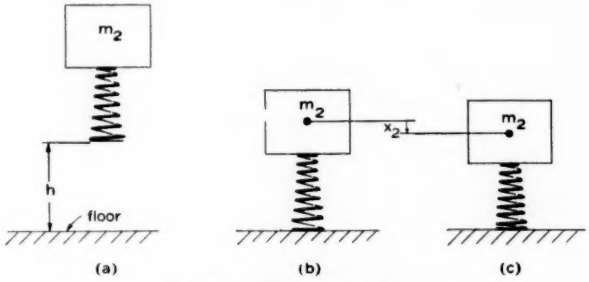

Fig. 1.2.1—Elementary system.

Fig. 1.2.2—Free body diagram for elementary system.
(a) Spring not in contact with floor.
(b) Spring in contact with floor.

on the mass, opposing the weight. The total downward force on m_2 is thus $m_2 g - P$. By the second law of motion, the product of the mass and its acceleration at any instant is equal to the applied force:

$$m_2 \ddot{x}_2 = m_2 g - P, \tag{1.2.3}$$

where the symbol $\ddot{x}_2$, representing the acceleration of m_2, stands for the second derivative of displacement with respect to time (d^2x_2/dt^2). Equation (1.2.3) is the law governing the motion of m_2 as long as the spring is in contact with the floor. When the spring is not in contact with the floor, it can exert no force on the mass so that, in writing the equation of motion that

governs before or after contact, the free-body diagram of Fig. 1.2.2(a) should be used. Then

$$\ddot{x}_2 = g. \tag{1.2.4}$$

Equation (1.2.4) holds (neglecting air resistance) from the instant the package starts to fall until the instant it strikes the floor and from it we can find the package velocity at the instant of first contact. Integrating (1.2.4) with respect to time, we find

$$\dot{x}_2 = gt + A, \tag{1.2.5}$$

where $\dot{x}_2$ is the velocity (dx_2/dt) and A is a constant of integration whose value is found from the initial condition that when $t = 0$ (the instant of release) $\dot{x}_2 = 0$. Thus $A = 0$ and

$$\dot{x}_2 = gt. \tag{1.2.6}$$

Integrating again,

$$x_2 = \tfrac{1}{2} gt^2 + B. \tag{1.2.7}$$

The value of the integration constant B is found from the initial condition that $x_2 = -h$ (the height of drop) when $t = 0$. Hence $B = -h$ and

$$x_2 = \tfrac{1}{2} gt^2 - h. \tag{1.2.8}$$

At the instant of contact, $x_2 = 0$ and, from (1.2.8), the time at first contact is given by $t_0^2 = 2h/g$. Substituting this value of t in (1.2.5) we find, for the velocity at first contact,

$$[\dot{x}_2]_{x_2=0} = \sqrt{2gh}. \tag{1.2.9}$$

We now have the initial conditions for finding the values of the integration constants in the solution of equation (1.2.3), which we proceed to obtain.

First multiply both sides of (1.2.3) by dx_2/dt and write $\ddot{x}_2 = \dfrac{d}{dt}\left(\dfrac{dx_2}{dt}\right)$:

$$m_2 \frac{dx_2}{dt} \frac{d}{dt}\left(\frac{dx_2}{dt}\right) + P \frac{dx_2}{dt} = m_2 g \frac{dx_2}{dt} \tag{1.2.10}$$

or

$$\tfrac{1}{2} m_2 \frac{d}{dt}\left(\frac{dx_2}{dt}\right)^2 + P \frac{dx_2}{dt} = m_2 g \frac{dx_2}{dt}.$$

Multiplying by dt and integrating once:

$$\tfrac{1}{2} m_2 \dot{x}_2^2 + \int^{x_2} P \, dx_2 = \int^{x_2} m_2 g \, dx_2 + C, \tag{1.2.11}$$

where C is a constant of integration whose value is determined by the initial conditions that $\dot{x}_2^2 = 2gh$ and $x_2 = 0$ at the instant of contact. Hence

$$C = m_2 gh + \int^0 P\, dx_2 .$$

Substituting the above value of C in (1.2.11), we have

$$\tfrac{1}{2} m_2 \dot{x}_2^2 + \int_0^{x_2} P\, dx_2 = m_2 g(h + x_2). \tag{1.2.12}$$

It may be observed that (1.2.12) is an energy equation in which the terms have the following meanings:

$\tfrac{1}{2} m_2 \dot{x}_2^2$ is the instantaneous kinetic energy of m_2,

$\int_0^{x_2} P\, dx_2$ is the energy stored in the spring at any instant. It is also equal to the area under the load-displacement curve up to the displacement x_2,

$m_2 g(h + x_2)$ is the potential energy of the mass at its initial height $h + x_2$ above the instantaneous position x_2.

Hence (1.2.12) expresses the law of conservation of energy.

Ordinarily h is very much larger than x_2 so that we may write, with good accuracy,

$$\tfrac{1}{2} m_2 \dot{x}_2^2 + \int_0^{x_2} P\, dx_2 = m_2 gh. \tag{1.2.13}$$

To the same approximation, equation (1.2.3) becomes

$$m_2 \ddot{x}_2 + P = 0. \tag{1.2.14}$$

Equation (1.2.14) and its first integral, equation (1.2.13), are convenient forms for calculating events at any time during contact. Their use will be illustrated in Part II. For calculating only maximum displacement and acceleration, the equations become simpler. Let

W_2 = weight of the packaged article ($= m_2 g$),

d_m = maximum displacement of the packaged article,

G_m = absolute value of maximum acceleration of the packaged article in terms of number of times gravity ($G_m = |\ \ddot{x}_2/g\ |_{\max}$),

P_m = maximum force exerted on packaged article by cushioning.

We shall limit our study to the practical regions where $P > 0$ when $x_2 > 0$. Then it may be seen from (1.2.13) that x_2 is a maximum when $\dot{x}_2$ is zero, hence

$$\int_0^{d_m} P\, dx_2 = W_2 h, \tag{1.2.15}$$

and, from (1.2.14),

$$G_m = \frac{P_m}{W_2}, \tag{1.2.16}$$

where P_m is the maximum value of P. If $P(x_2)$ is a monotonic function, P_m may be obtained from (1.2.2) by substituting d_m for x_2:

$$P_m = P(d_m). \tag{1.2.17}$$

In the unusual case where $P(x_2)$ is not monotonic, the maximum value of P in the interval $0 \leq x_2 \leq d_m$ must be chosen instead of equation (1.2.17).

The general procedure is to calculate d_m from (1.2.15), P_m from (1.2.17) and then G_m from (1.2.16). If P can be expressed analytically in terms of x_2 and if the integral in (1.2.15) can be evaluated in terms of elementary functions, simple formulas can be found for d_m and G_m. If this is not possible, then the integration can be performed graphically or numerically. Both of these procedures will be illustrated. In either case the maximum acceleration and displacement are obtained in terms of the weight of the packaged item, the height of drop and parameters descriptive of the load-displacement characteristics of the cushioning.

1.3 Linear Elasticity

For cushioning with a linear load-displacement relation, equation (1.2.1) applies. Substituting this value of P in (1.2.15), and performing the integration, we find

$$d_m = \sqrt{\frac{2hW_2}{k_2}}. \tag{1.3.1}$$

From (1.3.1) and (1.2.17),

$$P_m = \sqrt{2hW_2k_2}, \tag{1.3.2}$$

and, from (1.3.2) and (1.2.16),

$$G_m = \sqrt{\frac{2hk_2}{W_2}}. \tag{1.3.3}$$

Notice that equation (1.3.3) holds only if there is space available for a displacement d_m and if the cushioning is linear and capable of transmitting a force P_m. Also, from (1.3.3) and (1.3.1),

$$d_m = \frac{2h}{G_m} \tag{1.3.4}$$

and

$$k_2 = \frac{W_2G_m^2}{2h} = \frac{2hW_2}{d_m^2}. \tag{1.3.5}$$

Example: Find the properties of the linear cushioning required so that the maximum acceleration will be 50g in a 3 ft. drop of a 20 lb. article.

From (1.3.4),

$$\text{necessary travel, } d_m = \frac{2 \times 36}{50} = 1.44 \text{ inches.}$$

From (1.3.5),

$$\text{spring rate, } k_2 = \frac{20 \times (50)^2}{2 \times 36} = 694 \text{ lbs/in.}$$

From (1.2.16)

Maximum force $P_m = 20 \times 50 = 1000$ lbs.

1.4 Cushioning with Non-Linear Elasticity

In practice it is rarely that a packaging system has linear spring characteristics. Departure from linearity may be due to

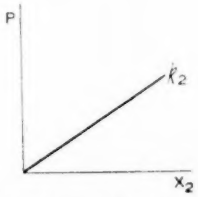

Fig. 1.4.1—Linear elasticity. Class A.

1. Non-linear geometry, such as in the tension spring package described in Section 1.7.

2. Non-linear characteristics of distributed cushioning materials such as excelsior and rubber.

3. Abrupt change of stiffness such as occurs if the packaged item can strike the wall of the container.

For the purpose of developing design formulas it is desirable to have analytical functions to represent load-displacement characteristics. It is not feasible to have only one family of functions with adjustable parameters to fit all possible shapes of load-displacement curves. Therefore, all the practical shapes have been divided into six general classes, most of which are associated with simple functions having one or two adjustable parameters. The six classes are as follows:

Class A—Linear Elasticity. This has already been treated. Its load-displacement function is

$$P = k_2 x_2. \tag{1.4.1}$$

Class B—Cubic Elasticity. This includes cushioning which does not bottom in the anticipated range of use, but the slope of the load-displacement function generally increases with increasing displacement as in the curved full line of Fig. 1.4.2. A suitable load-displacement function is

$$P = k_0 x_2 + r x_2^3 . \tag{1.4.2}$$

k_0 is the initial spring rate of the cushioning, as shown by the slope of the dashed straight line in Fig. 1.4.2, and r determines the rate of increase of the spring rate. The same function can be used if the slope of the curve decreases gradually with increasing load as shown by the curved dashed line in Fig. 1.4.2. In this case the parameter r is negative.

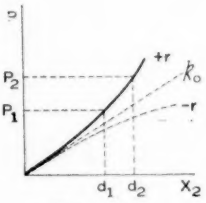

Fig. 1.4.2

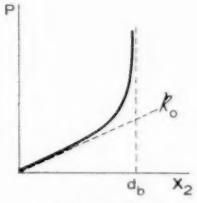

Fig. 1.4.3

Fig. 1.4.2—Cubic elasticity. Class B.
Fig. 1.4.3—Tangent elasticity. Class C.

Class C—Tangent Elasticity. Cushioning that bottoms, but not very abruptly, can be represented by the load-displacement function

$$P = \frac{2k_0 d_b}{\pi} \tan \frac{\pi x_2}{2d_b} . \tag{1.4.3}$$

Referring to Fig. 1.4.3, k_0 is the initial spring rate and d_b is the maximum available displacement. The figure shows how the stiffness of the cushioning (i.e., the slope of the curve) increases as the displacement approaches the maximum available (d_b) at hard bottoming. The shape of the curve is typical of load-displacement curves for a great variety of packages with distributed cushioning.

Figure 1.4.7 illustrates the wide variety of shapes of non-linear cushioning characteristics that can be obtained with the single function given by equation (1.4.3) simply by varying the parameter k_0; and a similar set is given by each value of d_b. Although these families of curves do not include all possible shapes, one of them can usually be found to fit a practical shape for cushioning of this class over the anticipated range of use.

Class D—Bi-linear Elasticity. This is characterized by a load-displace-

ment curve consisting of two straight line segments. The load displacement function is (see Fig. 1.4.4)

$$\left.\begin{aligned} P &= k_0 x_2 \qquad 0 \leqq x_2 \leqq d_s \\ P &= k_b x_2 - (k_b - k_0) d_s \quad x_2 \geqq d_s \end{aligned}\right\}. \tag{1.4.4}$$

It is useful especially in situations where very abrupt bottoming is possible.

Class E—Hyperbolic Tangent Elasticity. When the mechanism of the cushioning is such as to limit the maximum force that can be transmitted over a considerable displacement range, the load-displacement function

$$P = P_0 \tanh \frac{k_0 x_2}{P_0} \tag{1.4.5}$$

is useful. P_0 is the asymptotic value of the force and k_0 is the initial spring rate (see Fig. 1.4.5).

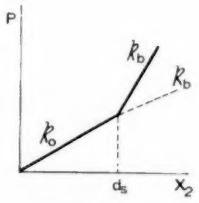

Fig. 1.4.4

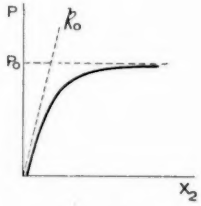

Fig. 1.4.5

Fig. 1.4.4—Bi-linear elasticity. Class D.
Fig. 1.4.5—Hyperbolic tangent elasticity. Class E.

Class F—Anomalous Elasticity. In occasional instances the load-displacement curve of the cushioning cannot be matched accurately enough by any of the five preceding functions. In such cases a numerical integration procedure can be used, as described in Section 1.15.

1.5 Cushioning with Cubic Elasticity (Class B)

Substituting (1.4.2) in (1.2.15) and performing the integration, we have:

$$\frac{k_0 d_m^2}{2} + \frac{r d_m^4}{4} = W_2 h. \tag{1.5.1}$$

Now, let

$$d_0 = \sqrt{\frac{2W_2 h}{k_0}}, \tag{1.5.2}$$

that is, d_0 is the displacement that would take place if the elasticity were linear (see equation (1.3.1)) with a constant spring rate k_0 equal to the initial spring rate of the cubic elasticity. Also let

$$B = \frac{4W_2 hr}{k_0^2}. \tag{1.5.3}$$

Then, from (1.5.1), (1.5.2) and (1.5.3)

$$\frac{d_m}{d_0} = \sqrt{\frac{2}{B}(-1 + \sqrt{1 + B})}. \tag{1.5.4}$$

Equation (1.5.4) is plotted in Fig. 1.5.1 which shows graphically how the maximum displacement d_m compares with the "equivalent linear displacement d_0" as the parameter B is varied. Note that B depends on the weight of the packaged item, the height of drop and the shape of the load displacement curve (as determined by k_0 and r).

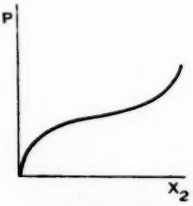

Fig. 1.4.6—Anomalous elasticity. Class F.

Similarly we can compare the maximum acceleration G_m with the maximum (G_0) that would obtain if the load displacement curve were linear with spring rate k_0. The latter acceleration is given by

$$G_0 = \sqrt{\frac{2hk_0}{W_2}} \tag{1.5.5}$$

and the former is obtained by finding P_m from (1.2.17) and then, from (1.2.16),

$$\frac{G_m}{G_0} = \sqrt{\frac{2}{B}(1 + B)(-1 + \sqrt{1 + B})}. \tag{1.5.6}$$

Equation (1.5.6) is plotted in Fig. 1.5.2.

1.6 Procedure for Finding Maximum Acceleration and Displacement for Cushioning with Cubic Elasticity

If the load-displacement curve of a cushioning system has the general appearance of Fig. 1.4.2 (where the slope increases or decreases gradually

with displacement) the following procedure may be used for estimating the effectiveness of the cushioning.

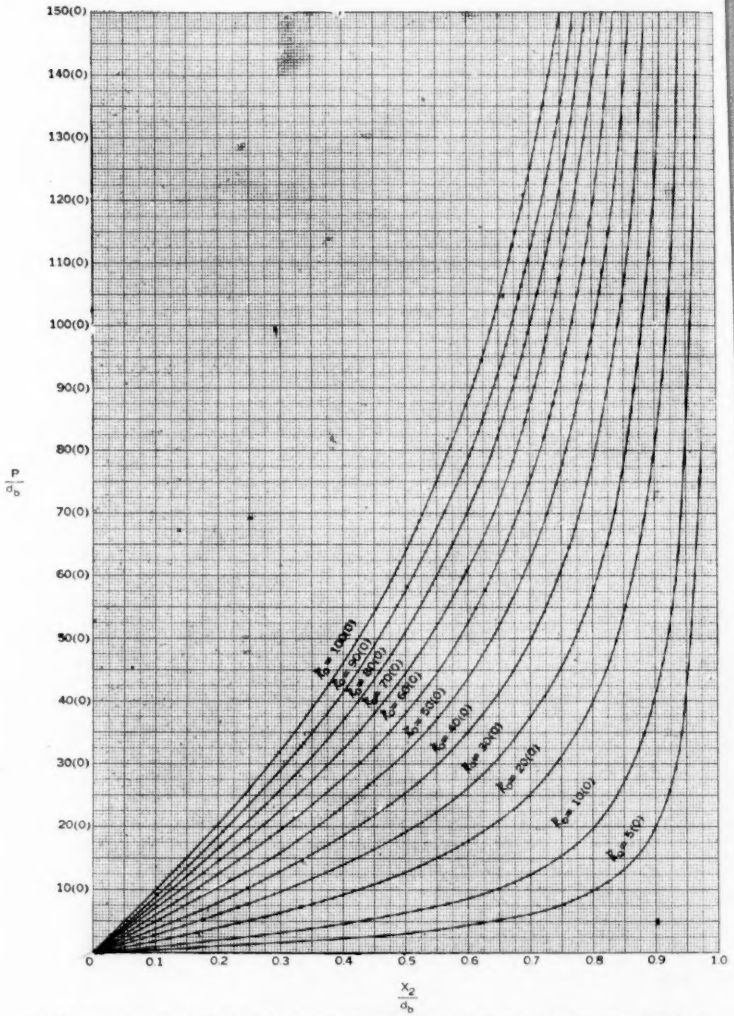

Fig. 1.4.7—Family of load displacement curves for cushioning with tangent elasticity.

a. Select the point on the load-displacement curve for which the load is equal to the weight of the packaged item multiplied by the allowable G_m. Call this load P_2 and the corresponding displacement d_2.

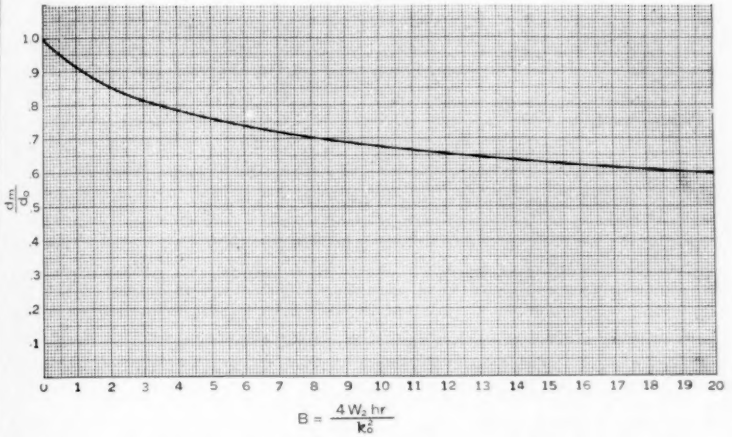

Fig. 1.5.1—Maximum displacement for cushioning with cubic elasticity. See equation (1.5.4).

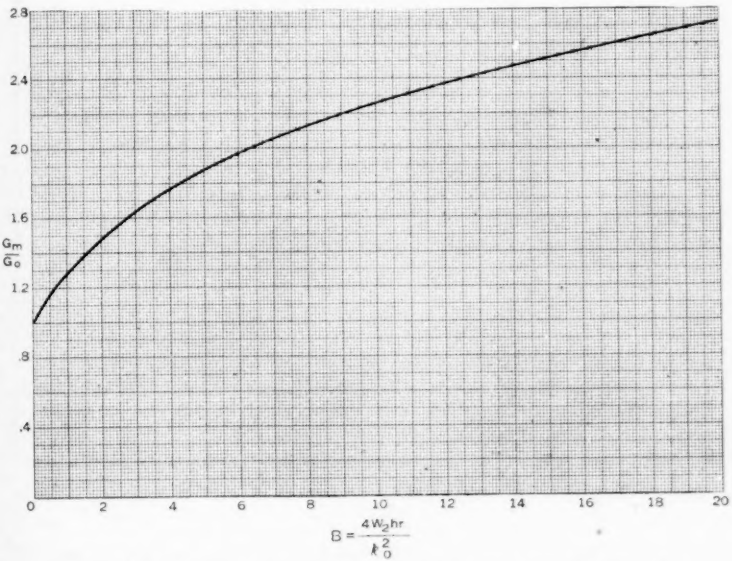

Fig. 1.5.2—Maximum acceleration for cushioning with cubic elasticity. See equation (1.5.6).

b. Select another point (d_1, P_1) about half way toward the origin from (d_2, P_2). See Fig. 1.4.2.

c. Calculate

$$k_0 = \frac{\frac{P_1}{d_1} d_2^2 - \frac{P_2}{d_2} d_1^2}{d_2^2 - d_1^2} \tag{1.6.1}$$

and

$$r = \frac{\frac{P_2}{d_2} - \frac{P_1}{d_1}}{d_2^2 - d_1^2}. \tag{1.6.2}$$

d. Using the known weight, W_2, of the packaged item, the specified height of drop h, and k_0 and r from (1.6.1) and (1.6.2), calculate B, d_0 and G_0 from (1.5.2), (1.5.3) and (1.5.5). Then calculate the maximum acceleration G_m and maximum displacement d_m from (1.5.6) and (1.5.4) or find their values from Figs. 1.5.1 and 1.5.2.

Example: A large vacuum tube, weighing 22.5 lbs, was packed in a 7″ x $7\frac{3}{4}$″ x 15″ carton which was supported on corrugated cardboard spring pads in a $10\frac{1}{2}$″ x $11\frac{1}{2}$″ x $18\frac{1}{2}$″ carton. The latter was, in turn, packed in 28 pounds of excelsior in a 25″ x 25″ x 30″ carton. The tube is rated at 50g and the package is intended for a drop of three feet.

A rod was inserted through a hole cut through the three cartons to the tube. Load was applied to the rod and the displacement of the tube was measured. The data obtained were

P (load in lbs)	x_2 (displacement in inches)
0	0
100	$\frac{5}{16}$
200	$\frac{5}{8}$
300	$\frac{7}{8}$
400	$1\frac{1}{16}$
500	$1\frac{3}{16}$
600	$1\frac{3}{8}$
700	$1\frac{1}{2}$
800	$1\frac{9}{16}$
900	$1\frac{5}{8}$
1000	$1\frac{3}{4}$
1100	$1\frac{13}{16}$
1200	$1\frac{7}{8}$
1300	$1\frac{15}{16}$
1400	2

The data are plotted in Fig. 1.6.1. The resulting curve is suitable for classification as either Class B or Class C cushioning. Considering it, for the present, as Class B, we take $P_2 = 22.5 \times 50 = 1225$, and from the curve, $d_2 = 1.9$ inches. Also, from the curve, take $d_1 = 1$ inch and $P_1 = 365$

lbs. Substituting these values in (1.6.1) and (1.6.2), we find $k_0 = 255$ and $r = 108$. Then

$$B = \frac{4W_2hr}{k_0^2} = \frac{4 \times 22.5 \times 36 \times 108}{(255)^2} = 5.4,$$

$$G_0 = \sqrt{\frac{2hk_0}{W_2}} = \sqrt{\frac{2 \times 36 \times 255}{22.5}} = 28.6.$$

Entering Fig. 1.5.2 with $B = 5.4$ we find $G_m/G_0 = 1.9$. Hence

$$G_m = 28.6 \times 1.9 = 55$$

This is close enough to the 50g rating of the tube to call the cushioning safe insofar as maximum acceleration is concerned.

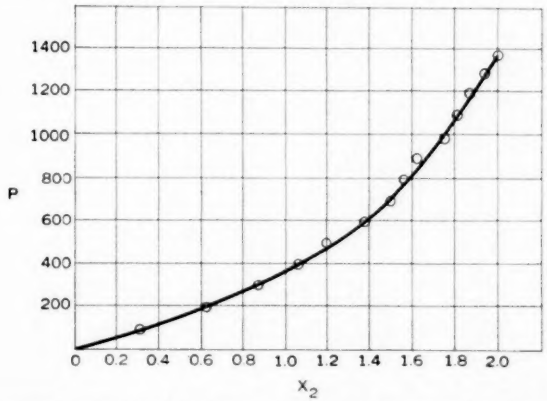

Fig. 1.6.1—Experimental load-displacement curve for a corrugated cardboard spring pad and excelsior cushion.

The maximum displacement, obtained by entering Fig. 1.5.1 with $B = 5.4$ and finding $d_m/d_0 = 0.75$. Then $d_m = 0.75 \times 2h/G_0 = 1.95$ inches. Hence, the package is much larger than necessary since approximately 8 inches of cushioning thickness is supplied to accommodate 2 inches of displacement.

1.7 The Tension-Spring Package (Class B)

The tension spring package is useful when the allowable G_m is so small and height of drop so great that a large displacement (say $d_m >$ several inches) is required. The decision as to whether or not a tension spring package is indicated may be made on the basis of a preliminary estimate of displacement based on the linear case. Suppose the height of drop is to be 60 inches and the allowable acceleration for the packaged item is

$20g$. Then, from Equation 1.3.4, the approximate displacement that will be required is

$$d_m = \frac{2 \times 60}{20} = 6 \text{ inches.} \tag{1.7.1}$$

The actual maximum displacement in a tension spring package will prove to be somewhat more than 6 inches, but the preliminary calculation shows the displacement to be large enough to warrant the use of this type of cushioning.

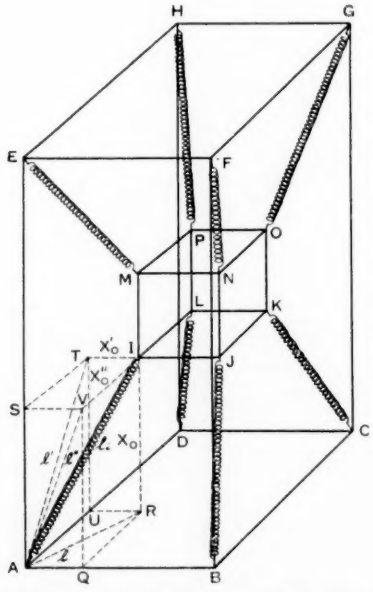

Fig. 1.7.1—Schematic diagram of a tension spring package.

A schematic diagram of a typical tension spring package is shown in Fig. 1.7.1 and a photograph of one design is given in Fig. 1.7.2. The packaged item is suspended on eight identical helical tension springs which diverge to the outer frame. The analysis and design procedures described in this and the following section apply equally well if the springs *converge* from the packaged item to the outer frame. With a slight modification, indicated in the next section, the procedure also applies if four of the springs (say, BJ, DL, EM, OG in Fig. 1.7.1) are omitted.

In all cases, however, we shall consider only systems having reflected symmetry about each of three mutually perpendicular planes through the center of gravity of the packaged article.

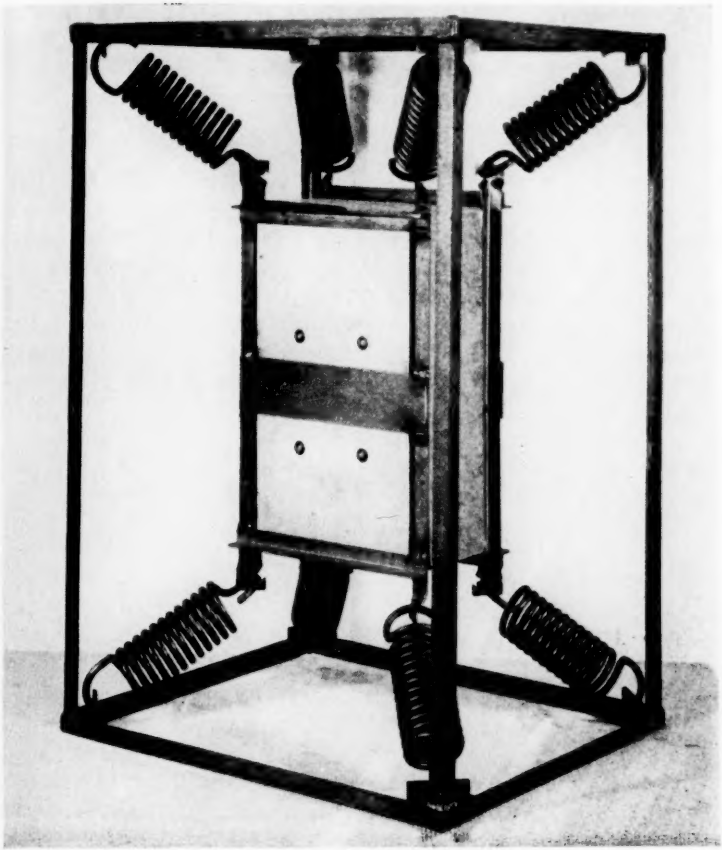

Fig. 1.7.2—A tension spring package.

The load-displacement characteristics of the spring system may be found by statical considerations. We shall examine, first, the displacement in the vertical direction in Fig. 1.7.1, using the following notations:

P = force applied to the suspended object,

x_2 = displacement of suspended object,

x_0 = perpendicular distance (IR, Fig. 1.7.1) from inner spring support point (I, Fig. 1.7.1) to nearest plane, perpendicular to displacement direction and containing four outer spring support points (A, B, C, D, Fig. 1.7.1);

ℓ_s = distance (IA) between spring support points when suspended article is in equilibrium position,
ℓ = projection of ℓ_s on plane $ABCD$,
f = ℓ minus length (between hooks) of unstretched spring,
k = spring rate of each spring.

Consider, first, the action of one pair of springs, say EM and GO of Fig. 1.7.1, independent of the remainder of the suspension. Since EM and GO lie in parallel vertical planes and the points M and O remain in the initial planes of their respective springs during a vertical displacement, the two springs may be considered to lie in the same plane, and to be translated horizontally in this plane so that their outer ends are separated by a distance 2ℓ. Hence Fig. 1.7.3 may be used to represent the independent action of this pair of springs and it is required to find the force Q' needed to transform Fig. 1.7.3(a) to Fig. 1.7.3(b). Initially there are two springs, each of length $\ell - f$

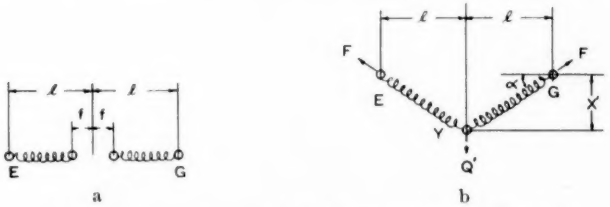

Fig. 1.7.3—Diagram used in discussion of tension spring package.

and spring constant k, with no initial tension in them. One end of one spring is fixed at point E and one end of the other spring is fixed at a point G distant 2ℓ from E. The springs are then stretched so that the two initially free ends are located at a point Y equidistant from E and G and distant x_2' from line EG. The axis of each spring makes an angle α with EG, where

$$\sin \alpha = \frac{x_2'}{\sqrt{\ell^2 + x_2'^2}}. \tag{1.7.2}$$

In this state the axial force F in each spring is

$$F = k[\sqrt{\ell^2 + x_2'^2} - \ell + f] \tag{1.7.3}$$

and the force Q', required to equilibrate the two forces F is $2F \sin \alpha$. Considering the force Q' as a function of the displacement x_2', we write

$$Q'(x_2') = \frac{2x_2'k}{\sqrt{\ell^2 + x_2'^2}}[\sqrt{\ell^2 + x_2'^2} - \ell + f] \tag{1.7.4}$$

or
$$Q'(z') = 2k\ell\left[z' + \frac{(1-b)z'}{\sqrt{1+z'^2}}\right] \tag{1.7.5}$$

where
$$z' = \frac{x_2'}{\ell}, \qquad b = \frac{f}{\ell}.$$

Consider, next, the configuration shown in Fig. 1.7.4(a), where one end of each of four springs is fixed at a corner of a rectangle of length 2ℓ and width $2x_0$. Each spring is again of length $\ell - f$. The four free ends of the springs are drawn together at a common point X at the center of the rectangle (see Fig. 1.7.4(b)). The system is in equilibrium in this position. A force Q is then applied at X in the plane of the rectangle and normal to the side 2ℓ.

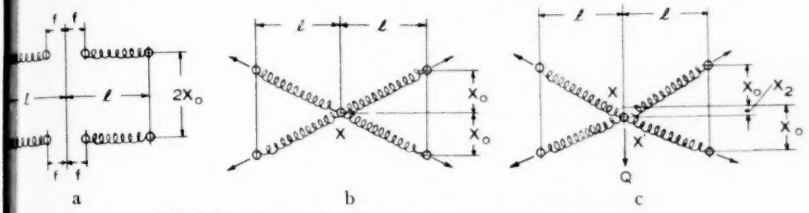

Fig. 1.7.4—Action of springs in a tension spring package.

The common point X is displaced a distance x_2 to X' (see Fig. 1.7.4(c)). Writing $z = x_2/\ell$, $a = x_0/\ell$, we observe that

$$Q(z) = Q'(z + a) + Q'(z - a), \tag{1.7.6}$$

or, from equation (1.7.5),

$$Q(z) = 2k\ell\left\{2z - (1-b)\left[\frac{z+a}{\sqrt{1+(z+a)^2}} + \frac{z-a}{\sqrt{1+(z-a)^2}}\right]\right\}. \tag{1.7.7}$$

The standard tension spring package has two sets of four springs so that the force P required to displace the common point X a distance x_2 is

$$P(z) = 2Q(z). \tag{1.7.8}$$

If x_2 is small in comparison with ℓ (i.e., z is small in comparison with unity), equation (1.7.8) may be written approximately as

$$P(z) = 4k\ell\left[2z - \frac{(1-b)z(2-z^2)}{(1+a^2)^{3/2}}\right]. \tag{1.7.9}$$

Even when x_2 becomes almost as large as ℓ, equation (1.7.9) has been found, experimentally, to be remarkably accurate.
Writing

$$K = 8k\left[1 - \frac{1-b}{(1+a^2)^{3/2}}\right] \tag{1.7.10}$$

and

$$c = \frac{(1 + a^2)^{3/2}}{1 - b} - 1, \tag{1.7.11}$$

equation (1.7.9) becomes

$$P = K\ell\left(z + \frac{z^3}{2c}\right). \tag{1.7.12}$$

It is seen, by comparison with (1.4.2) that this is Class B cushioning (cubic elasticity). K is the initial spring rate and c determines the rate of increase of stiffness with displacement. With the notation k_0, r of Section 1.5, we see that

$$k_0 = K \tag{1.7.13}$$

$$r = \frac{K}{2c\ell^2}. \tag{1.7.14}$$

Hence equations (1.5.6) and (1.5.4) may again be used to calculate maximum acceleration and displacement. B has the same meaning as before (Eq. 1.5.3).

To predict the performance, in the vertical direction (Fig. 1.7.1), of an existing tension spring package the same procedure as outlined in Section 1.6 may be used, except that it is not necessary to have a load-displacement curve for calculating k_0 and r. Instead, these parameters may be calculated directly from equations (1.7.10), (1.7.11), (1.7.13) and (1.7.14). The remainder of the procedure is the same as in Section 1.6(d).

To predict the performance perpendicular to another face, say $AEHD$ of Fig. 1.7.1, it is only necessary, in the calculation of k_0 and r, to substitute x_0' for x_0, ℓ' for ℓ (see Fig. 1.7.1) and, in place of b:

$$b' = 1 - \frac{\ell}{\ell'}(1 - b). \tag{1.7.15}$$

The initial spring rate K for any direction of acceleration may be calculated from the initial spring rates K_1, K_2, K_3 in the three directions normal to the faces of the frame by using the relation

$$\frac{1}{K^2} = \frac{s^2}{K_1^2} + \frac{t^2}{K_2^2} + \frac{u^2}{K_3^2}, \tag{1.7.16}$$

where s, t, u are the direction cosines of the acceleration direction with respect to the normals to the faces of the frame. It is seen, from (1.7.16), that the spring rate is given by the radius to the surface of an ellipsoid whose principal semi-axes are K_1, K_2, K_3.

The displacement direction does not necessarily coincide with the acceleration direction. The angle θ between them is given by

$$\cos\theta = K\left[\frac{s^2}{K_1} + \frac{t^2}{K_2} + \frac{u^2}{K_3}\right] \tag{1.7.17}$$

where K is defined by equation (1.7.16).

The spring characteristics may be made the same in all directions and the displacement direction may be made to coincide with the acceleration direction by setting

$$x_0 = x_0' = x_0'' = \frac{\ell}{\sqrt{2}}$$

and

$$\ell = \ell' = \ell''$$

(see Fig. 1.7.1). This makes $b = b' = b''$, $c = 0.828$ and $k/K = 0.274$ in the calculations of the next section.

1.8 Procedure for Designing Tension Spring Packages

The design of a tension spring package, as contrasted with the analysis of one, must proceed without initial knowledge of values for the parameters k_0 and r, since these cannot be known until the springs are designed. Therefore equations (1.5.4) and (1.5.6) cannot be used directly. For design purposes they are transformed to the following set of formulas:

$$\sqrt{c} = \sqrt{\frac{(1+a^2)^{3/2}}{1-b} - 1} \tag{1.8.1}$$

$$L = \frac{h}{\sqrt{c}\,\ell G_m} = \frac{1}{8}\sqrt{(\sqrt{N}+\sqrt{N+8})^2 + \frac{16}{N}} \tag{1.8.2}$$

$$\frac{d_m}{\sqrt{c}\,\ell} = \sqrt{2(-1+\sqrt{1+B})} \tag{1.8.3}$$

$$M^2 = N = \frac{W_2 G_m^2}{2hK} = \frac{2}{B}(1+B)(-1+\sqrt{1+B}) \tag{1.8.4}$$

$$\frac{e}{\ell} - b = -1 + \sqrt{1 + \frac{d_m + x_0}{\ell}}. \tag{1.8.5}$$

These formulas have been converted to design curves which are given in Figs. 1.8.1 to 1.8.5. The curves are for use in connection with the following routine procedure which has been found useful in designing the springs for tension spring packages. Reference should be made to Table I.

1. Enter, on Line 1, Table I, the weight (W_2) in pounds, of the suspended item. This includes the weight of the cradle or other holding arrangement and one-third the estimated weight of the springs.

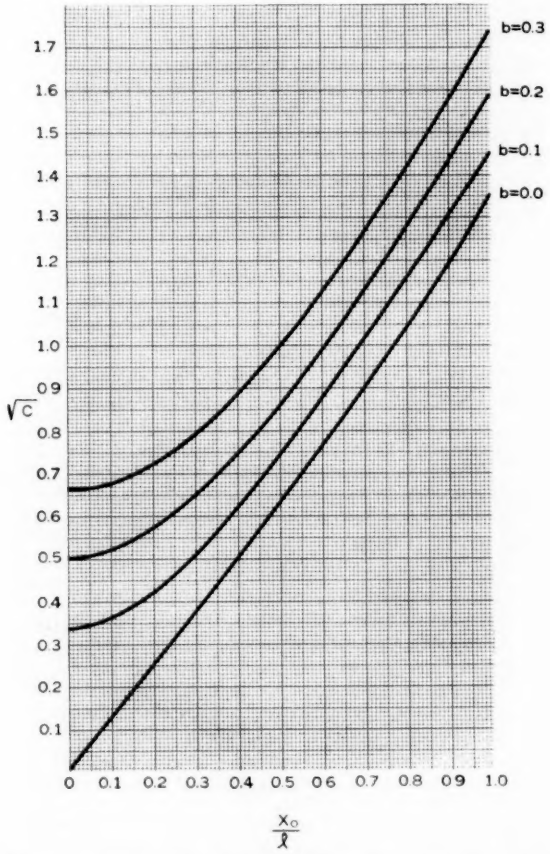

Fig. 1.8.1—Tension spring package design curve. Equation (1.8.1).

2. Enter, on Line 2, the height of drop (h) in inches.
3. Enter, on Line 3, the maximum allowable acceleration (G_m) in units of "number of times gravity." This should be determined beforehand from tests on the item to be packaged.
4. Enter, on Line 4, the dimension x_0 (inches).

5. Enter, on Line 5, the dimension ℓ (inches). For a package to have the same spring rate in all directions, $\ell = x_0\sqrt{2}$ is a necessary condition.
6. Enter, on Line 6, the value chosen for b. As b becomes greater than zero, the stiffness of the whole suspension increases for a given stiffness of individual springs. The reverse happens for b less than zero.

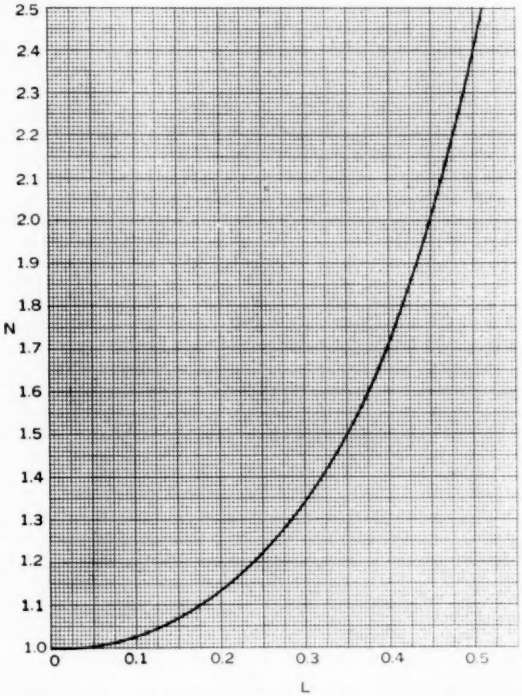

Fig. 1.8.2—Tension spring package design curve. Equation (1.8.2).

7. Calculate x_0/ℓ.
8. Enter Fig. 1.8.1 with x_0/ℓ and find $\sqrt{c}$.
9. Calculate $L = h/(\sqrt{c}\,\ell G_m)$.
10. Enter Fig. 1.8.2 with L and find N.
11. Calculate $K = (W_2 G_m^2)/(2hN)$. This is the initial spring rate of the suspension in the direction of x_0.
12. Calculate $f = 3.13\,(K/W_2)^{\frac{1}{2}}$. This is the natural frequency of vibration (cycles per second) of the suspension for small amplitudes in the x_0 direction. This should not be close to the natural frequency of

vibration of any element in the packaged item, which should be determined by test beforehand (see, also, Section 4.2). *In any case it is advisable to provide damping for the suspension.*

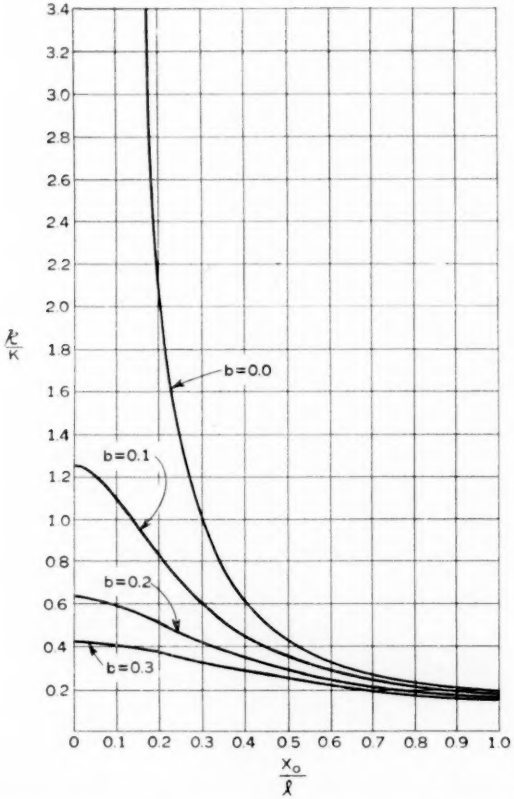

Fig. 1.8.3—Tension spring package design curve. Equation (1.7.10).

13. Enter Fig. 1.8.3 with x_0/ℓ and find k/K. If a four-spring package is desired, instead of an eight-spring package, (see Section 1.7) the value of k/K found on Fig. 1.8.3 should be multiplied by two before entering it on Line 13 in Table I. This is the only change required in the procedure.

14. Calculate $k = K\left(\frac{k}{K}\right)$. This is the spring rate of each of the springs in pounds per inch.

15. Calculate $B = (2W_2h)/(Kc\ell^2)$.
16. Enter Fig. 1.8.4(a) or (b) with B and find $d_m/(\sqrt{c}\,\ell)$.
17. Calculate $d_m/\ell = \sqrt{c}\cdot d_m/\sqrt{c}\,\ell$.
18. Calculate $d_m = \ell\cdot d_m/\ell$.
19. Calculate $(d_m/\ell) + (x_0/\ell)$.

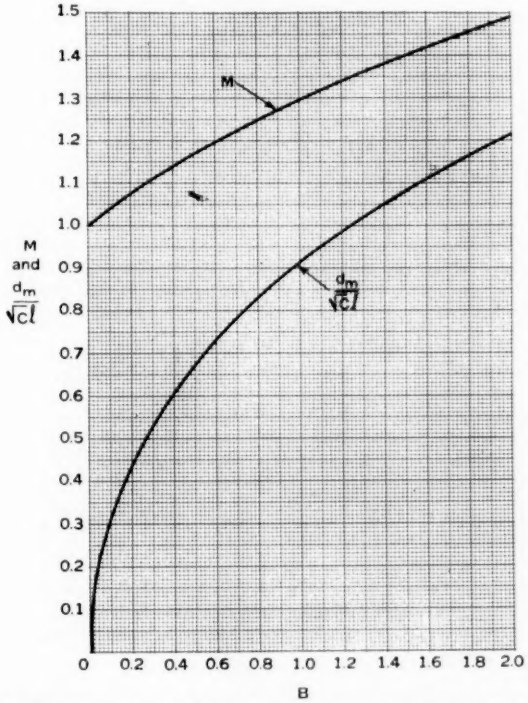

Fig. 1.8.4(a)—Tension spring package design curve. Equations (1.8.3) and (1.8.4).

20. Enter Fig. 1.8.5 with $(d_m/\ell) + (x_0/\ell)$ and find $(e/\ell) - b$. e is the stretch of each spring (in inches) when the displacement is d_m inches.
21. Calculate $F_m = k\cdot(e/\ell)\cdot\ell$. This is the maximum load (in pounds) on each spring.

22, 23, 24, 25, 26. These are the coil diameter, wire diameter, number of turns, fiber stress and length of coils. These quantities are calculated from the ordinary formulas, charts or slide rules for helical springs, using the values of k and F_m from Lines 14 and 21.

27. The length inside hooks is entered on Line 27 to group all of the spring specifications.

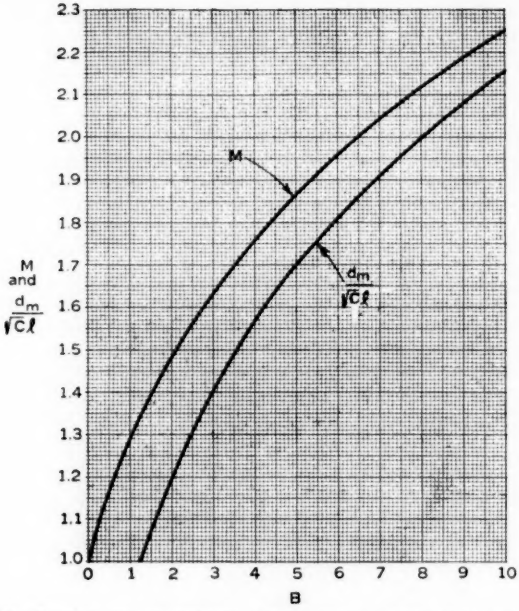

Fig. 1.8.4(b)—Tension spring package design curve. Equations (1.8.3) and (1.8.4).

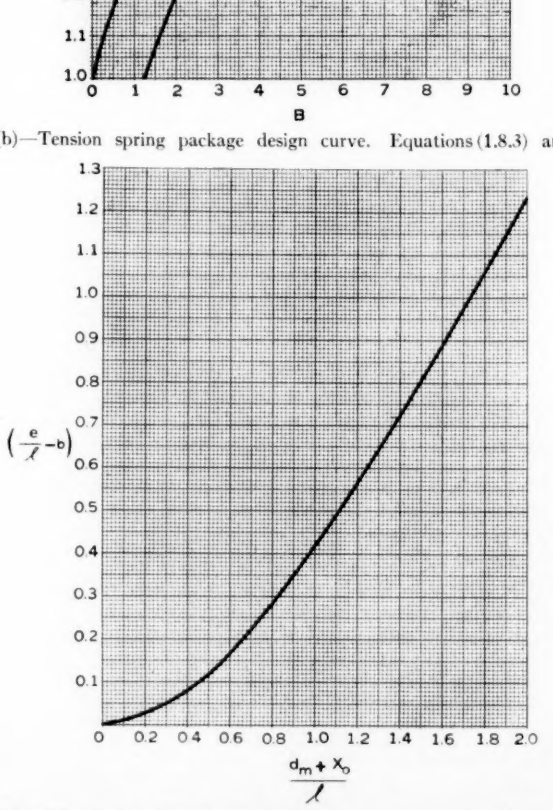

Fig. 1.8.5—Tension spring package design curve. Equation (1.8.5).

As an example of the calculations, Table I contains the entries for the design of springs for a 21 pound article (including $\frac{1}{3}$ the estimated spring weight) which is to be packaged so as not to exceed $35g$ in a five-foot drop.

TABLE I

Computation Form for Tension Spring Packages

1. W_2 (lbs.)	21
2. h (ins.)	60
3. G_m	35
4. x_0 (ins.)	5
5. ℓ (ins.)	7.07
6. b	0
7. Calc. x_0/ℓ	0.707
8. Find $\sqrt{c}$ from Fig. 1.8.1	0.91
9. Calc. $h/\sqrt{c}\,\ell G_m = L$	0.269
10. Find N from Fig. 1.8.2	1.265
11. Calc. $W_2G_m^2/2hN = K$ (lbs/in.)	169.0
12. Calc. $f = 3.13\ (K/W_2)^{\frac{1}{2}}$ (cyc./sec.)	8.9
13. Find k/K from Fig. 1.8.3	0.274
14. Calc. $k = K \cdot k/K$ (lbs/in.)	46.5
15. Calc. $B = 2W_2h/Kc\ell^2$	0.368
16. Find $d_m/\sqrt{c}\,\ell$ from Fig. 1.8.4	0.575
17. Calc. $d_m/\ell = \sqrt{c} \cdot d_m/\sqrt{c}\ell$	0.518
18. Calc. $d_m = \ell \cdot d_m/\ell$ (ins.)	3.68
19. Calc. $d_m/\ell + x_0/\ell$	1.220
20. Find e/ℓ from Fig. 1.8.5 and line 6	0.580
21. Calc. $F_m = k \cdot e/\ell \cdot \ell$ (lbs)	191.0
22. Coil diameter (ins.)	1.40
23. Wire diameter (ins.)	0.207
24. Number of turns	19
25. Fiber Stress (lbs./sq. in.) $\cdot\ 10^{-3}$	80
26. Length of Coils (ins.)	3.93
27. Length inside hooks (ins.)	7.07

1.9 Cushioning with Tangent Elasticity (Class C)

This is one of the most frequently encountered classes of cushioning since it includes a very common type of bottoming (Figs. 1.4.3 and 1.4.7). The load-displacement function (equation (1.4.3)) takes into account the fact that the cushioning can be compressed only to a definite amount d_b.

To find formulas for maximum acceleration and displacement, we proceed as follows. Substitute equation (1.4.3) in (1.2.15) and perform the integration, obtaining

$$\frac{4k_0d_b^2}{\pi^2}\log\cos\frac{\pi d_m}{2d_b} = -W_2h, \tag{1.9.1}$$

which may be written as

$$\tan\frac{\pi d_m}{2d_b} = \sqrt{\exp\left(\frac{\pi^2 W_2 h}{2k_0 d_b^2}\right) - 1}\,. \tag{1.9.2}$$

Equation (1.9.2) can then be substituted into (1.4.3) to obtain the maximum force P_m in accordance with (1.2.17):

$$P_m = \frac{2k_0 d_b}{\pi} \sqrt{\exp\left(\frac{\pi^2 W_2 h}{2k_0 d_b^2}\right) - 1}. \tag{1.9.3}$$

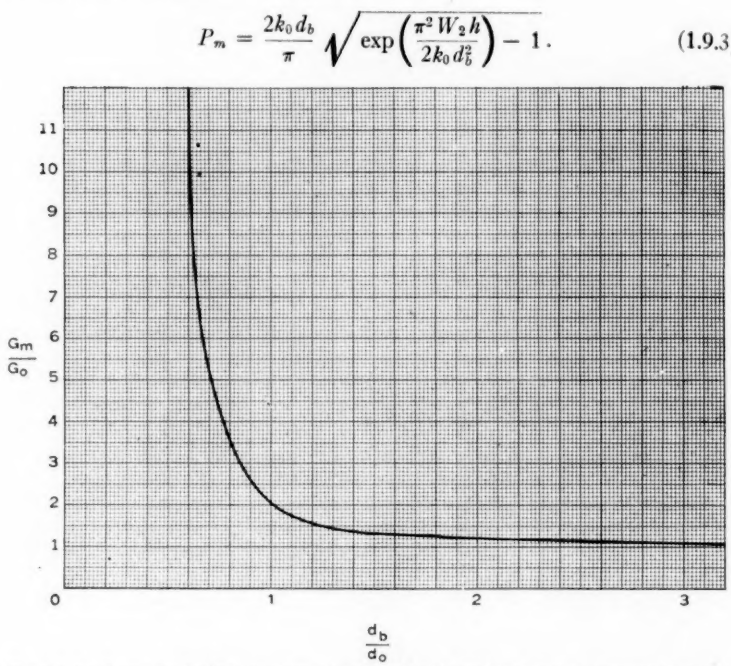

Fig. 1.9.1—Curve for finding maximum acceleration for cushioning with tangent elasticity. See equation (1.9.4).

The maximum acceleration is then obtained from (1.2.16) and may be written in the form

$$\frac{G_m}{G_0} = \frac{2d_b}{\pi d_0} \sqrt{\exp\left(\frac{\pi d_0}{2d_b}\right)^2 - 1}, \tag{1.9.4}$$

where d_0 and G_0 are defined just as in (1.5.2) and (1.5.5). G_0 is the maximum acceleration that would obtain if the cushioning did not bottom, that is, if the spring rate remained constant at its initial value k_0. d_0 is the maximum displacement that would be reached under the same linear conditions. Hence G_m/G_0 is a multiplying factor to be applied to a hypothetical linear cushioning to take into account the effect of bottoming. The multiplying factor depends only on the ratio (d_b/d_0) of the amount of space actually available to the amount of space that would be used under linear conditions.

The ratio G_m/G_0 is plotted against the ratio d_b/d_0 in Fig. 1.9.1. It may be seen that the multiplying factor increases very rapidly as the displacement ratio (d_b/d_0) falls below unity. For example, if the cushioning, with tangent elasticity, reaches hard bottoming (d_b) when only 80% of the required displacement (d_0) is attained, the acceleration is multiplied by 3.5; if only 60% of the required displacement is available, the acceleration is multiplied by 11.5.

Example: To illustrate with a numerical example, consider the case already discussed in Section 1.3, where we found that a spring rate of 694 lbs/in and a displacement of 1.44 inches were required to limit a 20-pound article

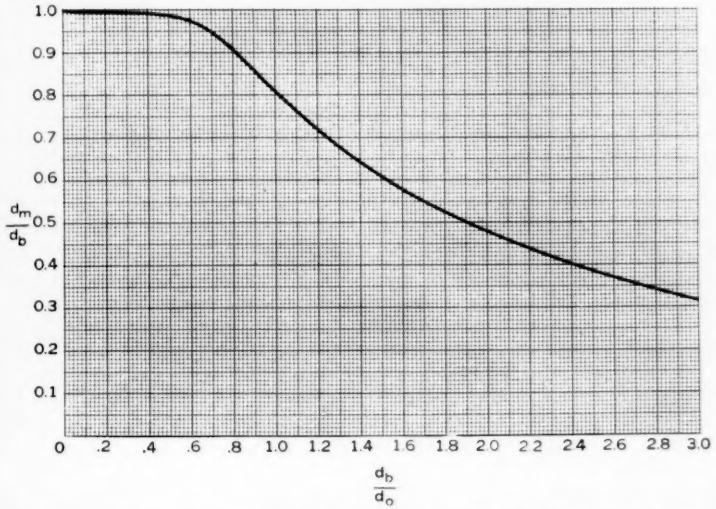

Fig. 1.9.2—Curve for finding maximum displacement for cushioning with tangent elasticity. See equation (1.9.5).

to an acceleration of 50g in a 3-foot drop with linear cushioning. Let us suppose that only 1.15 inches are available, instead of 1.44 inches, and that the cushioning has tangent elasticity starting with a spring rate of 694 lbs./in. Entering the curve of Fig. 1.9.1 at $d_b/d_0 = 1.15/1.44$ we find $G_m/G_0 = 3.5$. Hence the maximum acceleration will be 175g instead of the required 50g. This illustrates the wide variations in acceleration that may occur as a result of minor variations of dimensions in high G packages.

It is not necessarily true that the 175g test is 3.5 times as severe as the 50g test for all elements of the supported structure, since the severity depends also on the shape and scale of the acceleration-time relation. The factor may be more or less than 3.5 but it will be very close to this value for

all high-frequency elements of the structure. This subject is treated in detail in Parts II and III.

The maximum displacement d_m, in the case of tangent elasticity, may be calculated from equation (1.9.2) or, in terms of d_b/d_0, from

$$\frac{d_m}{d_b} = \frac{2}{\pi} \cos^{-1} \exp\left[-\frac{\pi^2}{8}\left(\frac{d_0}{d_b}\right)^2\right]. \tag{1.9.5}$$

The ratio d_m/d_b is plotted against d_b/d_0 in Fig. 1.9.2.

The use of Fig. 1.9.2 can be illustrated with the example already calculated, in which $d_b/d_0 = 1.15/1.44 = 0.8$. Entering the abscissa of Fig. 1.9.2 with $d_b/d_0 = 0.8$ we find $d_m/d_b = 0.915$. Hence the maximum displacement will be $0.915 \times 1.15 = 1.05$ inches.

1.10 Optimum Shape of Load-Displacement Curve for Tangent Elasticity

It is possible to choose the best shape for the load-displacement curve of the cushioning from those represented in Fig. 1.4.7. This will be, of course, not the best of all possible curves, but only the best among "tangent elasticity" curves. The best shape is defined as the one that yields the smallest maximum acceleration (G_m) for a given weight (W_2), height of drop (h) and available space (d_b). This leaves the initial spring rate (k_0) as the only remaining variable. To find its optimum value (say k_0'), set equal to zero the derivative of G_m (equation (1.9.4)) with respect to k_0, remembering that G_0 and d_0 are functions of k_0. The result is

$$\left(1 - \frac{\pi^2 W_2 h}{4 d_b^2 k_0'}\right) \exp\left(\frac{\pi^2 W_2 h}{2 d_b^2 k_0'}\right) - 1 = 0, \tag{1.10.1}$$

from which

$$k_0' = \frac{3.1 W_2 h}{d_b^2}. \tag{1.10.2}$$

Substituting (1.10.2) in (1.9.4) we find the minimum value (G_m') of maximum acceleration to be

$$G_m' = \frac{3.9h}{d_b}. \tag{1.10.3}$$

To illustrate the application of equations (1.10.2) and (1.10.3), consider again the case of the 20-pound article dropped from a height of three feet. We found that a linear spring, with a spring constant of 694 lbs/in, would limit the maximum acceleration to 50g if 1.44 inches of displacement were available. If only 1.15 inches of displacement are available, and the initial spring rate is kept at 694 lbs/in, we found the maximum acceleration to be

175g if the cushioning bottoms with tangent elasticity. Now, according to equation (1.10.2), the best initial spring rate for cushioning with tangent elasticity would be

$$k_0' = \frac{3.1 \times 20 \times 36}{(1.15)^2} = 1690 \text{ lbs/in.}$$

In this case, equation (1.10.3) gives, for the maximum acceleration,

$$G_m' = \frac{3.9 \times 36}{1.15} = 122g.$$

Hence, confronted with a space limitation less than that required for a 50g linear spring, it is better to use an initial spring rate higher than that for the 50g linear spring in order to strike an economical balance between displacement and bottoming. The best balance, among cushionings having tangent elasticity, is obtained by using equation (1.10.2).

If no factor of safety is considered, it would be still better not to use a bottoming type of cushion at all. From equations (1.3.5) and (1.3.3) it can be seen that a linear spring with a constant of 1090 lbs/in will give only 63g with a displacement of 1.15 inches. Such a spring, though, would bottom very sharply at a drop slightly higher than 3 ft. and would give an acceleration much greater than cushioning with tangent elasticity which bottoms more gradually. This may be important if there are high-frequency, brittle elements in the packaged article (see Part III).

1.11 Procedure for Finding Maximum Acceleration and Displacement for Cushioning with Tangent Elasticity (Class C)

To illustrate the use of the equations and curves for Class C cushioning, the same example used for Class B will be used, as it was observed that the experimental load-displacement curve in that example (Fig. 1.6.1) is a border line one which can be treated as either B or C.

By laying a straight edge along the first part of the curve (Fig. 1.6.1), the average initial spring rate is found to be 305 lbs/in. This value is taken as k_0 in the present case.

The next step is to find a value of d_b such that a graph of P/d_b vs x_2/d_b will fall slightly above the curve $k_0 = 30(0)$ in Fig. 1.4.7; d_b must be greater than 2 inches, since that displacement was obtained in the experiment. As a trial take $d_b = 2.25$ inches and test it at one point, say the experimental point $P = 300$ lbs., $x_2 = \frac{7}{8}$ in. Then $P/d_b = 133$ and $x_2/d_b = 0.39$. The point (0.39, 133) falls below the curve $k_0 = 30(0)$ in Fig. 1.4.7. Next try $d_b = 2.5$ inches. In this case, for the experimental point $P =$

300, $x_2 = \frac{7}{8}$, we find $P/d_b = 120$, $x_2/d_b = .35$. This falls slightly above the $k_0 = 30(0)$ curve as required. The whole experimental curve is then plotted to the coordinates $P/2.5$ vs $x_2/2.5$ and is found to fit as closely as necessary. Hence the parameters are adopted as $k_0 = 305$, $d_b = 2.5$.

We can now calculate the maximum acceleration that the tube will receive in, say, a three-foot drop test. First calculate, from equations (1) and (2),

$$d_0 = \sqrt{\frac{2hW_2}{k_0}} = \sqrt{\frac{2 \times 36 \times 22.5}{305}} = 2.31,$$

$$G_0 = \sqrt{\frac{2hk_0}{W_2}} = \sqrt{\frac{2 \times 36 \times 305}{22.5}} = 31.3.$$

Then $d_b/d_0 = 1.08$. Entering Fig. 4 with this value we find $G_m/G_0 = 1.82$. Hence the maximum acceleration is:

$$G_m = 31.3 \times 1.82 = 57g.$$

Finally, entering Fig. 5 with $d_b/d_0 = 1.08$ we find $d_m/d_b = 0.8$. Hence the maximum displacement is $d_m = 0.8 \times 2.5 = 2.0$ inches. This indicates that the load-displacement test was carried far enough to cover the range up to a three-foot drop.

It may be observed that the results obtained, by treating the same data as Class B or Class C cushioning, agree within a few per cent. This is because, in the example chosen, both B and C curves can be made to fit the experimental load-displacement curve.

1.12 Consequences of Abrupt Bottoming (Class D)

It is useful to examine cushioning systems that can bottom more abruptly than Class C cushioning. Abrupt bottoming is possible, for example, in a tension spring package lacking a snubbing device. An estimate of the increase in acceleration can be made by studying the case of bilinear elasticity (Fig. 1.4.4). Here we have a spring rate k_0 up to a displacement d_s, following which the cushioning has a different spring rate k_b. k_0 represents the average spring rate before bottoming and k_b can represent the much greater stiffness of the wall of the container.

If $d_0 > d_s$, that is, if

$$\sqrt{\frac{2W_2h}{k_0}} > d_s, \tag{1.12.1}$$

the suspended article will bottom and the maximum displacement and acceleration are obtained by using both of the equations (1.4.4) in evaluating the integral in (1.2.15). Thus,

$$\int_0^{d_s} k_0 x_2 \, dx_2 + \int_{d_s}^{d_m} [k_b x_2 - (k_b - k_0)d_s] \, dx_2 = W_2 h. \tag{1.12.2}$$

The remainder of the procedure for finding G_m is the same as before. The value of d_m found from (1.12.2) is substituted for x_2 in the second of

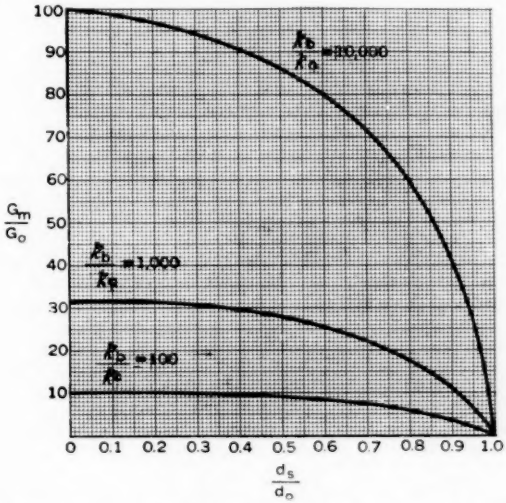

Fig. 1.12.1—Curves for finding maximum acceleration as a result of abrupt bottoming. See equation (1.12.3).

(1.4.4) and the value of P_m, thus obtained, is used, in (1.2.16), with the result:

$$G_m = G_0 \sqrt{\frac{k_b}{k_0} + \frac{d_s}{d_0^2}\left(1 - \frac{k_b}{k_0}\right)}, \tag{1.12.3}$$

where G_0 is the acceleration that would be reached if a displacement d_0 were available:

$$G_0 = \sqrt{\frac{2hk_0}{W_2}}. \tag{1.12.4}$$

The ratio G_m/G_0 is plotted against d_s/d_0 in Fig. 1.12.1 for several values of k_b/k_0. Since, in practice, k_b might be thousands of times as great as k_0, it may be seen that the increase in maximum acceleration can be very large even when d_s is only slightly less than d_0. It is apparent that a snubbing device is desirable in a tension spring suspension. This is especially true when considering high-frequency elements of the packaged article. It will be shown, in Part III, that low-frequency elements are not affected as much as might be expected from consideration of maximum acceleration alone.

1.13 Cushioning with Hyperbolic Tangent Elasticity (Class E)

In the preceding sections, there have been considered four types of elasticity (linear, cubic, tangent and bilinear) that fit the load-displacement characteristics of the more common cushioning materials and devices. There now remains the problem of finding more nearly ideal shapes of elasticity. By "more nearly ideal" is meant a shape which will result in a smaller maximum displacement for a given maximum acceleration. This is important in the packaging of very delicate articles if shipping space is limited.

It may be observed (equation (1.2.15)) that the total area under the load-displacement curve is equal to the maximum energy of the system. The maximum ordinate of the enclosed area is proportional to the maximum acceleration. Hence, if we wish to (1) limit the maximum acceleration (2) accomodate a given kinetic energy and (3) have as small a displacement as possible, the best shape for the load displacement function is $P =$ constant, where the constant is the product of the supported mass and the maximum allowable acceleration.

It is not practical to obtain this ideal shape exactly, for there will always be a finite initial spring rate and a rounding off of the load-displacement curve to the limiting maximum load. A function which represents this practical condition (and also includes the ideal case) is the hyperbolic tangent function mentioned in Section 1.4:

$$P = P_0 \tanh \frac{k_0 x_2}{P_0}. \tag{1.13.1}$$

The formulas for maximum acceleration and displacement are found in the same way as for the other classes of cushioning with the results:

$$d_m = \frac{P_0}{k_0} \cosh^{-1} \exp\left(\frac{W_2 h k_0}{P_0^2}\right) \tag{1.13.2}$$

or

$$d_m = \frac{d_0 P_0}{W_2 G_0} \cosh^{-1} \exp\left(\frac{W_2^2 G_0^2}{2P_0^2}\right) \tag{1.13.3}$$

and

$$G_m = \frac{P_0}{W_2} \tanh \frac{k_0 d_m}{P_0} \tag{1.13.4}$$

or

$$G_m = \frac{P_0}{W_2} \sqrt{1 - \exp\left(-\frac{W_2^2 G_0^2}{P_0^2}\right)} \tag{1.13.5}$$

where, as before

$$d_0 = \sqrt{\frac{2hW_2}{k_0}}, \qquad G_0 = \sqrt{\frac{2hk_0}{W_2}}.$$

Equations (1.13.3) and (1.13.5) are plotted, in Figs. 1.13.1 and 1.13.2, against the dimensionless parameter P_0/W_2G_0. The latter is the ratio of the maximum force, that the hyperbolic tangent cushioning will transmit,

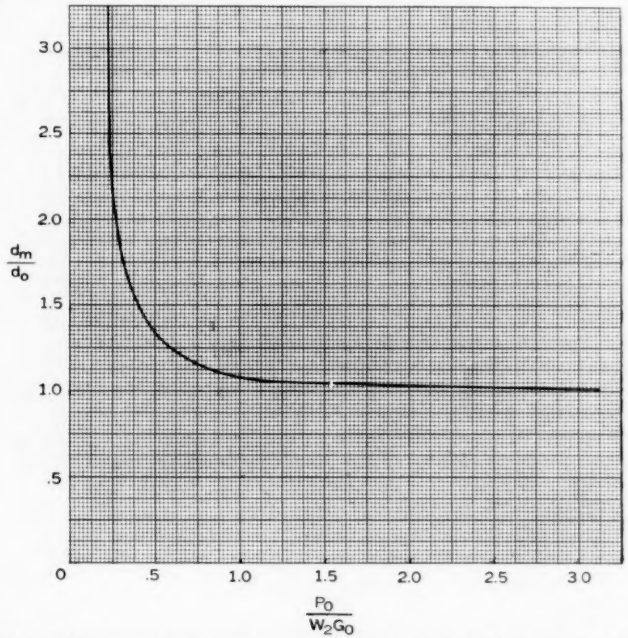

Fig. 1.13.1—Maximum displacement for cushioning with hyperbolic tangent elasticity. See equation (1.13.3).

to the force that linear cushioning would transmit under the conditions specified.

To find the value of k_0 which yields the minimum value of acceleration for a given maximum displacement, differentiate (1.13.4) with respect to k_0 and set the result equal to zero:

$$\operatorname{sech}^2 \frac{k_0 d_m}{P_0} = 0. \tag{1.13.6}$$

This is satisfied by $k_0 \to \infty$, which represents the rectangular load displacement curve and confirms the conclusion reached from energy considerations.

Taking the limit of (1.13.4) as $k_0 \to \infty$, we find the optimum acceleration to be

$$G'_m = \frac{P_0}{W_2}. \tag{1.13.7}$$

The corresponding maximum displacement is found, from (1.13.2) to be

$$d'_m = \frac{W_2 h}{P_0} = \frac{h}{G'_m}. \tag{1.13.8}$$

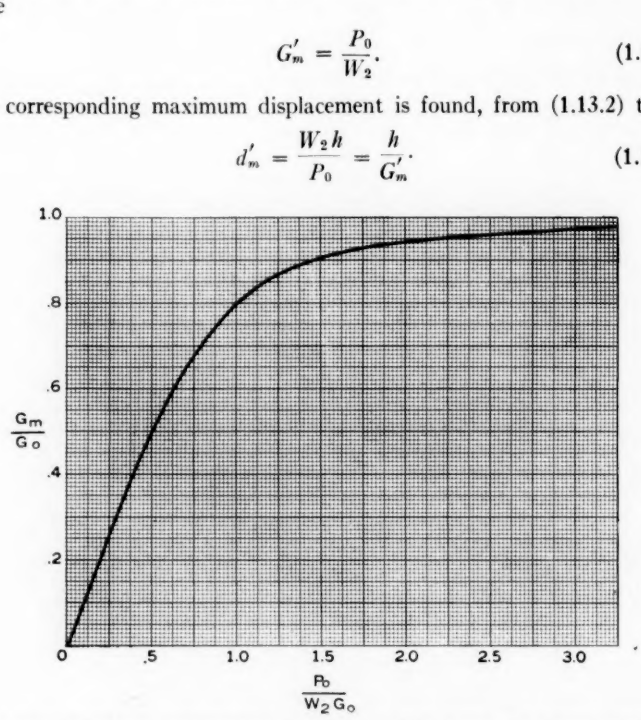

Fig. 1.13.2—Maximum acceleration for cushioning with hyperbolic tangent elasticity. See equation (1.13.5).

1.14 Minimum Space Requirements for Various Classes of Cushioning

It is interesting to compare the minimum amount of space for displacement that can be attained with the various kinds of cushioning that have been discussed.

Hyperbolic Tangent Elasticity	$d'_m = \frac{h}{G'_m}$
Linear Elasticity	$d_m = \frac{2h}{G_m}$
Tangent Elasticity	$d'_m = \frac{3.9h}{G'_m}$

Cubic elasticity will give a d_m somewhat more or less than $2h/G_m$ depending upon whether the parameter r is positive or negative.

It is seen that a factor of almost four can be gained, in the linear dimensions of the cushioning space required, by replacing the tangent type of cushioning with the hyperbolic tangent type.

There are several ways of obtaining a load-displacement curve with a shape similar to the hyperbolic tangent curve. One of the most interesting is suggested by the fact that the load-displacement curve of a strut has approximately this shape. Hence a bristle brush has the proper characteristics.

TABLE II

1	2	3	4	5	6	7	8
n	$\Delta(x_2)_n$	$(x_2)_n$	P_n	$\Delta A_n = \frac{1}{2}\Delta(x_2)_n \times (P_n + P_{n-1})$	$A_n = A_{n-1} + \Delta A_n$	$h_n = \frac{A_n}{W_2}$	$G_n = \frac{P_n}{W_2}$
0	—	0	0	0	0	0	0
1	0.500	0.500	120	30	30	1.6	6.5
2	0.100	0.600	150	13.5	43.5	2.4	8.1
3	0.100	0.700	205	17.0	61.3	3.3	11.1
4	0.100	0.800	290	24.8	86.1	4.7	15.7
5	0.100	0.900	410	35.0	121.1	6.6	22.2
6	0.100	1.000	585	49.8	170.9	9.2	31.6
7	0.050	1.050	730	32.9	203.8	11.1	39.5
8	0.050	1.100	950	42.0	245.8	13.3	51.4
9	0.050	1.150	1370	58.0	303.8	16.4	74.0
10	0.025	1.175	1680	38.1	341.9	18.5	91.0
11	0.025	1.200	2240	49.0	390.9	21.1	121.0
12	0.0125	1.2125	2620	30.4	421.3	22.8	141.5
13	0.0125	1.225	3200	36.4	457.7	24.7	173.0

1.15 Numerical Method for Analyzing Class F Cushioning

The numerical method to be described is one that has been adapted from a graphical one used by the Committee on Packing and Handling of Radio Valves of the British Radio Board. The method has advantages of simplicity in concept and ease of application, especially when the load-displacement curve of the cushioning does not resemble closely one of the Classes A to E described above. It has the disadvantage that it does not yield, directly, numerical factors by which the spring rate or depth of cushioning should be changed in the event that the analysis reveals inadequate or more than adequate protection.

The method is based on the fact that the area under the load-displacement curve of the cushioning represents the energy stored in, or absorbed by, the cushion. The total amount of energy that must be transferred is equal to the product of the weight (W_2) of the suspended item and the height (h) of drop. By finding the abscissa (x_2) and its ordinate (P) which

include an area W_2h, the maximum displacement is immediately x_2 and the maximum acceleration is the quotient P/W_2, in accordance with equations (1.2.15) and (1.2.16).

As actually applied in the present instance, the British method was modified slightly to make the procedure a routine numerical one. The

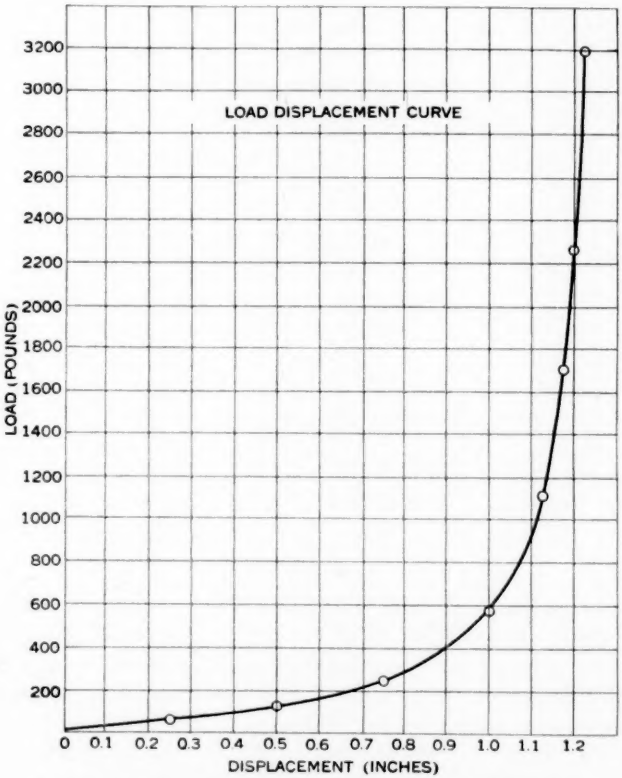

Fig. 1.15.1—Experimental load-displacement curve for Table II.

computing form is given in detail in Table II, in which the data are taken from an experimental load-displacement curve (Fig. 1.15.1) for the end spring pads of a vacuum tube package. The load-displacement data are listed in Columns 3 and 4 of Table II. The meaning of each column in the table is as follows.

Column 1. $n(= 1, 2, 3\cdots)$ is the number that identifies the displacement (and corresponding load) up to which the area under the load-displacement curve is to be calculated.

Column 2. $\Delta(x_2)_n$ is the increment of displacement between $(x_2)_{n-1}$ and $(x_2)_n$. $\Delta(x_2)_n = (x_2)_n - (x_2)_{n-1}$, see Fig. 1.15.2. Note that, as the curve becomes steeper, $\Delta(x_2)_n$ is taken smaller for better accuracy.

Column 3. $(x_2)_n$ is the displacement associated with the n^{th} point (see Fig. 1.15.2).

Column 4. P_n is the load that produces displacement $(x_2)_n$.

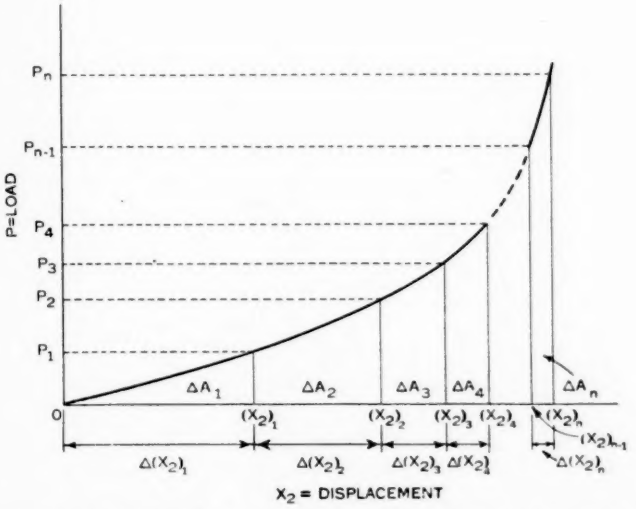

Fig. 1.15.2—Graphical illustration of numerical method of calculating area under load-displacement curve. See Table II.

Column 5. $\Delta A_n = \frac{1}{2}\Delta(x_2)_n(P_{n-1} + P_n)$ is the area of the trapezoid with altitude $\Delta(x_2)_n$ and bases P_{n-1} and P_n. It is approximately the energy absorbed by the cushioning in displacing from $(x_2)_{n-1}$ to $(x_2)_n$.

Column 6. A_n is the sum of all the trapezoidal areas from $x_2 = 0$ to $x_2 = (x_2)_n$. It is approximately the total energy the cushioning can absorb in displacing an amount $(x_2)_n$ beginning at zero displacement. Note that A_0 is always equal to zero.

Column 7. $h_n = A_n/W_2$ is the height of fall that will cause the cushioning to displace an amount $(x_2)_n$. In Table II, $W_2 = 18.5$ pounds.

Column 8. $G_n = P_n/W_2$ is the maximum acceleration experienced by the suspended mass when dropped from a height h_n.

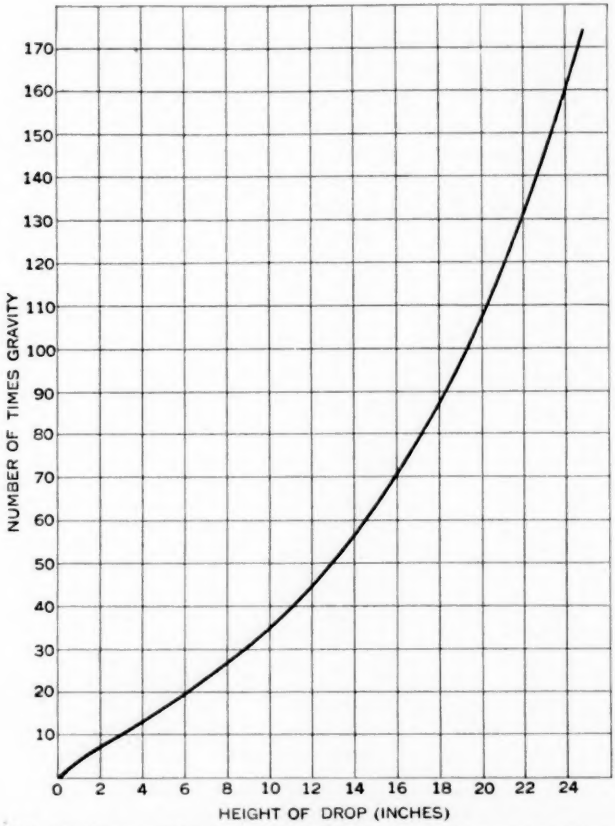

Fig. 1.15.3—Maximum acceleration vs. height of drop for an 18.5 pound article supported on cushioning with the load-displacement curve of Fig. 1.15.1. See Table II.

From the last two columns of the table a curve of height of drop vs. the corresponding acceleration may be plotted as in Fig. 1.15.3.

PART II

ACCELERATION-TIME RELATIONS

2.1 Introduction

In Part I we were concerned primarily with the *maximum* acceleration of the packaged item. In this part we shall study the details of the variation of acceleration with time in order to have this information available for our

study, in Part III, of its influence on the response of elements of the packaged item.

The first case to be considered will be the simple single mass and linear spring example described in Sections 1.2 and 1.3. Following this the phenomenon of rebound of the package will be considered. The influence of velocity damping and dry friction will be studied; and, finally, the effects of non-linearity of the cushion elasticity on the acceleration-time relation will be investigated.

2.2 Acceleration-time Relation for Linear Elasticity

Returning to the elementary example studied in Sections 1.2 and 1.3, we first write the equation of motion for the mass m_2, on its linear spring of spring rate k_2 (see Fig. 1.2.1.). Equation (1.2.3) becomes

$$m_2\ddot{x}_2 + k_2x_2 = m_2g. \tag{2.2.1}$$

Using the initial conditions

$$[x_2]_{t=0} = 0, \tag{2.2.2}$$

$$[\dot{x}_2]_{t=0} = \sqrt{2gh}, \tag{2.2.3}$$

the solution of (2.2.1) is

$$x_2 = \frac{\sqrt{g^2 + 2\omega_2^2 gh}}{\omega_2^2} \sin(\omega_2 t - \alpha) + \frac{g}{\omega_2^2} \tag{2.2.4}$$

or

$$x_2 = \sqrt{\frac{W_2^2}{k_2^2} + d_m^2} \sin(\omega_2 t - \alpha) + \frac{W_2}{k_2}, \tag{2.2.5}$$

where

$$\omega_2 = \sqrt{\frac{k_2}{m_2}} = 2\pi f_2 = \frac{2\pi}{T_2} \tag{2.2.6}$$

and

$$\alpha = \tan^{-1} \frac{g}{\omega_2\sqrt{2gh}} = \tan^{-1} \frac{W_2}{k_2 d_m}. \tag{2.2.7}$$

ω_2 is the circular frequency, f_2 is the frequency and T_2 is the period of vibration of the mass m_2 on its spring; d_m has the same definition as in Section 1.3 (equation (1.3.1)).

Now, W_2/k_2 is the static displacement of the mass m_2 on its spring. This is usually very small in comparison with the maximum displacement (d_m) during impact. Hence W_2/k_2 will be neglected, and (2.2.5) becomes

$$x_2 = d_m \sin \omega_2 t. \tag{2.2.8}$$

Differentiating (2.2.8) twice with respect to t, we find, for the acceleration

$$\ddot{x}_2 = -\omega_2^2 d_m \sin \omega_2 t = -\omega_2 \sqrt{2gh} \sin \omega_2 t. \tag{2.2.9}$$

Hence the absolute magnitude of the maximum acceleration is

$$G_m = \frac{|\ddot{x}_2|_{\max}}{g} = \frac{\omega_2^2 d_m}{g} = \sqrt{\frac{2hk_2}{W_2}} \tag{2.2.10}$$

as before.

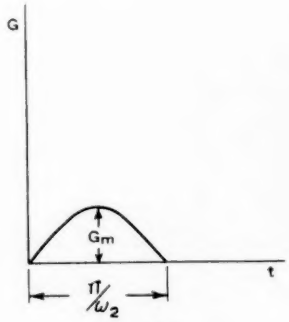

Fig. 2.2.1

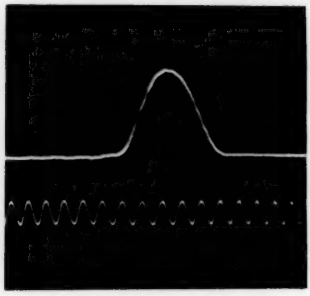

Fig. 2.2.2

Fig. 2.2.1—Half-sine-wave pulse acceleration. See equation (2.2.9).
Fig. 2.2.2—Oscillogram of a half-sine-wave pulse obtained with a piezo-crystal accelerometer.

Equation (2.2.9) shows that the acceleration varies sinusoidally with time. It rises from its initial zero value to its maximum in a time $\pi/2\omega_2$, at which time the displacement also reaches its maximum value. The acceleration returns to zero again at time π/ω_2. At this time the displacement is also zero. This is the end of the range of applicability of equation (2.2.9); for when t becomes slightly greater than π/ω_2, a tension in the spring is required. Since no mechanism, such as a large mass m_3 (Fig. 0.2.2), has been supplied, to allow a tension in the spring to develop, the system will rebound from the floor at the end of the half period π/ω_2. The acceleration is thus a half-sinusoidal pulse of duration $\pi/\omega_2 = T_2/2$ and amplitude $G_m g$ as illustrated in Fig. 2.2.1. An oscillogram of such a pulse obtained with a piezo-crystal accelerometer is shown in Fig. 2.2.2.

2.3 Package Rebound.

The presence of the mass of an outer container will affect the acceleration after the first half cycle of displacement. The outer container is represented by the mass m_3 in the general idealized system illustrated in Fig. 0.2.2 and in the simpler system (Fig. 2.3.1) that we shall consider now.

Two pairs of equations are necessary to describe the action of the system; one pair applies during the time of contact of m_3 with the floor and the second pair applies if rebound occurs.

The mass m_3 is assumed to be inelastic (see Section 0.2) so that, during the interval of its contact with the floor, the equation of motion for m_2 will be the same as before (2.2.1). In addition, there will be an equation of equilibrium for the mass m_3 :

$$R = k_2 x_2 + m_3 g \; ; \tag{2.3.1}$$

where R is the upward force exerted by the floor on m_3 .

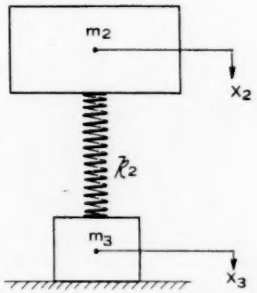

Fig. 2.3.1—Two-mass system representing packaged article, linear cushioning and outer container.

Equations (2.3.1) and (2.2.1) will hold as long as R is positive. To find out when $R > 0$, solve (2.2.1) for $k_2 x_2$ and substitute in (2.3.1):

$$R = W_2 + W_3 - m_2 \ddot{x}_2 \; . \tag{2.3.2}$$

That is, a necessary condition for rebound is that the mass of the cushioned article, multiplied by its maximum acceleration, exceeds the total weight of the package. The condition for rebound may be written

$$G_m > \frac{W_2 + W_3}{W_2} \; . \tag{2.3.3}$$

This is a necessary, but not a sufficient, condition for rebound because there will be energy losses as a result of damping and permanent deformation. G_m will generally have to be considerably greater than the right hand side of (2.3.3) for rebound to occur.

If rebound does not occur, equation (2.2.9) continues to apply, except for damping which will be considered in Section 2.5.

2.4 Motion After Rebound

If rebound occurs, the equations of motion for the two masses, m_2 and m_3, are

$$m_2\ddot{x}_2 + k_2(x_2 - x_3) = m_2 g, \tag{2.4.1}$$

$$m_3\ddot{x}_3 - k_2(x_2 - x_3) = m_3 g. \tag{2.4.2}$$

Multiplying (2.4.1) by m_3 and (2.4.2) by m_2 and subtracting, we find

$$m\ddot{y} + k_2 y = 0, \tag{2.4.3}$$

where

$$y = x_2 - x_3, \tag{2.4.4}$$

$$m = \frac{m_2 m_3}{m_2 + m_3}. \tag{2.4.5}$$

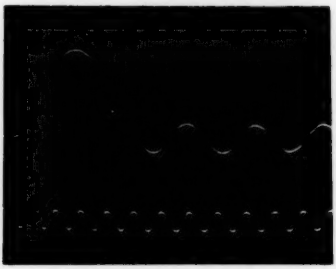

Fig. 2.4.1—Oscillogram illustrating the half-sine pulse followed by the higher frequency, lower amplitude vibration of the packaged article in a rebounding package.

Equation (2.4.3) is the equation governing the vibration of the two-mass system as a simple oscillator. The circular frequency of the vibration is

$$\omega = \sqrt{\frac{k_2}{m}} \tag{2.4.6}$$

and it may be noticed that this frequency is always greater than ω_2 (equation (2.2.6)). This fact is important in estimating the effect of vibrations on elements of the packaged item (Section 3.5).

ω is also the frequency of vibration of the packaged article during the interval of free fall. This vibration (usually of small amplitude) is initiated by the sudden release of the dead load displacement of the packaged article.

As an intermediate step in obtaining the acceleration after rebound we shall find the magnitude of the relative displacement (y) of the two masses. To do this it is necessary to solve equation (2.4.3) with the appropriate boundary conditions. Calling t_r the time at which m_3 leaves the floor, we

must find y and $\dot{y}$ at $t = t_r$. Since m_3 is motionless at $t = t_r$, the relative displacement and velocity at that time are identical with x_2 and $\dot{x}_2$ respectively. The former is simply the stretch of the spring necessary to just pull the mass m_3 off the floor, i.e.,

$$[y]_{t=t_r} = [x_2]_{t=t_r} = -\frac{W_3}{k_2}. \tag{2.4.7}$$

To find the velocity at $t = t_r$, substitute (2.4.7) in (2.2.4) and also substitute t_r for t in the latter. This gives an equation for determining t_r. Then, returning to (2.2.4), differentiate it once to obtain $\dot{x}_2$ and substitute for t the value t_r just found. The result is

$$[\dot{x}_2]_{t=t_r} = [\dot{y}]_{t=t_r} = -\sqrt{2gh - \frac{gW_3(2W_2 + W_3)}{W_2 k_2}}. \tag{2.4.8}$$

The solution of (2.4.3) with initial conditions (2.4.7) and (2.4.8) is

$$y = -\frac{1}{\omega}\sqrt{2gh - \frac{W_3 g}{k_2}} \sin(\omega t - \zeta), \tag{2.4.9}$$

where

$$\zeta = \omega t_r - \tan^{-1}\frac{\omega[y]_{t=t_r}}{[\dot{y}]_{t=t_r}}.$$

We are now in a position to find the acceleration of the packaged item after rebound. Substitute y of (2.4.9) for $x_2 - x_3$ in (2.4.1) to obtain

$$\ddot{x}_2 = g + \frac{\omega_2^2}{\omega}\sqrt{2gh - \frac{W_3 g}{k_2}} \sin(\omega t - \zeta). \tag{2.4.10}$$

To obtain a simple formula for the ratio of the maximum accelerations after and before rebound, let us assume that both are much greater than gravitational acceleration. Then if

G_r = maximum number of g's after rebound, (maximum of (2.4.10))

$G_m = \sqrt{\frac{2hk_2}{W_2}}$ = maximum number of g's before rebound,

we find, from (2.4.10), neglecting the term g outside the radical,

$$\frac{G_r}{G_m} = \frac{W_3}{W_2 + W_3}\sqrt{1 - \frac{W_3}{2hk_2}}. \tag{2.4.11}$$

Hence, the maximum acceleration after rebound is always less than the maximum acceleration before rebound. Therefore, conditions after rebound need only be examined when the frequency after rebound (see equation (2.4.6)) is near the natural frequency of vibration of a critical element of the packaged item (see Section 3.5).

The complete acceleration history of a rebounding package with undamped linear cushioning is thus a half sine wave pulse of amplitude $G_m = \sqrt{2hk_2/W_2}$ and duration π/ω_2 followed by an oscillating acceleration of amplitude given by (2.4.11) and frequency given by (2.4.6). Such a wave shape is shown in Fig. 2.4.1.

2.5 Influence of Damping on Acceleration

The presence of damping in cushioning is always desirable to prevent the building up of large amplitudes as a result of periodic disturbances. However, damping also has an effect on the maximum acceleration that is attained in a drop test. From the latter point of view there is an optimum amount of damping and an amount that should not be exceeded if the maximum undamped acceleration is not to be exceeded.

We shall consider the case of a linear cushion with damping proportional to velocity. The system is represented in Fig. 2.5.1. With the addition

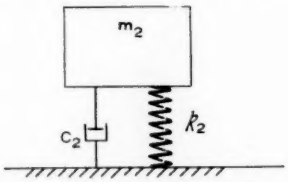

Fig. 2.5.1—Idealization of linear cushioning with velocity damping.

of the damping term the equation of motion of m_2, during contact of the package with the floor, is

$$m_2\ddot{x}_2 + c_2\dot{x}_2 + k_2x_2 = 0, \tag{2.5.1}$$

in which c_2 is the damping coefficient of the cushioning. Equation (2.5.1) is more conveniently expressed as

$$\ddot{x}_2 + 2\beta_2\omega_2\dot{x}_2 + \omega_2^2x_2 = 0, \tag{2.5.2}$$

where

$$\omega_2 = \sqrt{\frac{k_2}{m_2}}, \tag{2.5.3}$$

$$\beta_2 = \frac{c_2}{2m_2\omega_2}. \tag{2.5.4}$$

ω_2 is the undamped circular frequency of vibration of m_2 on its spring and β_2 is the fraction of critical damping. $\beta_2 = 0$ means no damping and $\beta_2 = 1$ means just enough damping so that there will be no oscillation if the packaged article is displaced and released.

The acceleration solution of (2.5.2), with the initial conditions of the drop test (see (2.2.2) and (2.2.3)) is

$$\ddot{x}_2 = -\frac{\omega_2\sqrt{2gh}}{\sqrt{1-\beta_2^2}}\, e^{-\beta_2\omega_2 t}\cos\left(\omega_2 t\sqrt{1-\beta_2^2}+\gamma\right) \qquad (2.5.5)$$

where

$$\tan\gamma = \frac{2\beta_2^2-1}{2\beta_2\sqrt{1-\beta_2^2}}. \qquad (2.5.6)$$

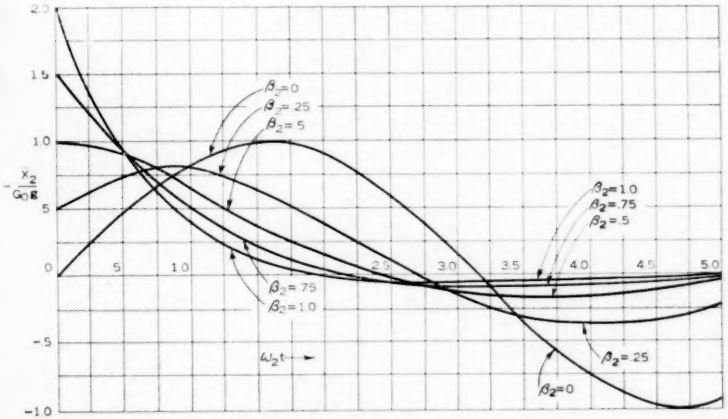

Fig. 2.5.2—Acceleration-time curves for linear cushioning with various amounts of damping (no rebound). See equation (2.5.5).

The acceleration is thus a damped sinusoid with an abruptly reached initial value whose magnitude depends upon the amount of damping. For small damping, the initial acceleration is small and then the acceleration increases, but never reaches the value that would be reached without any damping. For high damping ($\beta_2 > 0.5$) the initial value is greater than without any damping and falls off thereafter. Figure 2.5.2 shows the shapes of the acceleration time curves for several values of β_2. All of the curves are for no rebound. It may be seen, from equation (2.5.5) and Fig. 2.5.2 that the addition of damping changes the shape of the acceleration-time relation in three ways. First, a damped sinusoid replaces the pure sinusoid; second, the frequency is reduced; and, third, the initial phase is changed.

It is useful to consider in detail the effect of damping on *maximum* acceleration. Let

G_m = maximum number of g's with damping

$G_0 = \sqrt{\dfrac{2hk_2}{W_2}}$ = maximum number of g's without damping.

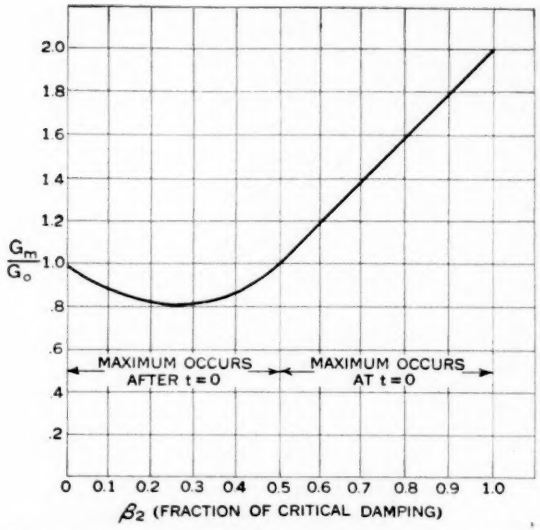

Fig. 2.5.3—Influence of velocity damping on maximum acceleration. See equation (2.5.5).

Then, from (2.5.5), at $t = 0$

$$\frac{G_m}{G_0} = 2\beta_2 \tag{2.5.7}$$

and, after $t = 0$,

$$\frac{G_m}{G_0} = e^{-\beta_2\omega_2 t_m}, \tag{2.5.8}$$

where t_m, the time at which the maximum occurs, is given by

$$\tan \omega_2 t_m \sqrt{1 - \beta_2^2} = \frac{(1 - 4\beta_2^2)\sqrt{1 - \beta_2^2}}{\beta_2(3 - 4\beta_2^2)}. \tag{2.5.9}$$

The largest value of G_m/G_0 from (2.5.7) and (2.5.8) is plotted against β_2 in Fig. 2.5.3. It is shown there that, as the damping is increased from zero, the maximum acceleration first decreases to a minimum of 80% of G_0 and then increases to G_0 at 50% of critical damping. In this interval the maximum acceleration occurs after $t = 0$. For damping greater than $\beta_2 = 0.5$ the maximum acceleration occurs at the instant of contact and increases in direct proportion to β_2.

2.6 Influence of Damping on Rebound

In considering rebound without damping, it was found that rebound does not occur unless the product of the maximum acceleration and the sus-

pended mass exceeds the total weight of the package. It was not necessary to distinguish between maximum acceleration on the first downstroke and first upstroke, since these are the same when there is no damping. With damping, however, the maximum acceleration on the first downstroke is

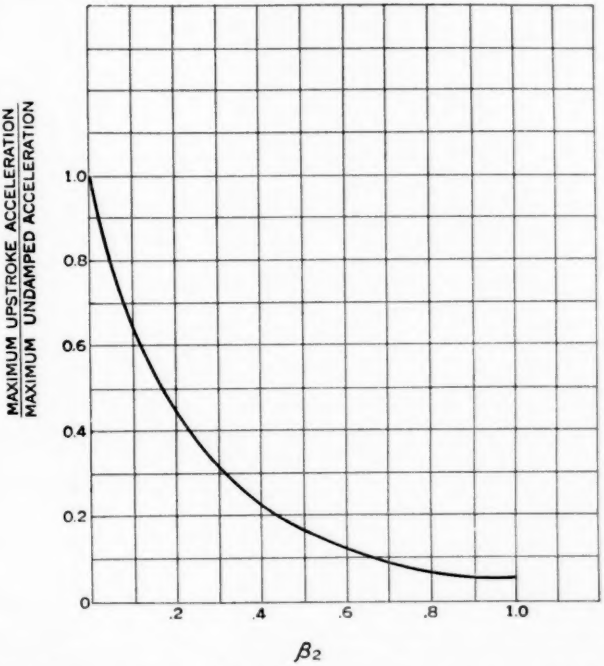

Fig. 2.6.1—Influence of velocity damping on maximum upstroke acceleration. See equation (2.5.5).

greater than that on the first upstroke (Fig. 2.5.2) and it is the latter that controls rebound. Hence damping inhibits rebound.

For example, with 50% of critical damping ($\beta_2 = 0.5$), equations (2.5.8) and (2.5.9) and Fig. 2.5.2 show that for the first downstroke $G_m/G_0 = 1$ while for the first upstroke $G_m/G_0 = 0.164$. Hence the tendency to rebound is reduced by a factor of six when damping to the extent of 50% of critical is added to an undamped package.

The ratio of the maximum acceleration on the first upstroke to the maximum undamped acceleration is plotted in Fig. 2.6.1 for various values of β_2.

2.7 Influence of Dry Friction on Acceleration and Displacement

By "dry friction" is meant friction that is independent of velocity except for sign. During contact of the package with the floor the motion of m_2 might be opposed by a constant friction force F. Such a force is developed, for example, in a package with corrugated spring pad cushioning by rubbing against the side and end pads in a top or bottom drop. A typical idealized

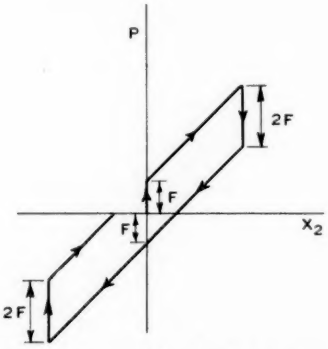

Fig. 2.7.1—Load vs. displacement for cushioning with dry friction.

load-displacement curve is shown in Fig. 2.7.1. For the first downstroke of m_2, the equation of motion of m_2 is

$$m_2\ddot{x}_2 + k_2x_2 = -F. \tag{2.7.1}$$

With initial conditions

$$[x_2]_{t=0} = 0, \qquad [\dot{x}_2]_{t=0} = \sqrt{2gh} \tag{2.7.2}$$

the solution of (2.7.1) is

$$x_2 = \sqrt{d_0^2 + \left(\frac{F}{k_2}\right)^2}\sin(\omega_2 t + \alpha) - \frac{F}{k_2} \tag{2.7.3}$$

where

$$d_0 = \sqrt{\frac{2W_2h}{k_2}},$$

$$\tan\alpha = \frac{F}{k_2 d_0} = \frac{F}{W_2 G_0},$$

$$G_0 = \sqrt{\frac{2hk_2}{W_2}}.$$

d_0 and G_0 are the maximum displacement and acceleration that would obtain if no friction were present. From (2.7.2) the maximum displacement with friction is

$$d_m = \sqrt{d_0^2 + \left(\frac{F}{k_2}\right)^2} - \frac{F}{k_2}. \tag{2.7.4}$$

Hence, the presence of friction decreases the maximum displacement since $d_m < d_0$.

From (2.7.3) the acceleration is

$$\frac{\ddot{x}_2}{g} = -\sqrt{G_0^2 + \left(\frac{F}{W_2}\right)^2} \sin(\omega_2 t + \alpha), \tag{2.7.5}$$

so that the maximum acceleration is

$$G_m = \sqrt{G_0^2 + \left(\frac{F}{W_2}\right)^2}, \tag{2.7.6}$$

which is greater than the maximum acceleration without friction.

It would appear, at first glance, that cushioning with friction always gives a greater acceleration than the corresponding cushioning without friction. However, the reverse is actually true provided we allow the same displacement in both cases. This may be done, as may be seen from (2.7.4), by decreasing the spring rate in the cushioning with friction to

$$k_F = k_2 - \frac{2F}{d_0}. \tag{2.7.7}$$

The maximum acceleration in the cushioning with friction is then, from (2.7.6),

$$G_F = G_0 - \frac{F}{W_2}, \qquad 0 \leqq \frac{F}{W_2} \leqq \frac{G_0}{2}. \tag{2.7.8}$$

That is, for the same maximum displacement, the maximum acceleration is reduced by the addition of dry friction.

2.8 Acceleration-Time Relation for Cubic Elasticity

As an example of the effect of nonlinearity of the cushioning on the shape of the acceleration-time function, the case of cubic elasticity (Class B) will be analyzed. The system to be considered is illustrated in Fig. 1.2.1, and the load-displacement relation for the cushioning is given by

$$P = k_0 x_2 + r x_2^3. \tag{2.8.1}$$

Substituting (2.8.1) in (1.2.13) and performing the indicated integration, we find

$$\dot{x}_2^2 = 2gh - \frac{k_0}{m_2} x_2^2 - \frac{r}{2m_2} x_2^4. \tag{2.8.2}$$

Remembering that $\dot{x}_2 = dx_2/dt$, we solve (2.8.2) for dt:

$$dt = \frac{dx_2}{\sqrt{2gh - \frac{k_0}{m_2} x_2^2 - \frac{r}{2m_2} x_2^4}}. \tag{2.8.3}$$

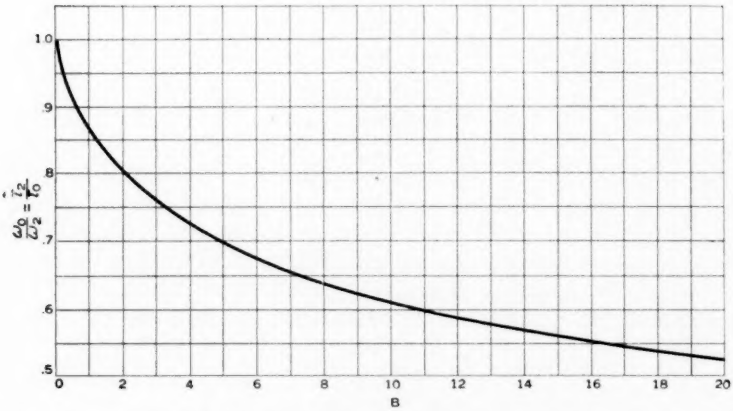

Fig. 2.8.1—Duration of acceleration pulse for cushioning with cubic elasticity. See equation (2.8.10).

Then, with the initial condition $x_2 = 0$ when $t = 0$, the integral of (2.8.3) is

$$t = \int_0^{x_2} \frac{dx_2}{\dot{x}_2} = \int_0^{x_2} \frac{dx_2}{\sqrt{2gh - \frac{k_0}{m_2} x_2^2 - \frac{r}{2m_2} x_2^4}}. \tag{2.8.4}$$

To integrate (2.8.4), let

$$Z = \frac{x_2}{\sqrt{k^2(x_2^2 - d_m)^2 + d_m^2}}, \tag{2.8.5}$$

where

$$k^2 = \tfrac{1}{2}\left\{1 - \frac{1}{\sqrt{1+B}}\right\} \tag{2.8.6}$$

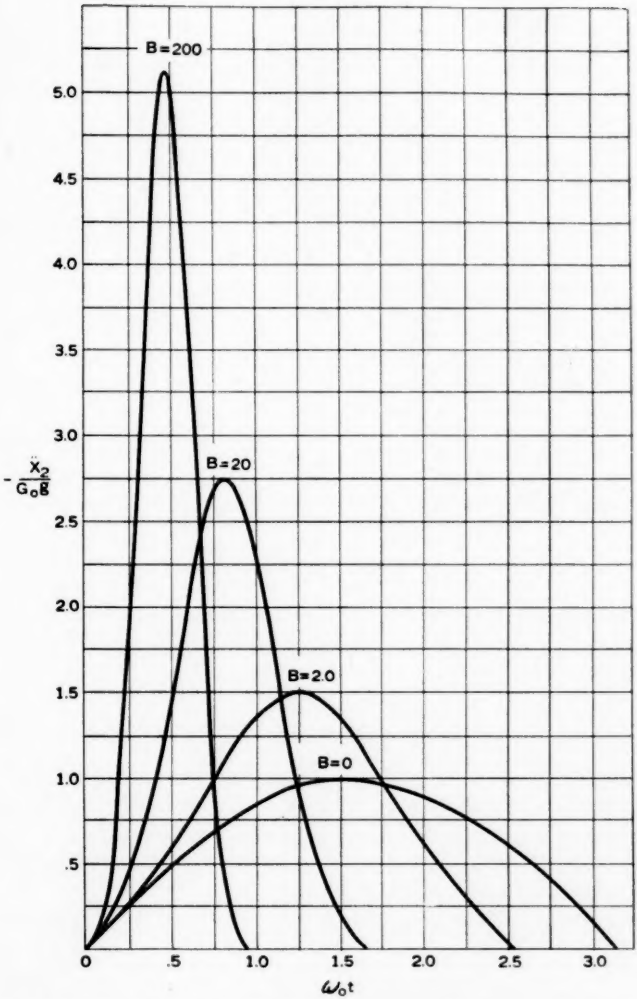

Fig. 2.8.2—Acceleration-time curves for cushioning with cubic elasticity. See equation (2.8.14).

and B and d_m are as given in Part I:

$$B = \frac{4W_2 hr}{k_0^2} \tag{1.5.3}$$

$$d_m = d_0 \sqrt{\frac{2}{B}(-1 + \sqrt{1 + B})}\,. \tag{1.5.4}$$

Then (2.8.4) becomes

$$t = \frac{1}{\omega_c} \int_0^Z \frac{dZ}{\sqrt{(1 - Z^2)(1 - k^2 Z^2)}}, \tag{2.8.7}$$

in which the integral is the elliptic integral of the first kind (see Hancock "Elliptic Integrals," John Wiley and Sons, New York, 1917). In (2.8.7),

$$\omega_c = \omega_0 (1 + B)^{1/4}, \tag{2.8.8}$$

where $\omega_0 = \sqrt{k_0/m_2}$ is the radian frequency that would obtain if the cushioning were linear with spring rate k_0. The motion for the linear case has a half period, or pulse duration $\tau_0 = \pi/\omega_0$. The half-period (τ_2) of the motion with cubic elasticity is twice the time required for x_2 to increase from 0 to d_m.

From 2.8.5

$$\begin{aligned} [Z]_{x_2=0} &= 0, \\ [Z]_{x_2=d_m} &= 1. \end{aligned} \tag{2.8.9}$$

Hence, from (2.8.7), the half-period is

$$\tau_2 = \frac{2}{\omega_c} \int_0^1 \frac{dZ}{\sqrt{(1 - Z^2)(1 - k^2 Z^2)}} = \frac{2K}{\omega_c} \tag{2.8.10}$$

where K is the complete elliptic integral of the first kind. The duration of the acceleration pulse is therefore $2K/\omega_c$. We can define a radian frequency of the acceleration by

$$\omega_2 = \frac{\pi}{\tau_2} = \frac{\pi\omega_c}{2K} = \frac{\pi\omega_0(1 + B)^{1/4}}{2K}. \tag{2.8.11}$$

The ratio ω_0/ω_2 (i.e., τ_2/τ_0) is plotted in Fig. 2.8.1 which illustrates how the pulse duration decreases as the parameter B increases. Hence, for a given cushioning with cubic elasticity, the pulse duration decreases as the height of drop increases. This is in contrast to the linear case in which the duration is independent of the height of drop.

To find the acceleration $\ddot{x}_2$, we return to (2.8.7) and write it in the form of an elliptic function:

$$\operatorname{sn} \omega_c t = Z. \tag{2.8.12}$$

Substituting the expression for Z given in (2.8.5) and solving for x_2, we find

$$x_2 = d_m cn(\omega_c t - K). \tag{2.8.13}$$

Finally, differentiating (2.8.13) twice with respect to t, we find the acceleration to be

$$\ddot{x}_2 = \omega_c^2 d_m [2k^2 sn^2(\omega_c t - K) - 1] cn(\omega_c t - K). \tag{2.8.14}$$

The ratio $-\ddot{x}_2/G_0 g$ is plotted in Fig. 2.8.2 against a radian coordinate ($\omega_0 t$) for several values of B. It may be seen that, as B increases, the maximum acceleration increases, the duration of the pulse decreases (see Fig. 2.8.1) and the acceleration-time curve becomes bell shaped. For reference, the sinusoid for the linear case ($B = 0$) is plotted in the figure.

Figure 2.8.2 is plotted for perfect rebound. If rebound does not occur, the curves continue, mirrored in the time axis, so as to form a periodic vibration of period $2\tau_2$.

2.9 Acceleration-Time Relation for Tangent Elasticity

In this section the effect of tangent elasticity on the shape of the acceleration-time relation will be studied. The shape of the load displacement curve is given by

$$P = \frac{2k_0 d_b}{\pi} \tan \frac{\pi x_2}{2d_b}. \tag{1.4.3}$$

The system considered is again that shown in Fig. 1.2.1. Referring to the energy equation (1.2.13):

$$\frac{m_2 \dot{x}_2^2}{2} + \int_0^{x_2} P dx_2 = m_2 gh, \tag{1.2.13}$$

we substitute the above value of P and perform the indicated integration to obtain, for the velocity,

$$\dot{x}_2 = \sqrt{2gh + \frac{8k_0 d_b^2}{m_2 \pi^2} \log \cos \frac{\pi x_2}{2d_b}}. \tag{2.9.1}$$

Then, as in Section 2.8,

$$t = \int_0^{x_2} \frac{dx_2}{\dot{x}_2} = \int_0^{x_2} \frac{dx_2}{\sqrt{2gh + \frac{8k_0 d_b^2}{m_2 \pi^2} \log \cos \frac{\pi x_2}{2d_b}}} \tag{2.9.2}$$

and the half-period (τ_2) of the motion is again twice the time required for x_2 to increase from 0 to d_m. Hence

$$\tau_2 = 2 \int_0^{d_m} \frac{dx_2}{\sqrt{2gh + \frac{8k_0 d_b^2}{m_2 \pi^2} \log \cos \frac{\pi x_2}{2d_b}}} \tag{2.9.3}$$

where, from Section 1.9,

$$d_m = \frac{2d_b}{\pi} \cos^{-1} \exp\left[-\frac{\pi^2}{8}\left(\frac{d_0}{d_b}\right)^2\right]. \tag{1.9.5}$$

The radian frequency of the acceleration is

$$\omega_2 = \frac{\pi}{\tau_2}$$

and this is to be compared with the frequency

$$\omega_0 = \frac{\pi}{\tau_0} = \sqrt{\frac{k_0}{m_2}}$$

that would obtain if the cushioning were linear with spring rate k_0. The ratio ω_0/ω_2 (i.e., τ_2/τ_0) was obtained by numerical integration of (2.9.3)

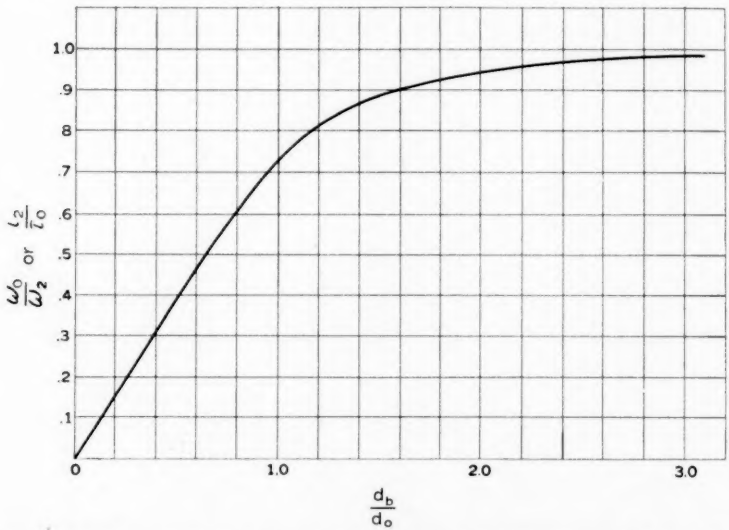

Fig. 2.9.1—Duration of acceleration pulse for cushioning with tangent elasticity. See equation (2.9.3).

and is plotted in Fig. 2.9.1 against the ratio d_b/d_0. The figure shows that for $d_b/d_0 < 1$, the pulse duration varies almost linearly with d_b/d_0. As the bottoming distance becomes larger than that required for linear cushioning with spring rate k_0, the pulse duration approaches asymptotically the duration π/ω_0 for the linear case.

As d_b/d_0 decreases, the pulse duration becomes shorter, but the maximum acceleration increases, in accordance with equation (1.9.4) and Fig. 1.9.1. The shapes of the acceleration-time curves for several values of d_b/d_0 are illustrated in Fig. 2.9.2. They are more sharply peaked than the corresponding curves for cubic elasticity (Fig. 2.8.2) as might be expected from

the fact that the load-displacement curve for tangent elasticity rises more rapidly than that for cubic elasticity; that is, the bottoming is harder.

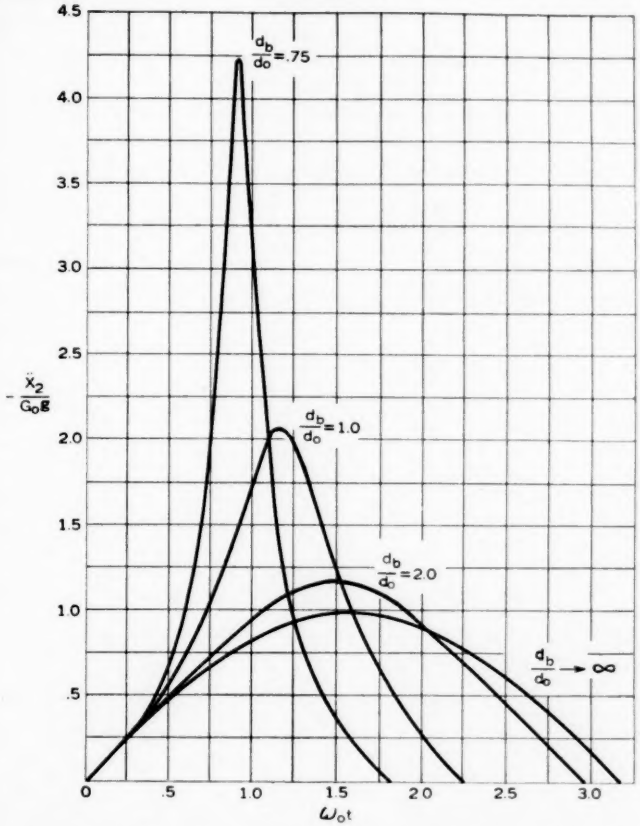

Fig. 2.9.2—Acceleration-time curves for cushioning with tangent elasticity.

The curves of Fig. 2.9.2 were obtained by numerical integration of equation (2.9.2), to obtain x_2 as a function of t, following which these values were substituted in the equation

$$m_2 \ddot{x}_2 + \frac{2k_0 d_b}{\pi} \tan \frac{\pi x_2}{2d_0} = 0$$

to obtain $\ddot{x}_2$. It may be observed that the maximum values of the curves are the values dictated by equation (1.9.4).

In performing the numerical integrations of equations (2.9.2) and (2.9.3), it is found that the integrand becomes infinite when $x_2 = d_m$ since at this point the velocity is zero. In order to avoid this difficulty, it was assumed[1] that, for a small distance in the neighborhood of d_m, the acceleration is constant with magnitude $G_m g$ as obtained from equation (1.9.4). The procedure is described in further detail in Section 2.12.

Figure 2.9.2 gives the acceleration-time curve for perfect rebound. If rebound does not occur, the acceleration is a periodic vibration, each successive half period having the shape shown, with alternating sign.

2.10 Acceleration-Time Relation for Abrupt Bottoming

By abrupt bottoming, we mean bilinear cushioning (Class D) as treated in Section 1.12. The load-displacement relation is (see equation (1.4.4) and Fig. 1.4.4)

$$\left.\begin{aligned} P &= k_0 x_2 \qquad 0 \leqq x_2 \leqq d_s \\ P &= k_b x_2 - (k_b - k_0) d_b \qquad x_2 \geqq d_s \end{aligned}\right\}. \tag{1.4.4}$$

Considering, again, the system illustrated in Fig. 1.2.1, the equation of motion of m_2, before bottoming, is

$$m_2 \ddot{x}_2 + k_0 x_2 = 0 \qquad 0 \leqq x_2 \leqq d_s \tag{2.10.1}$$

with initial conditions

$$[x_2]_{t=0} = 0, \qquad [\dot{x}_2]_{t=0} = \sqrt{2gh}. \tag{2.10.2}$$

The solution of (2.10.1) is then

$$x_2 = \frac{\sqrt{2gh}}{\omega_0} \sin \omega_0 t, \qquad 0 \leqq x_2 \leqq d_s, \tag{2.10.3}$$

where

$$\omega_0 = \sqrt{\frac{k_0}{m_2}}. \tag{2.10.4}$$

The time (t_s) at which x_2 reaches d_s is found from (2.10.3):

$$t_s = \frac{1}{\omega_0} \sin^{-1} \frac{\omega_0 d_s}{\sqrt{2gh}} = \frac{1}{\omega_0} \sin^{-1} \frac{d_s}{d_0}, \tag{2.10.5}$$

where

$$d_0 = \sqrt{\frac{2W_2 h}{k_0}};$$

[1] See Timoshenko, "Vibration problems in Engineering," D. Van Nostrand Co., New York, Second Edition (1937) page 123.

i.e., d_0 is the displacement that would have been reached if the spring rate remained constant.

The velocity of m_2 at time t_s is

$$[\dot{x}_2]_{t=t_s} = \sqrt{2gh}\cos\omega_0 t_s = \sqrt{2gh\left(1 - \frac{d_s^2}{d_0^2}\right)}. \tag{2.10.6}$$

If $\sqrt{2gh} > \omega_0 d_s$, the displacement will exceed d_s and the equation of motion becomes

$$m_2\ddot{x}_2 + k_b x_2 - (k_b - k_0)d_s = 0, \qquad x_2 \geqq d_s. \tag{2.10.7}$$

The solution of (2.10.7), with initial conditions

$$\left.\begin{aligned}[x_2]_{t=t_s} &= d_s \\ [\dot{x}_2]_{t=t_s} &= \sqrt{2gh\left(1 - \frac{d_s^2}{d_0^2}\right)},\end{aligned}\right\} \tag{2.10.8}$$

is

$$\left.\begin{aligned}x_2 = \frac{k_0 d_0}{k_b}\sqrt{\frac{k_b}{k_0} + \frac{d_s^2}{d_0^2}\left(1 - \frac{k_b}{k_0}\right)}\sin(\omega_b t + \alpha - \omega_b t_s) \\ + \left(1 - \frac{k_0}{k_b}\right)d_s \qquad x_2 \geqq d_s\end{aligned}\right. \tag{2.10.9}$$

where

$$\left.\begin{aligned}\tan^2\alpha &= \frac{k_0}{k_b\left(\frac{d_0^2}{d_s^2} - 1\right)} \\ \omega_b &= \sqrt{\frac{k_b}{m_2}}.\end{aligned}\right\} \tag{2.10.10}$$

By differentiating (2.10.3) and (2.10.9) twice with respect to t, the accelerations for the two regions are found to be

$$\ddot{x}_2 = -G_0 g\sin\omega_0 t, \qquad 0 \leqq x_2 \leqq d_s, \tag{2.10.11}$$

$$\ddot{x}_2 = -G_0 g\sqrt{\frac{k_b}{k_0} + \frac{d_s^2}{d_0^2}\left(1 - \frac{k_b}{k_0}\right)}\sin(\omega_b t + \alpha - \omega_b t_s), \tag{2.10.12}$$

$$x_2 \gtreqless d_s,$$

where

$$G_0 = \sqrt{\frac{2hk_0}{W_2}}. \tag{2.10.13}$$

Typical shapes of the acceleration pulse represented by equations (2.10.11) and (2.10.12) are shown in Fig. 2.10.1. The curves are drawn for $d_s/d_0 =$

0.5 and for several values of k_b/k_0. The peak values of the curves are the same as given by equation (1.12.3). The curve marked $k_b/k_0 = 1$ is the sinusoid of the linear case with duration

$$\tau_0 = \frac{\pi}{\omega_0}. \tag{2.10.14}$$

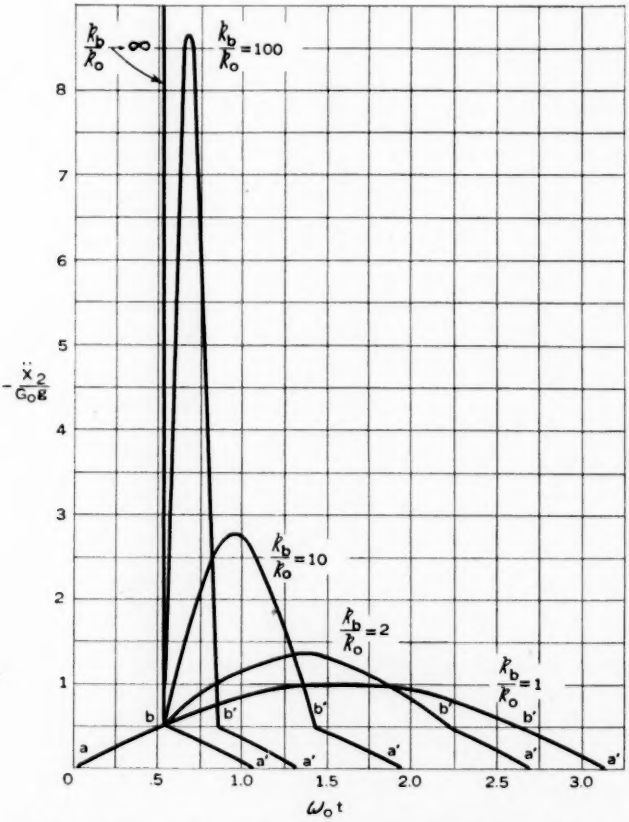

Fig. 2.10.1—Acceleration-time curves for cushioning with bi-linear elasticity. $d_s/d_0 = 0.5$. See equations (2.10.11) and (2.10.12).

As before, if the package does not rebound, the acceleration shown is mirrored in the time axis after each half cycle, to form a vibration of period $2\tau_2$.

It is useful to know the duration of the complete pulse (aa' in Fig. 2.10.1) and also the duration of bottoming (bb' in Fig. 2.10.1). Calling the former τ_2 and the latter τ_B, we have, from equations (2.10.11) and (2.10.12)

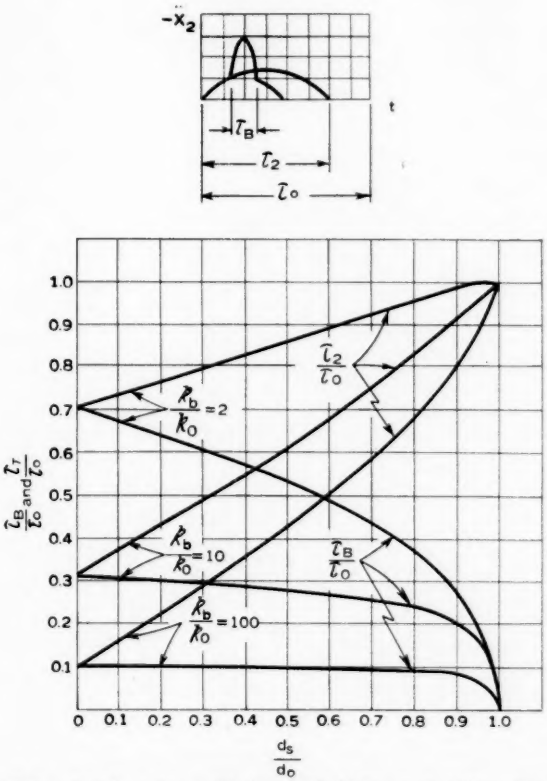

Fig. 2.10.2—Pulse durations for cushioning with bi-linear elasticity. See equations (2.10.15) and (2.10.16).

$$\frac{\tau_2}{\tau_0} = \frac{2}{\pi}\sin^{-1}\frac{d_s}{d_0} + \sqrt{\frac{k_0}{k_b}}\left[1 - \frac{2}{\pi}\tan^{-1}\sqrt{\frac{k_0}{k_b\left(\frac{d_0^2}{d_s^2} - 1\right)}}\right] \tag{2.10.15}$$

$$\frac{\tau_B}{\tau_0} = \sqrt{\frac{k_0}{k_b}}\left[1 - \frac{2}{\pi}\tan^{-1}\sqrt{\frac{k_0}{k_b\left(\frac{d_0^2}{d_s^2} - 1\right)}}\right]. \tag{2.10.16}$$

These two equations are plotted in Fig. 2.10.2 for several values of k_b/k_0.

2.11 Acceleration-Time Relation for Hyperbolic Tangent Elasticity

The relation between acceleration and time for hyperbolic tangent elasticity is found by the same procedure that was used for tangent elasticity

in Section 2.9. The system considered is that shown in Fig. 1.2.1 and the load displacement curve of the cushioning is given by

$$P = P_0 \tanh \frac{k_0 x_2}{P_0}.$$

Substituting the above expression for P in the energy equation (1.2.13), we find the velocity to be

$$\dot{x}_2 = \sqrt{2gh - \frac{2P_0^2}{m_2 k_0} \log \cosh \frac{k_0 x_2}{P_0}}. \tag{2.11.1}$$

Then, as before,

$$t = \int_0^{x_2} \frac{dx_2}{\dot{x}_2} \tag{2.11.2}$$

and the half period (τ_2) of the motion is twice the time required for x_2 to increase from 0 to d_m, or

$$\tau_2 = 2 \int_0^{d_m} \frac{dx_2}{\dot{x}_2}, \tag{2.11.3}$$

where, from Section 1.13,

$$d_m = \frac{d_0 P_0}{W_2 G_0} \cosh^{-1} \exp \left(\frac{W_2^2 G_0^2}{2P_0^2} \right). \tag{1.13.3}$$

The radian frequency of the acceleration is defined as

$$\omega_2 = \frac{\pi}{\tau_2}$$

and this is to be compared with the frequency

$$\omega_0 = \frac{\pi}{\tau_0} = \sqrt{\frac{k_0}{m_2}}$$

that would obtain if the cushioning had a constant spring rate equal to the initial spring rate (k_0) of the hyperbolic tangent cushioning. The ratio ω_0/ω_2 (or τ_2/τ_0) is plotted, in Fig. 2.11.1, against the dimensionless parameter P_0/W_2G_0 (see Section 1.13). It may be observed that the pulse duration becomes very long when P_0/W_2G_0 is small, i.e., when the horizontal portion of the load displacement curve (Fig. 1.4.5) comes into play. The influence on the shape of the acceleration-time curve is illustrated in Fig. 2.11.2. The curve marked $P_0/W_2G_0 \to \infty$ is the sinusoid for the linear case. For small values of P_0/W_2G_0 the curve approaches a square wave.

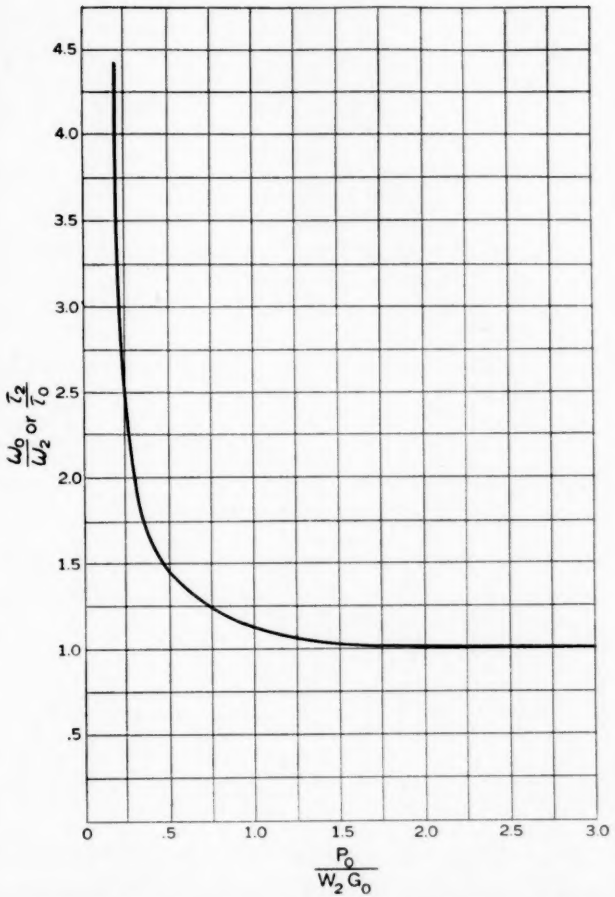

Fig. 2.11.1—Duration of acceleration pulse for cushioning with hyperbolic tangent elasticity.

2.12 Numerical Procedure for Finding Acceleration-Time Relation for Class F Cushioning

When the load-displacement curve does not resemble one of Classes A to E, the acceleration-time relation may be found by numerical integration. Combining the energy equation,

$$\frac{m_2 \dot{x}_2^2}{2} + \int_0^{x_2} P \, dx_2 = m_2 g h, \qquad (1.2.13)$$

with the equation relating time and velocity,

$$t = \int_0^{x_2} \frac{dx_2}{\dot{x}_2}, \tag{2.12.1}$$

we find

$$t = \sqrt{\frac{W_2}{2g}} \int_0^{x_2} \frac{dx_2}{\sqrt{W_2 h - \int_0^{x_2} P\, dx_2}}. \tag{2.12.2}$$

As an example, consider the problem of a 15-pound article supported on cushioning with the load-displacement curve shown in Fig. 2.12.1. The package is to be dropped from a height of 3 feet. The computations are

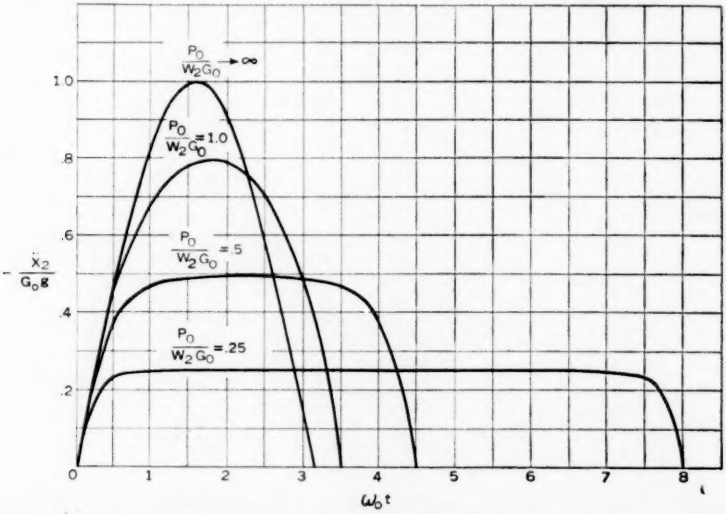

Fig. 2.11.2—Acceleration-time curves for cushioning with hyperbolic tangent elasticity.

given in detail in Tables III and IV. The headings of Columns (1) to (8) of Table III are the same as in Table II, Section 1.15. A_n is the integral under the radical of equation (2.12.2). Column (10) of Table III is the integrand of Equation (2.12.2), i.e., it is proportional to the reciprocal of the velocity expressed as a function of displacement. The function is plotted in Fig. 2.12.2 and its integration is performed in Table IV. In columns (11), (12) and (13), intervals of x_2 are chosen to suit the shape of the curve. The values for column (14) are taken from column (10). Columns (15) and (16) perform the same operations on the integrand $(W_2 h - A_n)^{-\frac{1}{2}}$ that are performed in Columns (5) and (6) of Table III on the integrand P.

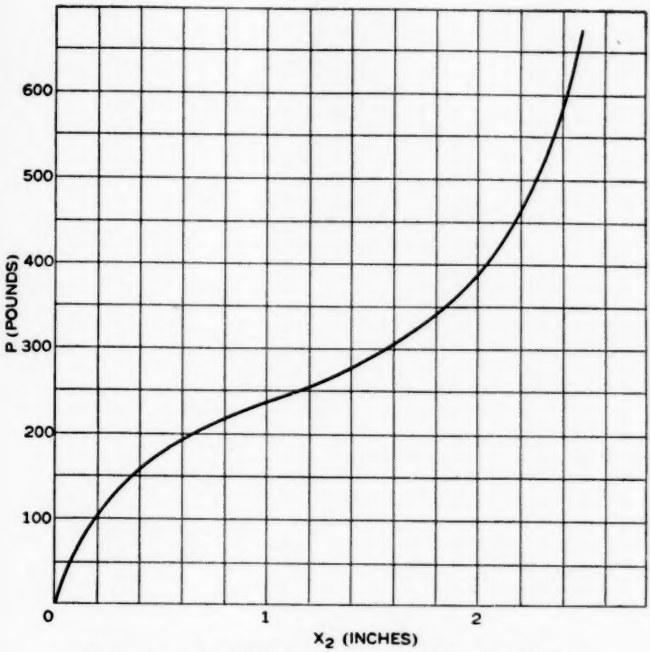

Fig. 2.12.1—A load displacement curve for Class F cushioning.

TABLE III

(1)	(2)	(3)	(4)	(5)	(6)	(7)	(8)	(9)	(10)
n	$\Delta(x_2)_n$	$(x_2)_n$	P_n	$\frac{\Delta(x_2)_n}{2}(P_n + P_{n-1})$	$A_n = \int_0^{(x_2)_n} P dx_2$	$h_n = \frac{A_n}{W_2}$	$G_n = \frac{P_n}{W_2}$	$W_2 h - A_n$	$\frac{1}{\sqrt{W_2 h - A_n}}$
0	0	0.0	0	0	0	0	0	540	0.0431
1	.20	0.2	105	10.5	10.5	0.7	7.0	529.5	0.0435
2	.20	0.4	155	26.0	36.5	2.4	10.3	503.5	0.0446
3	.20	0.6	192	34.7	71.2	4.8	12.8	468.8	0.0462
4	.20	0.8	217	40.9	112.1	7.5	14.5	427.9	0.0483
5	.20	1.0	237	45.4	157.5	10.5	15.8	382.5	0.0511
6	.20	1.2	257	49.4	206.9	13.9	17.1	333.1	0.0547
7	.20	1.4	277	52.9	259.8	17.3	18.5	280.2	0.0597
8	.20	1.6	305	58.2	318.0	21.2	20.3	222.0	0.0671
9	.20	1.8	342	64.7	382.7	25.5	22.8	157.3	0.0798
10	.20	2.0	392	73.4	456.1	30.4	26.1	83.9	0.109
11	.05	2.05	405	19.9	476.0	31.8	27.0	64.0	0.125
12	.05	2.10	422	20.7	496.7	33.2	28.1	43.3	0.152
13	.05	2.15	440	21.6	518.3	34.6	29.4	21.7	0.215
14	.01	2.16	445	4.42	522.7	34.8	29.7	17.3	0.240
15	.01	2.17	450	4.48	527.2	35.2	30.0	12.8	0.279
16	.01	2.18	455	4.52	531.7	35.5	30.3	8.3	0.347
17	.01	2.19	457	4.56	536.3	35.8	30.5	3.7	0.521
18	.01	2.20	462	4.60	540.9	36.1	30.8	0	∞

TABLE IV

(11)	(12)	(13)	(14)	(15)	(16)	(17)
n	$\Delta(x_2)_n$	$(x_2)_n$	$f_n = \frac{1}{\sqrt{W_2 h - A_n}}$	$\frac{\Delta(x_2)_n}{2}(f_n + f_{n-1})$	$D_n = \int_0^{(x_2)_n} \frac{dx_2}{\sqrt{W_2 h - A_n}}$	$t = D_n \times \sqrt{\frac{W_2}{2g}}$
0	0	0	0.0431	0	0	0
1	0.4	0.4	0.0446	0.0175	0.0175	0.0024
2	0.4	0.8	0.0483	0.0185	0.0360	0.0050
3	0.4	1.2	0.0547	0.0206	0.0566	0.0079
4	0.4	1.6	0.0671	0.0243	0.0809	0.0112
5	0.2	1.8	0.0798	0.0149	0.0958	0.0133
6	0.2	2.0	0.109	0.0189	0.1147	0.0160
7	0.1	2.1	0.152	0.0131	0.1278	0.0178
8	0.05	2.15	0.215	0.0092	0.1370	0.0190
9	0.03	2.18	0.347	0.0083	0.1453	0.0202
10	0.01	2.19	0.521	0.0043	0.1496	0.0208
11	0.01	2.20	∞			0.0221

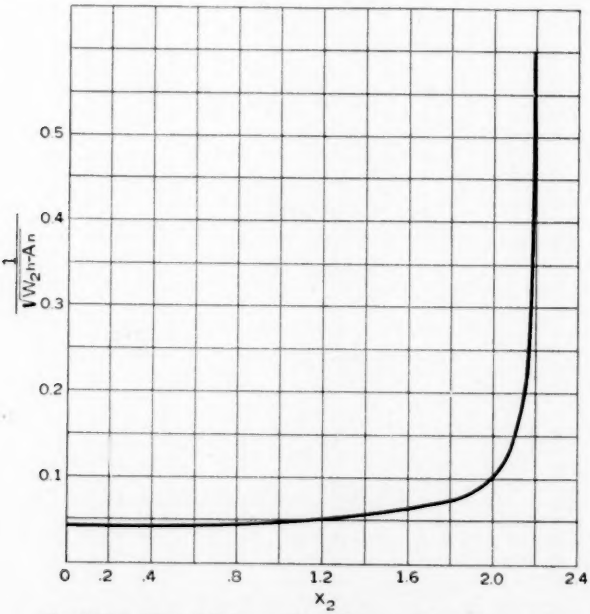

Fig. 2.12.2—Plot of Column (3) vs. Column (10) of Table III.

A difficulty arises because the integrand $(W_2h - A_n)^{-\frac{1}{2}}$ becomes infinite for the maximum displacement (see Column (14)). This is avoided by assuming that the acceleration is constant in the last interval[2] and has the

[2] Timoshenko, "Vibration Problems in Engineering," D. Van Nostrand Co., New York, Second Edition (1937) page 123.

value given in Column (8), Table III, for the maximum height of drop. Then,

$$\Delta(x_2)_n = \tfrac{1}{2} G_m g \Delta t^2 \tag{2.12.3}$$

or

$$\Delta t = \sqrt{\frac{2\Delta(x_2)_n}{G_m g}}. \tag{2.12.4}$$

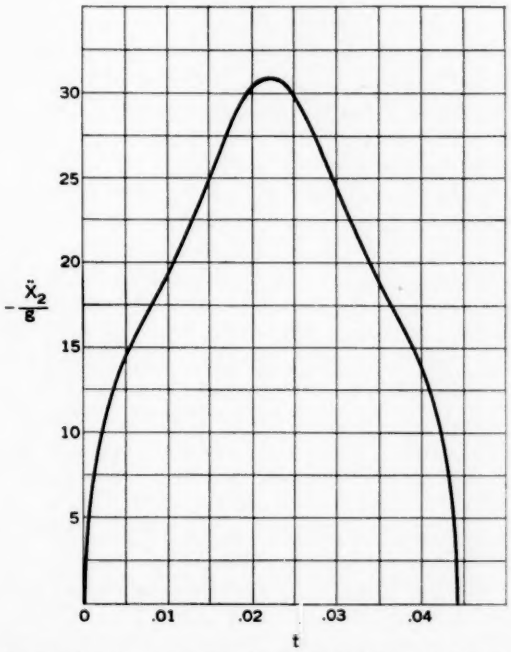

Fig. 2.12.3—Acceleration-time curve (for the cushioning shown in Fig. 2.12.1) obtained by numerical integration.

In the present instance,

$$(\Delta x_2)_n = 0.01 \text{ inches}$$

$$G_m g = 30.8 \times 386 = 11900 \text{ in/sec.}^2$$

Hence, from (2.12.4), $\Delta t = 0.0013$ sec. and the last entry in Column (17) is obtained by adding this value of Δt to the preceding entry.

The final curve of acceleration vs. time is obtained by plotting the entries of Column (17) against the entries of Column (8), Table III, for corresponding values of x_2. The result is shown in Fig. 2.12.3.

PART III

AMPLIFICATION FACTOR

3.1 Introduction

If the maximum acceleration, of the packaged article as a whole, is reached very slowly, the severity of the disturbance experienced by a structural element of the packaged article is very nearly proportional to the maximum acceleration. Roughly speaking, "very slowly" means that the time, during which the acceleration undergoes a major change in magnitude, is long in comparison with the natural period of vibration of the element under consideration. When this is so, no transient vibration is excited in the element. The displacement response of an element under very slowly varying conditions is called the "static response". Under more rapidly varying conditions the dynamic response to the same maximum acceleration may be greater or less than the static response. The ratio (A) of the maximum dynamic response to the static response is called the amplification factor. In general, for a given acceleration disturbance, very low-frequency elements have amplification factors less than unity, while the amplification factors are greater than unity for elements whose natural frequencies are near or above the disturbing frequencies. The numerical value of the amplification factor depends not only on the manner in which the disturbing acceleration varies with time, but also on the "reference acceleration", i.e., the value of acceleration for which the static response is calculated. Usually the reference acceleration chosen for calculating the static response is the maximum value (G_m) of the disturbing acceleration. However, when special circumstances are being investigated, such as the effect of damping or abrupt bottoming, the reference acceleration is taken to be G_0, which is the acceleration that would be reached if the damping or bottoming were absent. In such cases the amplification factor includes both the effect of rate of change of acceleration and the effect of the special conditions.

When the reference acceleration is G_m the amplification factor will be denoted by A_m and when the reference acceleration is G_0 the amplification factor will be denoted by A_0. The symbol G_e will be used to designate the slowly applied acceleration that would produce the same maximum displacement as the transient acceleration, i.e., $G_e = A_m G_m$ or $G_e = A_0 G_0$. The symbol G_s will be used to denote the safe value of G_e, for an element of the packaged article, as determined by a strength test or by calculation. In specifying G_s some judgement is required to take into account the effects of plastic deformation in comparing tests made on greatly different time scales. Good judgement is also necessary in deciding whether or not the

assumptions listed in Section 0.2 are valid in each application. The general procedure for using amplification factors is as follows. We first find the value of the reference acceleration (in units of *number of times gravity*) from Part I. From Part II we find the properties of the acceleration-time relation which give us the information required for entering one of the curves of Part III and finding the amplification factor. Then, the product of the reference acceleration and the amplification factor ($A_m G_m$ or $A_0 G_0$) is a number (G_e) by which the weight of the structure is to be multiplied when calculating its deflection or stress by the usual static methods of elementary strength of materials. Alternatively, G_e must be found not to exceed G_s.

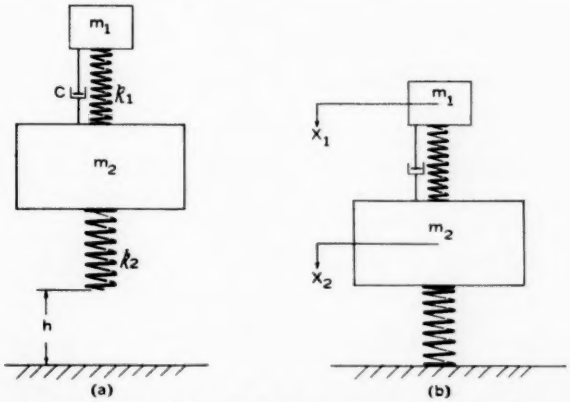

Fig. 3.2.1—Idealized system used in calculating amplification factors for linear undamped cushioning with perfect rebound. (a) initial position, (b) first contact with floor.

In the following sections the amplification factors for typical transient accelerations encountered in package drop tests are calculated. The amplification factor curves that are plotted are entirely analogous to the familiar "resonance curves" for steady sinusoidal vibration, except that in this case the disturbing forces are transients of various shapes. It will be seen from the curves that the maximum acceleration, as calculated by the methods of Part I or as measured by an accelerometer, is not always a true measure of the severity of the disturbance.

3.2 Amplification Factors for a Half-Sine-Wave Pulse Acceleration

The first case to be treated is the response of an element of the packaged item to the transient acceleration that would occur in a package with linear

undamped cushioning and perfect rebound. Figure 3.2.1 illustrates the idealized system, and it may be noted that the mass m_3 is omitted, as is required for perfect rebound (Section 2.3). At first we shall consider that the mass m_1 is undamped and later we shall consider the effect of damping in this element.

The mass m_1 is taken to be small in comparison with m_2, so that the motion of the latter is the same as we found it to be in Section 2.2 where m_1 was not considered. Hence the acceleration of m_2 is a half-sine wave pulse:

$$\ddot{x}_2 = -\omega_2 \sqrt{2gh} \sin \omega_2 t, \qquad (0 \leqq t \leqq \pi/\omega_2). \tag{3.2.1}$$

The equation of motion of m_1 is

$$m_1\ddot{x}_1 + k_1(x_1 - x_2) = 0. \tag{3.2.2}$$

Let x be the relative displacement of m_1 with respect to m_2, i.e.,

$$x = x_1 - x_2 . \tag{3.2.3}$$

x is proportional to the force in the spring (k_1x) and to the acceleration of m_1 and hence is proportional to the deflection, strain and stress in the element which the system m_1, k_1 represents.

Substituting (3.2.3) in (3.2.2), we find:

$$m_1\ddot{x} + k_1x = -m_1\ddot{x}_2 . \tag{3.2.4}$$

This equation holds for the duration π/ω_2 of the pulse $\ddot{x}_2$. The initial conditions for x are

$$[x]_{t=0} = [\dot{x}]_{t=0} = 0 \tag{3.2.5}$$

so that the solution of (3.2.4) is

$$x = \frac{\omega_2 \sqrt{2gh}}{\omega_2^2 - \omega_1^2}\left[\frac{\omega_2}{\omega_1} \sin \omega_1 t - \sin \omega_2 t\right], \qquad \left(0 \leqq t \leqq \frac{\pi}{\omega_2}\right). \tag{3.2.6}$$

It may be seen that x is composed of a forced displacement at the acceleration frequency ω_2, on which is superposed a free vibration at the natural frequency, ω_1, of the element. The maximum value of the relative displacement is

$$x_{\max} = \frac{\sqrt{2gh}}{\omega_1\left(\frac{\omega_1}{\omega_2} - 1\right)} \sin \frac{2n\pi}{\frac{\omega_1}{\omega_2} + 1}, \qquad \left(0 \leqq t \leqq \frac{\pi}{\omega_2}\right), \tag{3.2.7}$$

in which n is a positive integer chosen so as to make the sine term as large as possible while the argument remains less than π.

(3.2.7) gives the maximum dynamic response of the element m_1 during the interval of impact. To find the amplification factor we must compare

x_{max} with the "static response" i.e. with the value (x_{st}) that x would have if the acceleration $\ddot{x}_2$ reached the same maximum value $(\omega_2\sqrt{2gh})$ in a very long time. The resulting value may be found from (3.2.4) by omitting the transient term $m_1\ddot{x}$. Then

$$x_{st} = \omega_2 \sqrt{2gh}\,\frac{m_1}{k_1}$$

or

$$x_{st} = \frac{\omega_2}{\omega_1^2}\sqrt{2gh}. \tag{3.2.8}$$

The amplification factor for the interval $0 \leqq t \leqq \pi/\omega_2$ is then

$$A_m = \frac{x_{max}}{x_{st}} = \frac{\dfrac{\omega_1}{\omega_2}}{\dfrac{\omega_1}{\omega_2} - 1} \sin\frac{2n\pi}{\dfrac{\omega_1}{\omega_2} + 1}, \qquad (0 \leqq t \leqq \pi/\omega_2). \tag{3.2.9}$$

It should be observed that A_m depends only on the frequency ratio ω_1/ω_2. That is, since $\omega_1/\omega_2 = \tau_2/\tau_1$, the amplification factor depends only on the ratio of the pulse duration to the half period of vibration of the element.

Thus far we have studied only the motion in the interval $0 \leqq t \leqq \pi/\omega_2$. We must not, however, overlook the possibility of larger displacements of m_1 with respect to m_2 occurring after rebound. In fact, examination of (3.2.6) reveals that x has no maximum in the interval $0 \leqq t \leqq \pi/\omega_2$ when $\omega_1 < \omega_2$. It is very likely, then, that larger values will occur at later times.

After rebound, m_1 executes free vibrations with respect to m_2. We have to compare the magnitude of x_{max}, in the interval $0 \leqq t \leqq \pi/\omega_2$, with the amplitude of the free vibration. Calling the relative displacement during free vibration x' and measuring a time coordinate t' from the instant the package leaves the floor, we have

$$m_1\ddot{x}' + k_1x' = 0, \tag{3.2.10}$$

with initial conditions

$$\begin{aligned} [x']_{t'=0} &= [x]_{t=\pi/\omega_2}, \\ [\dot{x}']_{t'=0} &= [\dot{x}]_{t=\pi/\omega_2}. \end{aligned} \tag{3.2.11}$$

The solution of (3.2.10) with initial conditions (3.2.11) is

$$\begin{aligned} x' &= \frac{\omega_2^2\sqrt{4gh\left(1 + \cos\dfrac{\omega_1}{\omega_2}\pi\right)}}{\omega_1(\omega_2^2 - \omega_1^2)} \sin\left(\omega_1 t' + \frac{\omega_1\pi}{2\omega_2}\right), \\ t &\geqq \frac{\pi}{\omega_2}. \end{aligned} \tag{3.2.12}$$

Then

$$A_m = \frac{x'_{max}}{x_{st}} = \frac{2\frac{\omega_1}{\omega_2}\cos\frac{\pi\omega_1}{2\omega_2}}{1-\frac{\omega_1^2}{\omega_2^2}}, \qquad \left(t \leqq \frac{\pi}{\omega_2}\right). \tag{3.2.13}$$

We find, on comparing (3.2.13) with (3.2.9) that for $\omega_1 < \omega_2$ equation (3.2.13) gives the larger value of A_m, while for $\omega_1 > \omega_2$ equation (3.2.9)

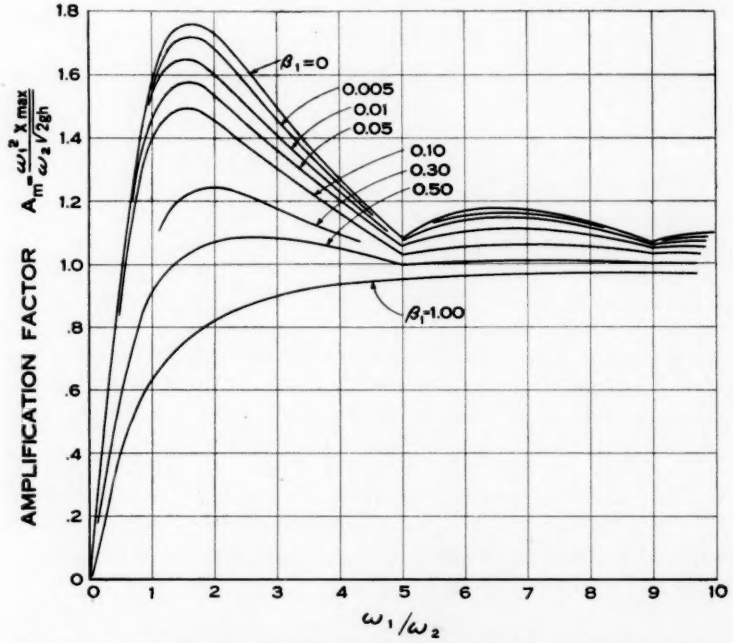

Fig. 3.2.2—Amplification factors for linear undamped cushioning with perfect rebound. See Fig. 3.2.1 and equations (3.2.9) and (3.2.13).

gives the larger value of A_m. That is, when the duration of impact is shorter than the half-period of vibration of the element, the maximum displacement (and stress) in the element occurs after the impact is over.

The curve marked $\beta_1 = 0$ in Fig. 3.2.2 is a plot of the largest value of A_m from (3.2.9) and (3.2.13) with the frequency ratio ω_1/ω_2 as abscissa. (3.2.13) was used for $\omega_1/\omega_2 \leqq 1$ and (3.2.9) for $\omega_1/\omega_2 \geqq 1$. The maximum value of A_m is 1.76 and occurs at $\omega_1/\omega_2 = 1.6$. Hence, at this frequency ratio, the deformation of the element is 1.76 times as great as would be expected from a calculation using the maximum value of acceleration alone as in Part I.

On the other hand, for frequency ratios $\omega_1/\omega_2 < 0.5$ the severity of the shock can be very much less than might be expected from the calculations of Part I. For very small values of ω_1/ω_2 the amplification factor may be seen from (3.2.13) to be equal to $2\omega_1/\omega_2$. For large values of ω_1/ω_2 (stiff elements) Fig. 3.2.2 shows that the amplification factor is very nearly unity and the methods of Part I can be used without additional calculation.

When damping of the element of the packaged article is considered, the amplification factors are less than without damping. The applicable equations of motion during and after impact are obtained by inserting velocity damping terms in (3.2.4) and (3.2.10):

$$m_1\ddot{x} + c_1\dot{x} + k_1x = -m_1\ddot{x}_2, \qquad 0 \leqq t \leqq \frac{\pi}{\omega_2} \tag{3.2.14}$$

$$m_1\ddot{x}' + c_1\dot{x}' + k_1x' = 0, \qquad t \geqq \frac{\pi}{\omega_2}. \tag{3.2.15}$$

If we express the damping of the element m_1 as the fraction of critical damping

$$\beta_1 = \frac{c_1}{2\sqrt{m_1k_1}}, \tag{3.2.16}$$

(as in Section 2.5) equations (3.2.14) and (3.2.15) become

$$\ddot{x} + 2\beta_1\omega_1\dot{x} + \omega_1^2x = -\ddot{x}_2, \qquad 0 \leqq t \leqq \frac{\pi}{\omega_2}, \tag{3.2.17}$$

$$\ddot{x}' + 2\beta_1\omega_1\dot{x}' + \omega_1^2x' = 0, \qquad t \geqq \frac{\pi}{\omega_2}. \tag{3.2.18}$$

The amplification factors for equations (3.2.17) and (3.2.18), with boundary conditions (3.2.5) and (3.2.11), respectively, were obtained on the Westinghouse Mechanical Transients Analyzer[3] for $\beta_1 = 0.005, 0.01, 0.05, 0.10, 0.30, 0.50$ and 1.00. The curves are shown in Fig. 3.2.2.

3.3 Application of Half-Sine-Wave Amplification Factors

As an example of the use of the amplification factor curves of Fig. 3.2.2, let us consider the following problem:

[3] Arrangements for performing these calculations were made through the courtesy of Mr. A. C. Monteith, Manager of Industry Engineering, and Mr. C. F. Wagner, Manager of Central Station Engineering, Westinghouse Electric and Manufacturing Co. Dr. G. D. McCann, Transmission Engineer, was in immediate charge of the project. For a description of the analyzer see "A New Device for the Solution of Transient-Vibration Problems by the Method of Electrical-Mechanical Analogy" by H. E. Criner, G. D. McCann and C. E. Warren, *Journal of Applied Mechanics*, Vol. 12, No. 3 (1945) pp. A-135 to A-141.

It is required to judge the suitability of a proposed package for a large vacuum tube weighing 10 pounds. Strength tests have been made on the tube in a shock testing machine which produces a half-sine-wave acceleration pulse of 25 milliseconds duration. The weakest element of the tube is found to be the cathode structure, for which the safe maximum acceleration in the drop testing machine is 200g. The cathode structure has a natural vibration frequency of 120 cycles per second and has 1% of critical damping. The proposed package has essentially linear, undamped cushioning with a spring rate of 3300 pounds per inch and an available displacement of $\frac{3}{4}$ inch. The outer container weighs much less than the tube so that the package may be expected to rebound. Is the cushioning suitable for protecting the cathode in a drop of 5 feet?

First find the maximum G that the tube will experience in a 5 ft. drop of the package (equation 1.3.3):

$$G_m = \sqrt{\frac{2hk_2}{W_2}} = \sqrt{\frac{2 \times 60 \times 3300}{10}} = 199.$$

The accompanying maximum displacement is, from equation (1.3.4),

$$d_m = \frac{2h}{G_m} = \frac{2 \times 60}{199} = 0.6 \text{ in.}$$

The available displacement ($\frac{3}{4}$ inches) is therefore sufficient and the maximum acceleration (199g) is slightly less than the safe maximum acceleration (200g) found with the shock testing machine. However, before the cushioning is approved it is necessary to investigate the frequency effects. The duration of acceleration in both the shock machine and in the package must be considered.

The amplification factor for the element tested in the shock machine is found as follows. First find the frequency corresponding to the 25 millisecond pulse:

$$f_2 = \frac{1}{2 \times .025} = 20 \text{ c.p.s.}$$

The ratio of the element frequency to the shock machine frequency is

$$\frac{f_1}{f_2} = \frac{\omega_1}{\omega_2} = \frac{120}{20} = 6.$$

Entering Fig. 3.2.2 with $\omega_1/\omega_2 = 6$, we read, from the curve $\beta_1 = 0.01$, $A_m = 1.14$. The 200g test in the shock machine is, therefore, equivalent to a slowly applied acceleration of $G_s = 200 \times 1.14 = 228g$.

To find the corresponding quantity for the package drop, first find the cushion frequency:

$$f_2 = \frac{1}{2\pi}\sqrt{\frac{k_2}{m_2}} = \frac{1}{2\pi}\sqrt{\frac{3300 \times 386}{10}} = 57 \text{ c.p.s.}$$

The ratio of the element frequency to the package frequency is therefore

$$\frac{f_1}{f_2} = \frac{\omega_1}{\omega_2} = \frac{120}{57} = 2.1.$$

Entering Fig. 3.2.2 with $\omega_1/\omega_2 = 2.1$ we read, from the curve $\beta_1 = 0.01$, $A_m = 1.59$. The $199g$ acceleration pulse in the package drop is therefore equivalent to a slowly applied acceleration of $G_e = 199 \times 1.59 = 316g$. This is almost 40% in excess of the value ($228g$) found to be safe from the shock machine data. The cushioning is therefore judged to be inadequate. The procedure for finding the correct spring rate for the cushioning is as follows. It is known that we must have

$$G_e \gtrless G_s.$$

Therefore, take

$$G_e = A_m G_m = 228.$$

Now

$$G_m = \sqrt{\frac{2hk_2}{W_2}} = \omega_2\sqrt{\frac{2h}{g}}.$$

Therefore

$$A_m\omega_2 = 409 \text{ rad/sec.}$$

Also

$$\omega_1 = 2\pi \times 120 = 754 \text{ rad/sec.}$$

Then, with successive trial values of ω_2, we calculate ω_1/ω_2, enter Fig. 3.2.2, read the corresponding value of A_m from curve $\beta_1 = 0.01$ and test to see if the product $A_m\omega_2 = 409$. The combination which satisfies the test is found to be

$$\omega_2 = 280 \text{ rad/sec.}$$

$$\omega_1/\omega_2 = 2.69$$

$$A_m = 1.47.$$

Then

$$k_2 = \omega_2^2 m_2 = \frac{(280)^2 \times 10}{386} = 2030 \text{ lbs./in.}$$

$$G_m = \sqrt{\frac{2hk_2}{W_2}} = 155$$

$$d_m = \frac{2h}{G_m} = .77 \text{ in.}$$

Hence the spring rate of the cushioning should be reduced from 3300 lbs./in. to 2030 lbs./in. and the available space should be increased to accomodate the 0.77 inch maximum displacement before bottoming.

3.4 Special Treatment of Strong, Low Frequency Elements

The product of the amplification factor (A_m) and the maximum acceleration (G_m) must be equal to or less than the maximum allowable slowly applied acceleration (G_s):

$$G_e = A_m G_m \leqq G_s . \tag{3.4.1}$$

For frequency ratios

$$\frac{\omega_1}{\omega_2} < \frac{1}{2}, \tag{3.4.2}$$

Figure 3.2.2 shows that, approximately,

$$A_m = 2\frac{\omega_1}{\omega_2} \tag{3.4.3}$$

for $\beta_1 \lessapprox 0.10$. When this is so, we may combine (3.4.1) and (3.4.3) to obtain the criterion

$$2\frac{\omega_1}{\omega_2} G_m \lessapprox G_s . \tag{3.4.4}$$

Now,

$$G_m = \sqrt{\frac{2hk_2}{W_2}} = \omega_2 \sqrt{\frac{2h}{g}} . \tag{3.4.5}$$

Hence the criterion (3.4.4) may be written as

$$2\omega_1 \sqrt{\frac{2h}{g}} \lessapprox G_s \tag{3.4.6}$$

or

$$f_1 \lessapprox \frac{1.1\, G_s}{\sqrt{h}} \tag{3.4.7}$$

where h is in inches and f_1 is in cycles per second.

It may be observed that (3.4.7) *is independent of the properties of the cushioning.* Hence, as long as (3.4.2) is satisfied, any cushioning at all may be used for an element that satisfies (3.4.7) regardless of the magnitude of the maximum acceleration G_m. In particular, rigid mounting is suitable for such an element. The only precaution to be observed is that the maximum acceleration and duration must not be unfavorable for other elements of the packaged article.

Example: A 9-pound vacuum tube has an anode structure for which the safe maximum acceleration is $200g$ as determined in a centrifuge test. The natural vibration frequency of the anode is 35 cycles per second and the damping is 1% of critical. What cushioning around the tube is required to protect the anode from damage in a package drop of 3 feet?

Calculate

$$\frac{1.1G_s}{\sqrt{h}} = \frac{1.1 \times 200}{\sqrt{36}} = 36.7 \text{ c.p.s.}$$

This is greater than $f_1 = 35$ c.p.s and hence any cushioning is safe for the anode. The results of calculations for cushioning with spring rates of 50, 500, 5000, 5×10^5 and 5×10^7 pounds per inch are given in the following table:

k_2(lbs./in.)	G_m	$\frac{\omega_1}{\omega_2}$	A_m	A_mG_m
50	20	4.74	1.12	22
500	63	1.47	1.65	106
5×10^3	200	.474	0.9	180
5×10^5	2,000	.0474	0.09	180
5×10^7	20,000	.0047	0.009	180

In each case the product of A_mG_m is less than the allowable 200 and, as long as the combination of G_m and the amplification factors for other elements does not exceed the allowable A_mG_m for those elements, the cushioning is suitable. The precaution to observe is that higher-frequency elements shall not have amplification factors such that A_mG_m may be excessive for them.

3.5 Amplification Factors for Damped Sinusoidal Acceleration

If the outer container of the package is heavy enough (see Section 2.3) there will be no rebound and the packaged item will vibrate in the cushioning after impact. For linear cushioning with velocity damping, the acceleration produced by the vibration will be a damped sinusoid (equation (2.5.5) and Fig. 2.5.2). The system to be considered is shown in Fig. 3.5.1. To determine the effect of the damped vibration of m_2 on the mass m_1,

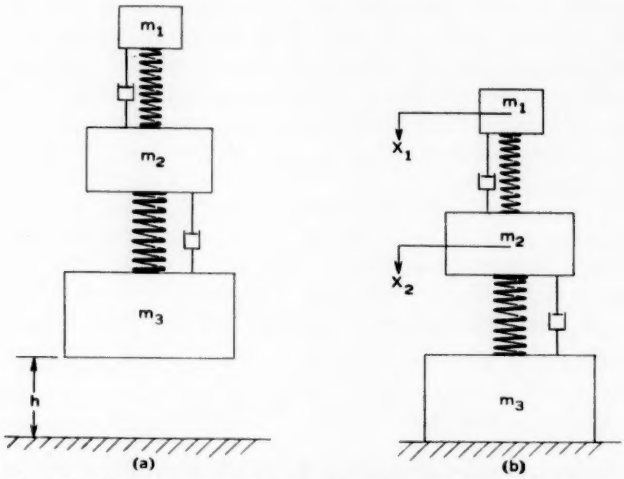

Fig. 3.5.1—Idealized system for linear damped cushioning with no rebound. (a) initial position, (b) first contact with floor.

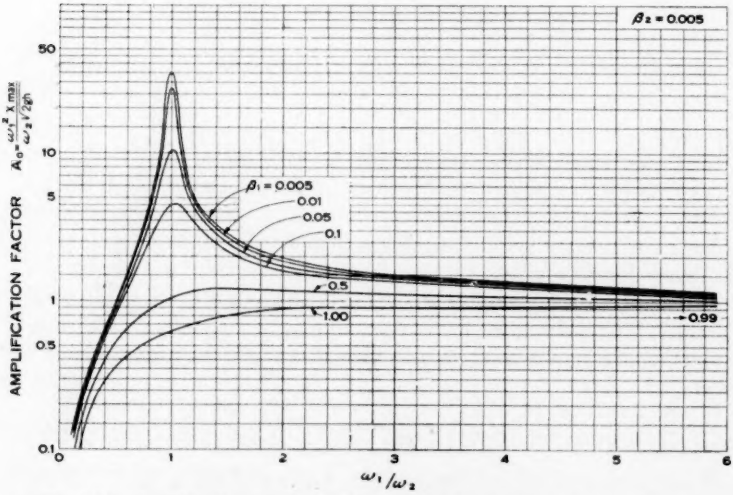

Fig. 3.5.2—Amplification factors for linear damped cushioning with no rebound. $\beta_2 = 0.005$. See equations (3.5.1) and (3.5.2).

we note that the equation of motion and initial conditions are identical with (3.2.17) except that for the acceleration $\ddot{x}_2$ we use the damped sinusoid, equation (2.5.5), instead of the half-sine pulse (3.2.1). The solution of (3.2.17), i.e. the relative displacement $(x_1 - x_2)$ of m_1 with respect to m_2, is

$$x = \frac{\omega_2^2 \sqrt{2gh}}{2\omega_2' \omega_1'} \{e^{-\beta_1 \omega_1 t}[A \sin(\omega_1' t + \gamma - \delta) + B \sin(\omega_1' t - \gamma - \zeta)] - e^{-\beta_2 \omega_2 t}[A \sin(\omega_2' t + \gamma - \delta) - B \sin(\omega_2' t + \gamma + \zeta)]\} \quad (3.5.1.)$$

where

$$\omega_1 = \sqrt{\frac{k_1}{m_1}}$$

$$\omega_2 = \sqrt{\frac{k_2}{m_2}}$$

$$\omega_1' = \omega_1 \sqrt{1 - \beta_1^2}$$

$$\omega_2' = \omega_2 \sqrt{1 - \beta_2^2}$$

$$1/A = \sqrt{(\beta_2 \omega_2 - \beta_1 \omega_1)^2 + (\omega_1' - \omega_2')^2}$$

$$1/B = \sqrt{(\beta_2 \omega_2 - \beta_1 \omega_1)^2 + (\omega_1' + \omega_2')^2}$$

$$\tan \gamma = \frac{2\beta_2^2 - 1}{2\beta_2 \sqrt{1 - \beta_2^2}}$$

$$\tan \delta = \frac{\omega_1' - \omega_2'}{\beta_2 \omega_2 - \beta_1 \omega_1}$$

$$\tan \zeta = \frac{\omega_1' + \omega_2'}{\beta_2 \omega_2 - \beta_1 \omega_1}.$$

The relative displacement of m_1 with respect to m_2 is seen to consist of a forced, damped vibration (ω_2, β_2) on which is superposed the free damped oscillations (ω_1, β_1) of m_1.

The amplification factor

$$A_0 = \frac{x_{\max}}{x_{st}} = \frac{\omega_1^2 x_{\max}}{\omega_2 \sqrt{2gh}} \quad (3.5.2)$$

is plotted in Figs. 3.5.2 to 3.5.7 for six values of β_1 and six values of β_2. These curves were obtained by direct solution of the differential equation on the Westinghouse Mechanical Transients Analyzer.[4] The amplification factor in this case includes the effect of damping; i.e., the reference acceleration is not the maximum acceleration of m_2, but is the maximum acceleration that m_2 would reach if the damping β_2 were zero. Consequently, the amplification factors for large values of ω_1/ω_2 do not approach

[4] See footnote, Section 3.2. Only enough data were obtained with the analyzer to find the general shapes of the curves, so that the fine structure is not revealed. Checks on the analyzer results were made by computing A_0 from equations (3.5.1) and (3.5.2) for $\omega_1/\omega_2 = 1$, $\beta_1 = \beta_2$; $\omega_1/\omega_2 = 0$; $\omega_1/\omega_2 \to \infty$.

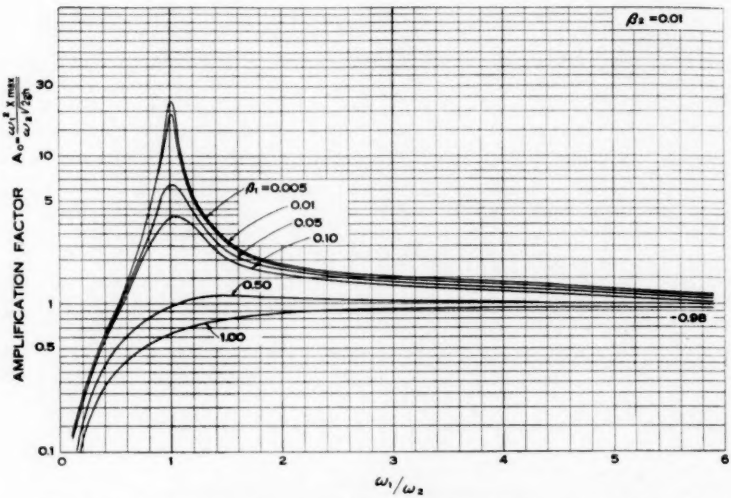

Fig. 3.5.3—Amplification factors for linear damped cushioning with no rebound. $\beta_2 = 0.01$. See equations (3.5.1) and (3.5.2).

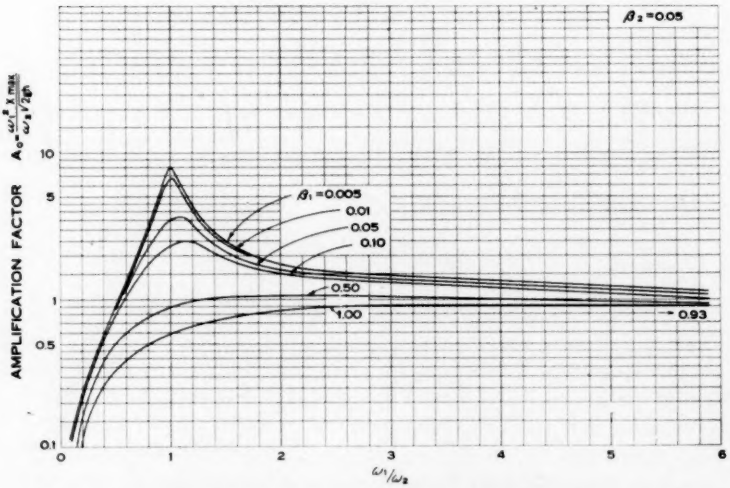

Fig. 3.5.4—Amplification factors for linear damped cushioning with no rebound. $\beta_2 = 0.05$. See equations (3.5.1) and (3.5.2).

unity. For example, the curve for $\beta_1 = 0.005, \beta_2 = 1$ (Fig. 3.5.7) approaches a value of nearly four as $\omega_1/\omega_2 \to \infty$. The factor four is composed of two

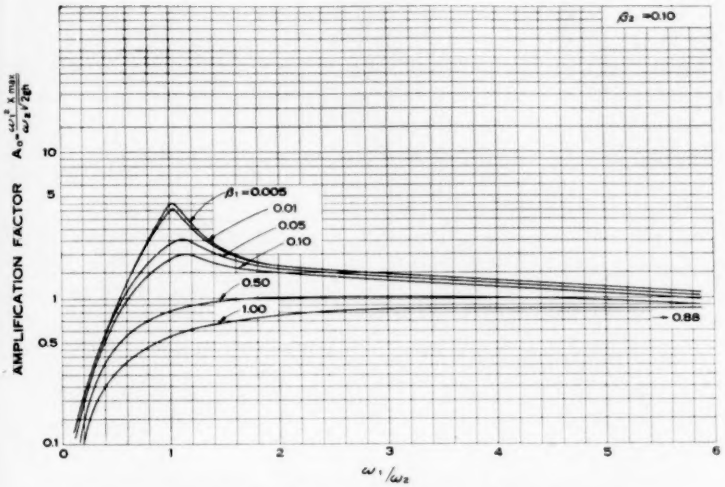

Fig. 3.5.5—Amplification factors for linear damped cushioning with no rebound. $\beta_2 = 0.1$. See equations (3.5.1) and (3.5.2).

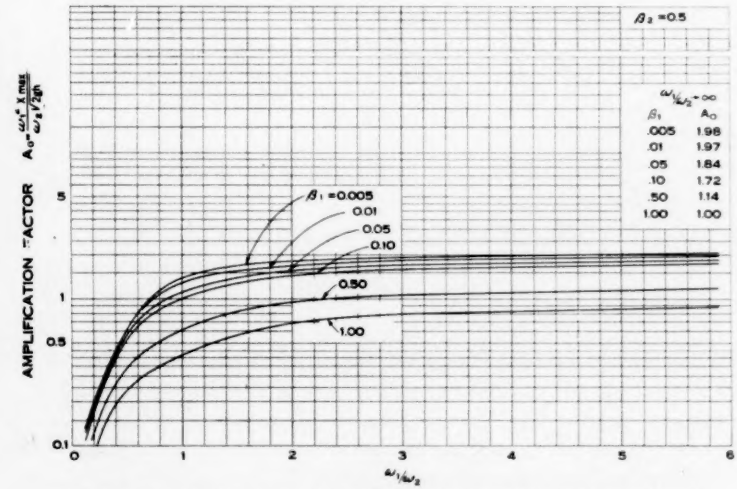

Fig. 3.5.6—Amplification factors for linear damped cushioning with no rebound. $\beta_2 = 0.5$. See equations (3.5.1) and (3.5.2).

factors of two. The first arises from the fact that the maximum value of acceleration, for $\beta_2 = 1$, is twice the value that would be reached if β_2

were equal to zero (see Fig. 2.5.3). The second factor (of nearly two) is due to the fact that the maximum acceleration is reached at time $t = 0$ when $\beta_2 = 1$ (see Fig. 2.5.2) and the response of an almost undamped system ($\beta_1 = 0.005$) to a suddenly applied and subsequently maintained acceleration is double the response to a slowly applied acceleration (see curve (a) Fig. 3.8.1). For $\beta_1 > 0$ and $\beta_2 < 1$ the amplification factor is less than four, as $\omega_1/\omega_2 \to \infty$, in accordance with the curves plotted in Fig. 3.5.8.

Example: A 1.5-pound vacuum tube is to be packed in a container whose estimated weight will be at least 50 pounds. The cathode structure of the tube has a natural frequency of 25 c.p.s. with damping 0.5% of critical

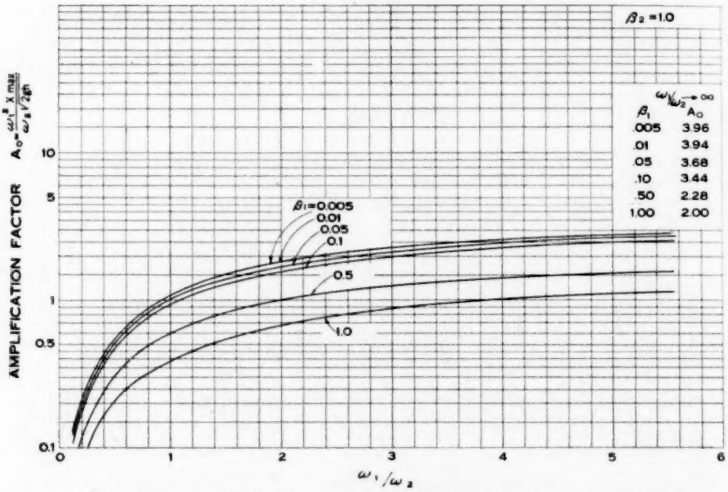

Fig. 3.5.7—Amplification factors for linear damped cushioning with no rebound. $\beta_2 = 1.0$. See equations (3.5.1) and (3.5.2).

and its safe acceleration, as determined in a centrifuge, is 90g. What spring rate of cushioning is suitable for protecting the cathode in a drop of five feet? It is specified that the cushioning shall have damping 50% of critical.

Assuming linear cushioning, the spring rate that would be prescribed, by considering maximum acceleration alone, is

$$k_2 = \frac{W_2 G_m^2}{2h} = \frac{1.5 \times (90)^2}{2 \times 60} = 101 \text{ lbs./in.}$$

Considering damping, Fig. 2.5.3 shows that 50% of critical damping does

not change G_m. To find the amplification factor we must first decide if the package will rebound. With 50% of critical damping, the maximum ac-

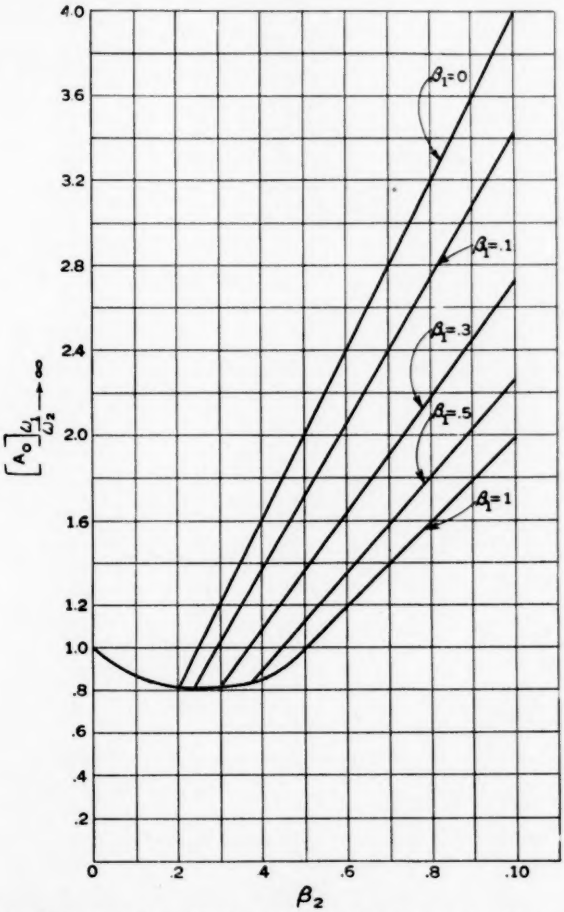

Fig. 3.5.8—Limiting values of amplification factors for linear damped cushioning with no rebound. $\omega_1/\omega_2 \to \infty$. See equations (3.5.1) and (3.5.2).

celeration on the first upstroke is 0.164 G_m (see Section 2.6 and Fig. 2.6.1). Then, $0.164 \times 90 \times 1.5 = 22$ lbs. which is less than the estimated weight of the outer container. The package will not rebound and Fig. 3.5.6 should be used for the amplification factor.

The frequency of vibration of the tube in its cushion will be

$$\omega_2 = \sqrt{\frac{k_2}{m_2}} = \sqrt{\frac{101 \times 386}{1.5}} = 159 \text{ rad./sec.}$$

Hence $\omega_1/\omega_2 = 2\pi \times 25/159 = 0.99$ and, from Fig. 3.5.6, $A_0 = 1.4$. Hence $G_e = 90 \times 1.4 = 126$, which is greater than the allowable $G_s = 90$, so that the 101 lb./in. cushion is unsatisfactory.

To obtain satisfactory cushioning, set

$$A_0 G_0 = 90,$$

that is

$$A_0 \omega_2 = \frac{90}{\sqrt{\frac{2h}{g}}} = 159 \text{ rad./sec.}$$

Noting that $\omega_1 = 2\pi \times 25 = 157$, we find from Fig. 3.5.6 that there are two values of ω_2 (90 and 600 rad/sec.) that satisfy the criterion $A_0\omega_2 = 159$ rad/sec. The first gives

$$\omega_2 = 90 \text{ rad/sec.}$$
$$A_0 = 1.8$$
$$k_2 = 31.5 \text{ lbs./in.}$$
$$G_0 = 50$$
$$G_e = 90$$
$$d_m = 2.4 \text{ in.}$$

The second gives

$$\omega_2 = 600 \text{ rad/sec.}$$
$$A_0 = 0.27$$
$$k_2 = 1400 \text{ lbs./in.}$$
$$G_0 = 335$$
$$G_e = 90$$
$$d_m = 0.36 \text{ in.}$$

The second solution requires less space for cushioning than the first but should be used only if the remainder of the tube can endure the high acceleration of $335g$. Otherwise the $50g$ package should be used.

3.6 Amplification Factors for the Pulse Acceleration of Cubic Cushioning

In a rebounding package with undamped Class B cushioning, the packaged article (m_2) will undergo a pulse acceleration of duration π/ω_2 as given by equation (2.8.11). The shape of the pulse is illustrated in Fig. 2.8.2 and its functional form is

$$\ddot{x}_2 = \frac{4K^2\omega_2^2 d_m}{\pi^2}\left[2k^2 sn^2\left(\frac{2K\omega_2 t}{\pi} - K\right) - 1\right] cn\left(\frac{2K\omega_2 t}{\pi} - K\right). \quad (2.8.14)$$

To determine the influence of the shape and duration of this pulse on the amplification factor, we proceed as before by substituting (2.8.14) in the

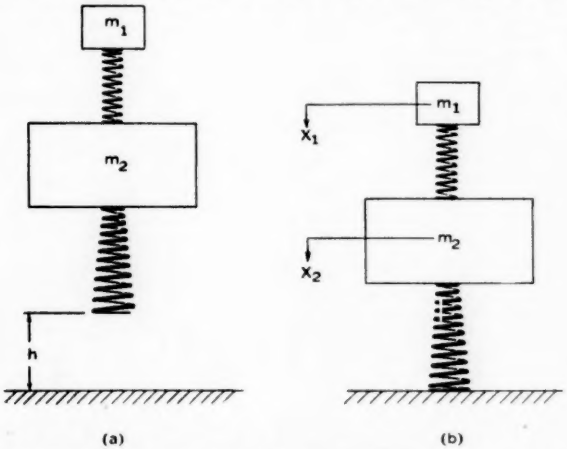

Fig. 3.6.1—Idealized system used in calculating amplification factors for non-linear, undamped cushioning with perfect rebound.

differential equation governing the relative displacement ($x = x_1 - x_2$) between m_1 and m_2 (see Fig. 3.6.1):

$$\ddot{x} + \omega_1^2 x = -\ddot{x}_2\,. \quad (3.6.1)$$

With boundary conditions $x(0) = \dot{x}(0) = 0$, the solution of (3.6.1) may be written as

$$x = \frac{1}{\omega_1}\int_0^t \ddot{x}_2(\lambda)\,\sin\,\omega_1(\lambda - t)\,d\lambda \quad (3.6.2)$$

and the maximum value of x may be expressed by

$$x_{max} = \frac{1}{\omega_1}\int_0^{t_m} \ddot{x}_2(\lambda)\,\sin\,\omega_1(\lambda - t_m)\,d\lambda, \quad (3.6.3)$$

where t_m is the time at which the largest value of x occurs.

The amplification factor, in this case, will be taken as the ratio of x_{max} to the relative displacement (x_{st}) resulting from a slow application of the maximum value of $\ddot{x}_2$. From (3.6.1),

$$x_{st} = \frac{|\ddot{x}_2|_{max}}{\omega_1^2} = \frac{G_m g}{\omega_1^2}, \tag{3.6.4}$$

where G_m is given by equation (1.5.6). Then

$$A_m = \frac{x_{max}}{x_{st}} = \frac{x_{max}\,\omega_1^2}{G_m g} \tag{3.6.5}$$

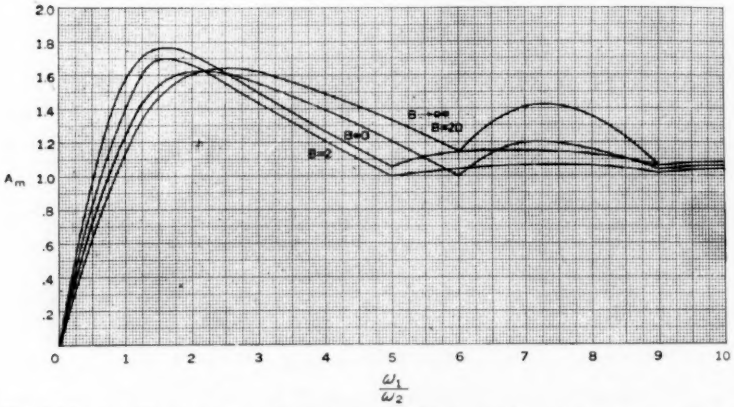

Fig. 3.6.2—Amplification factors for undamped cushioning with cubic elasticity. Perfect rebound. See equation (3.6.6).

or

$$A_m = \frac{\omega_1}{G_m g} \int_0^{t_m} \ddot{x}_2(\lambda) \sin \omega_1(\lambda - t_m)\, d\lambda. \tag{3.6.6}$$

A_m was evaluated, mostly by graphical methods, for four values of B (0, 2, 20 and ∞) and the results are plotted in Fig. 3.6.2. Observing that $B = 0$ corresponds to linear cushioning, it may be noted that cubic non-linearity in the cushioning does not change the amplification factor by more than 35% even in the most extreme case ($B \to \infty$). The severity of the shock, however, may be much greater for the cubic cushioning than for linear cushioning with a spring rate equal to the initial spring rate (k_0) of the cubic cushioning. This is because A_m is multiplied by G_m to obtain G_e and, for large values of B, G_m may be much larger than the maximum acceleration for the linear case. In other words, in comparing Class B

with Class A cushioning the difference in maximum acceleration, rather than the difference in amplification factors, is usually more important.

Example: Consider the example given in Section 1.6 and let it be required to determine the effect of pulse duration on a cathode structure with a 200 c.p.s. natural frequency of vibration. In Section 1.6 we found that

$$B = 5.4 \qquad k_0 = 255$$

$$G_0 = 28.6 \qquad r = 108.$$

$$G_m = 55$$

With $B = 5.4$, enter Fig. 2.8.2 and find

$$\frac{\omega_0}{\omega_2} = 0.88.$$

Now

$$\omega_0 = \sqrt{\frac{k_0 g}{W_2}} = \sqrt{\frac{255 \times 386}{22.5}} = 66.1 \text{ rad./sec.}$$

Hence

$$\omega_2 = \frac{66.1}{0.88} = 75 \text{ rad./sec.}$$

Then, with $\omega_1/\omega_2 = 2\pi \times 200/75 = 16.7$, enter Fig. 3.6.2 and find $A_m =$ approximately 1.0. Hence G_e is about the same as G_m and the conclusions reached for this problem in Section 1.6 are not altered.

3.7 Amplification Factors for Abrupt Bottoming

The amplification factors for bilinear elasticity have not been computed in complete detail. They can be obtained approximately by using the duration curves (Fig. 2.10.2) and the amplification curves for the linear case (Figs. 3.2.2 and 3.5.2 to 3.5.7). It is useful, however, to calculate the amplification factors for extremely abrupt bottoming ($k_b \rightarrow \infty$) to obtain a general understanding of the accompanying phenomena.

The system to be considered is illustrated in Fig. 3.7.1. It is assumed that the impact between m_2 and the base (occurring at $t = t_s$, $x_2 = d_s$) has a coefficient of restitution of unity. Hence m_2 will strike the base with velocity

$$[\dot{x}_2]_{t=t_s} = \sqrt{2gh\left(1 - \frac{d_s^2}{d_0^2}\right)}$$

(see equation (2.10.8)) and leave it at a velocity of the same magnitude but opposite sign. Perfect rebound of the whole package is also assumed.

The acceleration pulse will then look like the curve marked $k_b/k_0 \to \infty$ in Fig. 2.10.1.

There will be three regions in which to consider the relative displacement x:

Region 1 $\quad 0 < t < t_s$

Region 2 $\quad t_s < t < 2t_s$

Region 3 $\quad t > 2t_s$

The relative displacement ($x = x_1 - x_2$) of m_1 with respect to m_2 will have

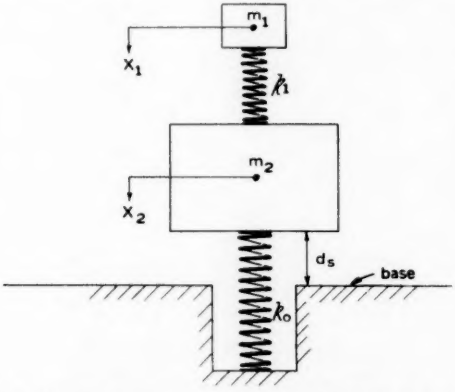

Fig. 3.7.1—Idealized system representing abrupt bottoming.

the same functional form for Region 1 as in the linear case (see equation (3.2.6)), and the amplification factor is, by analogy with (3.2.9),

$$A_0 = \frac{\dfrac{\omega_1}{\omega_0}}{\dfrac{\omega_1}{\omega_0} - 1} \sin \frac{2n\pi}{\dfrac{\omega_1}{\omega_0} + 1}, \qquad 0 < t < t_s, \tag{3.7.1}$$

where

$$\omega_0^2 = k_0/m_2 .$$

For Region 2, we use the differential equation

$$\ddot{x} + \omega_1^2 x = \omega_0 \sqrt{2gh} \sin \omega_0(t - 2t_s) \tag{3.7.2}$$

and, as initial conditions at $t = t_s$, we use the terminal conditions for Region 1 with the sign of $[\dot{x}_2]_{t=t_s}$ reversed. The amplification factor for this region is found to be (by the same method as in Section 3.2):

$$A_0 = \frac{\omega_1^2}{\omega_0\sqrt{2gh}}\sqrt{A^2+B^2}\sin(\omega_1 t_m + \eta - \omega_1 t_s) - \frac{1}{1-\left(\frac{\omega_0}{\omega_1}\right)^2}\sin\left(\omega_0 t_m - \omega_0 t_s - \sin^{-1}\frac{d_s}{d_0}\right), \quad (3.7.3)$$

$$t_s < t < 2t_s$$

where

$$\frac{\omega_1^2}{\omega_0\sqrt{2gh}}A = -\frac{\frac{\omega_0}{\omega_1}}{1-\left(\frac{\omega_0}{\omega_1}\right)^2}\sin\left(\frac{\omega_1}{\omega_0}\sin^{-1}\frac{d_s}{d_0}\right)$$

$$\frac{\omega_1^2}{\omega_0\sqrt{2gh}}B = \frac{\frac{\omega_0}{\omega_1}}{1-\left(\frac{\omega_0}{\omega_1}\right)^2}\left[2\frac{\omega_1^2}{\omega_0^2}\sqrt{1-\frac{d_s^2}{d_0^2}} - \cos\left(\frac{\omega_1}{\omega_0}\sin^{-1}\frac{d_s}{d_0}\right)\right]$$

$$\eta = \tan^{-1}\frac{A}{B}$$

and t_m is the root of

$$\frac{\omega_1^3}{\omega_0^2\sqrt{2gh}}\sqrt{A^2+B^2}\cos(\omega_1 t_m + \eta - \omega_1 t_s) - \frac{1}{1-\left(\frac{\omega_0}{\omega_1}\right)^2}\cos\left(\omega_0 t_m - \omega_0 t_s - \sin^{-1}\frac{d_s}{d_0}\right) = 0$$

that yields the largest value of A_0 in equation (3.7.3). Region 3 is governed by

$$\ddot{x} + \omega_1^2 x = 0 \quad (3.7.4)$$

and the initial conditions are the terminal conditions of Region 2. By the same method as was used in Section 3.2, we find

$$A_0 = \frac{2\frac{\omega_1}{\omega_0}}{\left(\frac{\omega_1}{\omega_0}\right)^2 - 1}\left[\left(\frac{\omega_1}{\omega_0}\right)^2\sqrt{1-\frac{d_s^2}{d_0^2}} - \cos\left(\frac{\omega_1}{\omega_0}\sin^{-1}\frac{d_s}{d_0}\right)\right], \quad (3.7.5)$$

$$t > 2t_s.$$

The largest value of A_0 from equations (3.7.1), (3.7.3) and (3.7.5) is plotted against ω_1/ω_0 in Fig. 3.7.2 for several values of d_s/d_0.

Notice that the amplification factor is A_0 rather than A_m. That is, the reference acceleration is G_0 rather than G_m. This is necessary because G_m is infinite in the present instance. Hence Fig. 3.7.2 cannot be compared directly with Figs. 3.2.2 and 3.6.2. However, it is interesting to observe that, for $\omega_1/\omega_2 < 0.5$, (low frequency elements) abrupt bottoming has no harmful effect. For high-frequency elements, the severity of bottoming is very great even when very nearly all of the required space (d_0) is available. For example, if 90% of the required space is available ($d_s/d_0 = 0.9$) and the frequency of the element is ten times the package frequency,

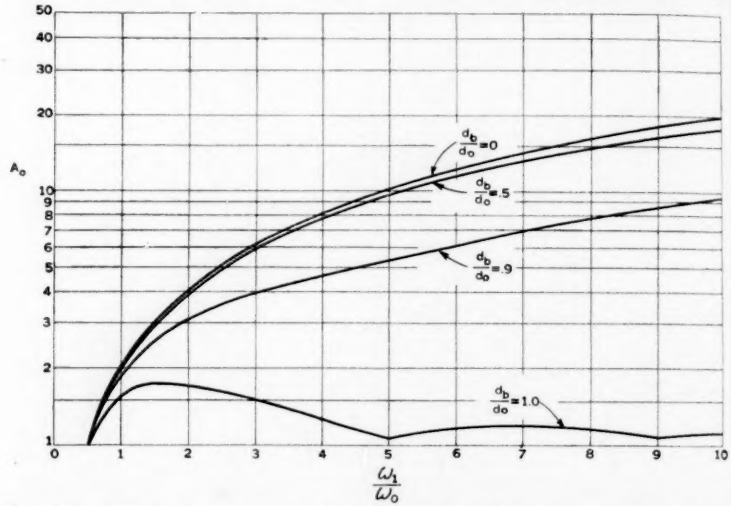

Fig. 3.7.2—Amplification factors for abrupt bottoming. See equations (3.7.1), (3.7.3) and (3.7.5).

the severity of the shock is almost ten times as great as it would be if the additional 10% of space were available.

3.8 General Influence of Shape of Acceleration-Time Curve on Amplification Factor

When amplification factor curves are not available for a special shape of acceleration-time curve, an approximate value of A_m may be obtained by interpolation between or extrapolation from the curves of the preceding sections. The shape of the acceleration-time curve and its duration (τ_2) or frequency (ω_2) should be found, first, by the methods described in Part II. The shape found should then be compared with the standard shapes shown in Part II, for which amplification factors are given in Part III.

The amplification factor found in this way will generally be within 25%

of the true value because amplification curves for pulse accelerations do not differ greatly even for very different acceleration-time curves as long as the

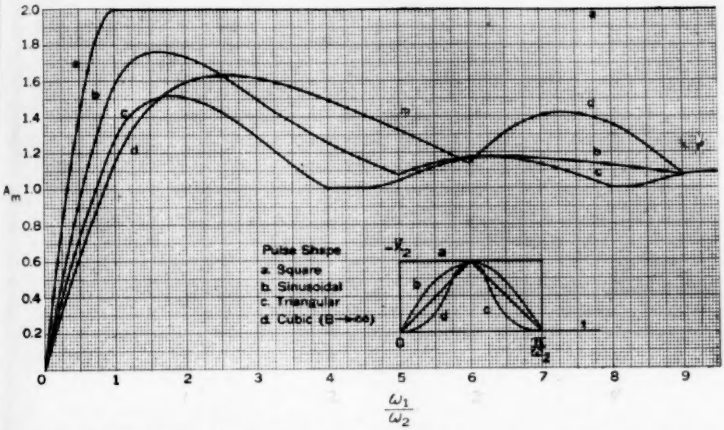

Fig. 3.8.1—Dependence of amplification factor on shape of symmetrical acceleration pulse.

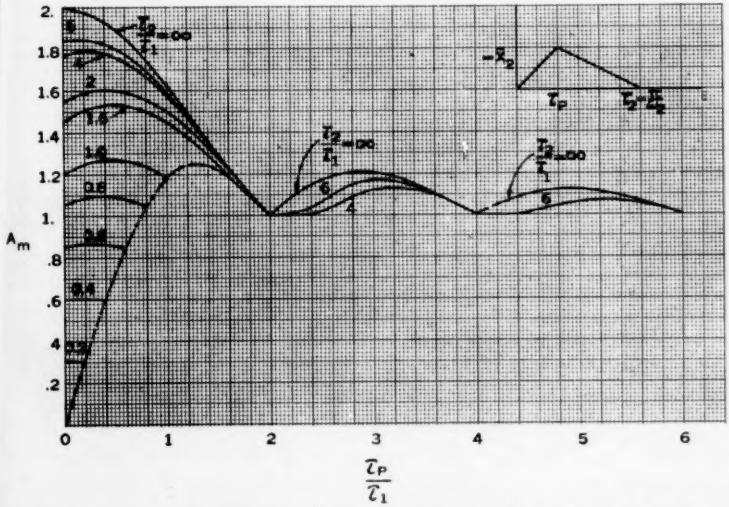

Fig. 3.8.2—Effect of asymmetry of an acceleration pulse on amplification factor.

amplitudes and frequencies are adjusted to the same scales. This is illustrated in Fig. 3.8.1 where the amplification factor curves are drawn for square wave, half-sine wave, triangular and cubic pulses.

Amplification factors for small values of ω_1/ω_2 may be calculated very accurately if it is observed that the initial slope of the amplification factor curve for a pulse acceleration is proportional to the area under the acceleration-time curve. For example, noting that the initial slope of the amplification factor curve for the half-sine wave pulse is 2, we assign the value 2 to the area under the half-sine wave. On the same scale, the area under a square wave pulse is π and under a triangular pulse is $\pi/2$. Accordingly, the initial slopes of the amplification factor curves for the latter two pulses are π and $\pi/2$ respectively.

As an additional aid in finding amplification factors for unusual cases, Fig. 3.8.2 is given to show the effect of asymmetry of an acceleration pulse. The pulse is triangular in shape but the time (τ_P) taken to reach the peak value of acceleration may have any value from zero to the total duration (τ_2) of the pulse.

PART IV

DISTRIBUTED MASS AND ELASTICITY

4.1 Introduction

It is important to be aware of the conditions under which the assumption of lumped parameters is permissible. In Parts I and II the cushioning medium was assumed to be massless, so that wave propagation (or surges) through it was ignored. Such surges will contribute to the acceleration imposed on the packaged article and we should be able to predict both the magnitudes and frequencies of the additional disturbances. If this is done, the information in Part III may be used to obtain at least a rough estimate of the resulting effects. In Part III itself the effects of accelerations were determined by studying the response of a system having only one degree of freedom; that is, an element of the packaged article was assumed to be a single mass supported by a massless spring. Every real element, of course, has an infinite number of degrees of freedom, so that it is important to discover the contribution, of the higher modes of vibration of an element, to the overall response.

Both of these problems (distributed parameters of mass and elasticity in the cushioning medium and in an element of the packaged article) are studied in this part. One example of each type is considered, and the choice of the example in each case was influenced by considerations of expediency, namely that the mathematical derivations be relatively simple and lead to solutions for which not too lengthy computations are necessary to yield results that can be applied practically. At the same time, the examples chosen are believed to give some insight into several of the physical phe-

nomena involved. The treatment is by no means complete, but a more detailed investigation is beyond the scope of this paper.

4.2 Effect of Distributed Mass and Elasticity of Cushioning on Acceleration of Packaged Article

Referring to Fig. 4.2.1, we consider the packaged article, of mass m_2, to be supported by distributed cushioning of mass m_c and depth ℓ. The cushioning may be a pad, say of rubber, in which case ℓ is the pad thickness, or it may be a helical metal spring, in which case ℓ is the coil length. The package is dropped vertically from a height h and has attained a velocity v at the instant of contact ($t = 0$) of the outer container and the floor. The outer container is assumed to be heavy enough so that there is no rebound. A horizontal plane in the cushioning is located by a coordinate x measured from the end of the cushioning attached to the outer container. The vertical

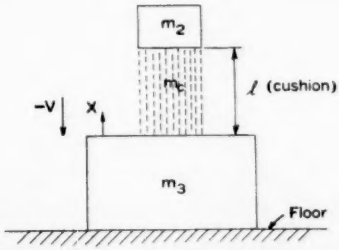

Fig. 4.2.1—Packaged article of mass m_2, supported on distributed cushioning of depth ℓ and mass m_c, depicted at the instant of first contact of the outer container (m_3) and the floor.

displacement of the plane x is designated by u. The undamped motion of the cushioning after contact is governed by the one-dimensional wave equation:

$$\frac{\partial^2 u}{\partial t^2} = a^2 \frac{\partial^2 u}{\partial x^2}, \tag{4.2.1}$$

in which a is the velocity of propagation of longitudinal waves in the cushioning. If the cushioning is continuous,

$$a^2 = \frac{E}{\rho}, \tag{4.2.2}$$

where E is the modulus of elasticity and ρ is the density of the cushioning. If the cushioning is a helical spring,

$$a^2 = \frac{k\ell^2}{m_c}, \tag{4.2.3}$$

where k is the spring rate.

The initial conditions of the system are

$$[u]_{t=0} = 0, \tag{4.2.4}$$

$$\left[\frac{\partial u}{\partial t}\right]_{t=0} = -v. \tag{4.2.5}$$

The boundary conditions are

$$[u]_{x=0} = 0, \tag{4.2.6}$$

$$k\ell\left[\frac{\partial u}{\partial x}\right]_{x=\ell} = -m_2\left[\frac{\partial^2 u}{\partial t^2}\right]_{x=\ell}. \tag{4.2.7}$$

Equation (4.2.7) expresses the requirement that the force on the upper end of the cushioning must balance the inertia force of the packaged article. For continuous cushioning $k\ell$ should be replaced by EA, where A is the cross-sectional area of the cushioning.

A solution of (4.2.1) satisfying conditions (4.2.4) and (4.2.6) is

$$u = \sum_{n=1}^{\infty} A_n \sin\frac{\omega_n x}{a} \sin\omega_n t, \tag{4.2.8}$$

where ω_n is the n^{th} root of a transcendental equation to be obtained from (4.2.7) and A_n is a constant to be determined by (4.2.5). Substituting (4.2.8) in (4.2.7) and equating coefficients of like terms of the series, we obtain the transcendental equation

$$\frac{\omega_n \ell}{a}\tan\frac{\omega_n \ell}{a} = \frac{m_c}{m_2}. \tag{4.2.9}$$

Substituting (4.2.8) in (4.2.5) we obtain, by the usual methods of expansion into trigonometric series,

$$A_n = -\frac{2v}{\omega_n\left(\frac{\omega_n \ell}{a} + \frac{1}{2}\sin\frac{2\omega_n \ell}{a}\right)}. \tag{4.2.10}$$

Hence the complete solution of the problem is

$$u = -\sum_{n=1}^{\infty} \frac{2v \sin\frac{\omega_n x}{a} \sin\omega_n t}{\omega_n\left(\frac{\omega_n \ell}{a} + \frac{1}{2}\sin\frac{2\omega_n \ell}{a}\right)}. \tag{4.2.11}$$

Our chief interest is in the acceleration of m_2. Making use of (4.2.7) and (4.2.9) we find, from (4.2.11), that this acceleration is

$$\left[\frac{\partial^2 u}{\partial t^2}\right]_{x=\ell} = v\omega_0 \sum_{n=1}^{\infty} B_n \sin\omega_n t, \tag{4.2.12}$$

where

$$\omega_0^2 = \frac{k}{m_2} \tag{4.2.13}$$

and

$$B_n = \frac{2\sqrt{\frac{m_c}{m_2}\left(\frac{m_c^2}{m_2^2} + \frac{\omega_n^2 l^2}{a^2}\right)}}{\frac{m_c}{m_2} + \frac{m_c^2}{m_2^2} + \frac{\omega_n^2 l^2}{a^2}}. \tag{4.2.14}$$

The acceleration of m_2 is, therefore, a sum of sinusoids of frequency ω_n and amplitude $v\omega_0 B_n$. Now, $v\omega_0$ is the maximum acceleration that m_2 would attain if the mass of the cushioning were negligible. Calling G_n the maximum acceleration in the n^{th} mode and G_0 the maximum acceleration neglecting the mass of the cushioning, as in Part I, we have

$$\frac{G_n}{G_0} = B_n. \tag{4.2.15}$$

But B_n depends only on the ratio m_c/m_2, as may be seen from equations (4.2.9) and (4.2.14). Similarly the ratio of the frequency (ω_n) of any mode to the frequency (ω_0) with massless cushioning depends only on m_c/m_2, as may be seen from equations (4.2.3), (4.2.9) and (4.2.13). *Hence, both the amplitude and frequency ratios for the acceleration in any mode depend only on the ratio of the mass of the cushioning to the mass of the packaged article.* The ratios G_n/G_0 and ω_n/ω_0 are plotted against m_c/m_2 in Figs. 4.2.2 and 4.2.3 for the first five modes. *It may be seen from these figures that the accelerations in the higher modes can be very important.* For example, if the cushioning weighs half as much as the packaged article the maximum acceleration in the second mode is about 40% of the acceleration in the first mode and the latter is about the same as found by the elementary method of Part I. This could have a disastrous effect on an element of the packaged article if the latter had a fundamental frequency near that of the second mode of the cushioning, the latter being found, from Fig. 4.2.3, to be about five times the fundamental frequency of the package.

It must be remembered that damping has been neglected in the above investigation and damping in the cushioning will serve to mitigate the severity of the higher mode accelerations to a great extent. However, the danger is always present at the start of a design and the possibilities of unfavorable combinations should be studied in every case.

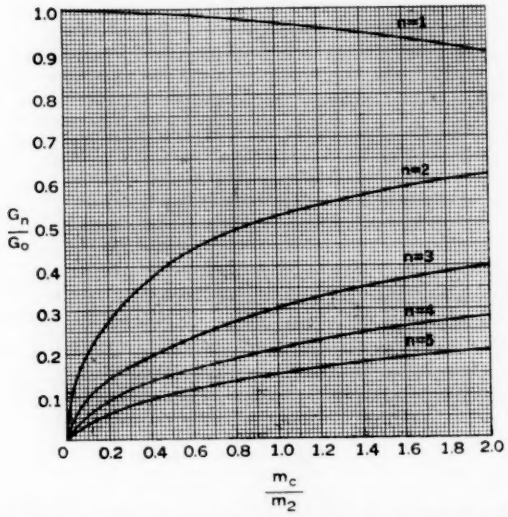

Fig. 4.2.2—Influence of ratio of mass of cushioning (m_c) to mass of packaged article (m_2) on acceleration ratio. The numerator of the acceleration ratio is the maximum acceleration (G_n) in the nth mode of vibration transmitted through the cushioning. The denominator of the acceleration ratio is the maximum acceleration ($G_0 = \sqrt{2hk_2/m_2g}$) that the mass m_2 would experience if the mass of the cushioning were negligible. See equations (4.2.15), (4.2.14), (4.2.9).

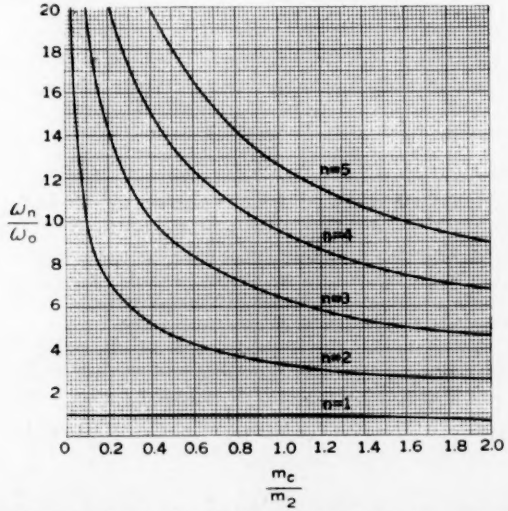

Fig. 4.2.3—Influence of ratio of mass of cushioning (m_c) to mass of packaged article on frequency ratio. The numerator of the frequency ratio is the frequency (ω_n) of the nth mode of vibration transmitted through the cushioning. The denominator of the frequency ratio is the frequency ($\omega_o = \sqrt{k_2/m_2}$) of vibration of the mass m_2 neglecting the effect of the mass of the cushioning. See equations (4.2.9), (4.2.13), and (4.2.3).

4.3 Effect of Distributed Mass and Elasticity, of an Element of the Packaged Article, on the Amplification Factor for a Half-Sine-Wave Pulse Acceleration

In this section we shall determine the contribution of the higher modes of vibration of a structural element to its total response to a half-sine-wave pulse acceleration. For the shape of the element, we choose a prismatic bar because this leads to the simplest mathematical formulation of the problem and such a bar is also a common structural element. Other considerations influence the choice of direction of acceleration with respect to the axis of the bar. The transverse direction (cantilever) is the most practical from a physical standpoint, but, for purposes of comparison with the one-degree-of-freedom system, the parallel (axial) direction of acceleration is the more logical. Both problems lead to solutions in the form of infinite series, but, in the latter case, the expression for the strain at a fixed

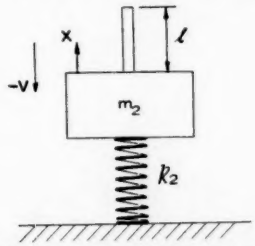

Fig. 4.3.1—The system studied in Section 4.3 depicted at the instant of contact with the floor.

end can be summed in terms of elementary functions without difficulty. Since it is necessary to determine maximum values of strain over a wide range of frequency ratios for the plotting of an amplification factor curve, an enormous reduction in the time required for accurate computations is obtained by choosing the axial case. Furthermore, the axial case appears to contain the essential features which might result in differences between the response of a one-degree-of-freedom system and a continuous one.

The complete system to be studied is illustrated in Fig. 4.3.1. To the mass m_2, supported on massless cushioning of constant spring rate k_2, is attached one end of an elastic prismatic bar, of length ℓ, cross sectional area A, modulus of elasticity E, and density ρ, with its axis oriented vertically. The system is dropped from a height h so that its velocity is v at the instant of contact of the cushioning with the floor. The mass of the bar is supposed to be small in comparison with m_2 and perfect rebound is assumed, so that the motion of m_2 during contact is a half-sine wave of frequency

$$\omega_2 = \sqrt{\frac{k_2}{m_2}}. \tag{4.3.1}$$

The maximum acceleration of m_2 is thus $v\omega_2$. If this magnitude of acceleration were reached very slowly, so as not to excite transient longitudinal waves in the bar, the maximum force between the bar and m_2 would be the product of the acceleration and the mass of the bar:

$$F = v\omega_2 \rho A \ell. \tag{4.3.2}$$

Hence the strain at the end of the bar attached to m_2 would be

$$\epsilon_0 = \frac{v\omega_2 \rho \ell}{E}. \tag{4.3.3}$$

Our problem is to find the ratio of the maximum transient strain to ϵ_0.

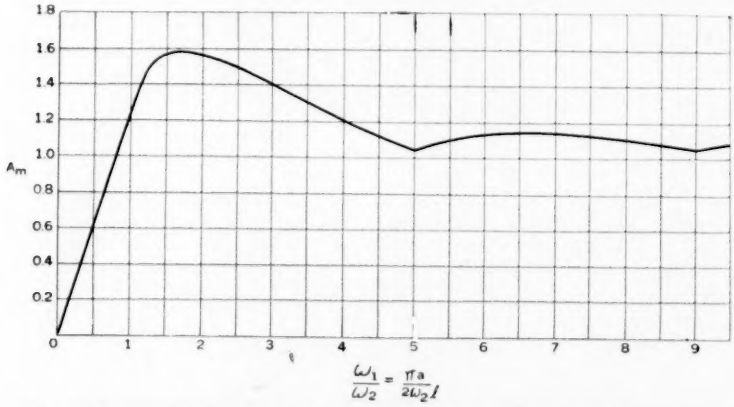

Fig. 4.3.2—Amplification factors for an element of the packaged article having distributed mass and elasticity. The package has linear undamped cushioning and perfect rebound. See equations (4.3.15), and (4.3.14).

Let u be the displacement of a transverse plane section of the bar distant x from the end attached to m_2. Then, the equation of motion of the bar is

$$\frac{\partial^2 u}{\partial t^2} = a^2 \frac{\partial^2 u}{\partial x^2}, \tag{4.3.4}$$

where a is the velocity of propagation of longitudinal waves in the bar:

$$a^2 = \frac{E}{\rho}. \tag{4.3.5}$$

Taking the instant of first contact of the cushioning with the floor to be $t = 0$, we know, from Part II, that the system will leave the floor when $t =$

π/ω_2. We shall therefore treat separately, as in Part III, the motion during contact

$$0 \leqq t \leqq \frac{\pi}{\omega_2}$$

and after rebound

$$t \geqq \frac{\pi}{\omega_2}.$$

During the first interval, the initial and boundary conditions are

$$[u]_{t=0} = 0, \tag{4.3.6}$$

$$\left[\frac{\partial u}{\partial t}\right]_{t=0} = -v, \tag{4.3.7}$$

$$[u]_{x=0} = \frac{-v}{\omega_2} \sin \omega_2 t, \tag{4.3.8}$$

$$\left[\frac{\partial u}{\partial x}\right]_{x=l} = 0. \tag{4.3.9}$$

The first and second conditions state that, at the instant of contact, all points in the bar are moving with the approach velocity v, without relative displacement. The third condition prescribes the half-sine wave motion of the end of the bar that is attached to m_2. The fourth condition states that the strain at the free end of the bar is always zero.

By the usual methods, a solution of (4.3.4) satisfying conditions (4.3.6) to (4.3.9) is found to be

$$u = -\frac{v \cos \frac{\omega_2}{a}(\ell - x) \sin \omega_2 t}{\omega_2 \cos \frac{\omega_2 \ell}{a}} + \frac{8v\ell}{\pi^2 a} \sum_{n=1,3,5\cdots}^{\infty} \frac{\sin \frac{n\pi x}{2\ell} \sin \frac{n\pi a t}{2\ell}}{n^2\left[\left(\frac{n\pi a}{2\omega_2 \ell}\right)^2 - 1\right]} \tag{4.3.10}$$

$$\left(0 \leqq t \leqq \frac{\pi}{\omega_2}, \frac{n\pi a}{2\omega_2 \ell} \neq 1\right).$$

The displacement is seen to be a forced vibration at the frequency (ω_2) of the applied acceleration, on which are superposed the free vibrations of the bar given by the series expression. The frequency of the fundamental mode of vibration of the bar is $\pi a/2\ell$ and the frequencies of the higher modes are the odd integral multiples of the fundamental.

The strain at the attached end of the bar is

$$\epsilon = \left[\frac{\partial u}{\partial x}\right]_{x=0}$$

$$= -\frac{v}{a}\left\{\tan\frac{\omega_2\ell}{a}\sin\omega_2 t - \frac{4}{\pi}\sum_{n=1,3,5\cdots}^{\infty}\frac{\sin\dfrac{n\pi at}{2\ell}}{n\left[\left(\dfrac{n\pi a}{2\omega_2\ell}\right)^2 - 1\right]}\right\} \quad (4.3.11)$$

$$\left(0 \leqq t \leqq \frac{\pi}{\omega_2},\ \frac{n\pi a}{2\omega_2\ell} \neq 1\right).$$

It may be verified that the sum of the series in (4.3.11) is given by

$$\frac{4}{\pi}\sum_{n=1,3,5\cdots}^{\infty}\frac{\sin\dfrac{n\pi at}{2\ell}}{n\left[\left(\dfrac{n\pi a}{2\omega_2\ell}\right)^2 - 1\right]} = \tan\frac{\omega_2\ell}{a}\sin\omega_2 t + \cos\omega_2 t - 1, \quad (4.3.12)$$

$$\left(0 < t < \frac{2\ell}{a}\right).$$

It should be observed that the summation is valid only in the interval $0 < t < 2\ell/a$. However, the series is periodic with half period $2\ell/a$ and includes only the odd terms, so that the function repeats itself with reversed sign after each interval $2\ell/a$. Hence the summation, valid for all t, can be written

$$\frac{4}{\pi}\sum_{n=1,3,5\cdots}^{\infty}\frac{\sin\dfrac{n\pi at}{2\ell}}{n\left[\left(\dfrac{n\pi a}{2\omega_2\ell}\right)^2 - 1\right]}$$

$$= (-1)^k\left[\tan\frac{\omega_2\ell}{a}\sin\omega_2\left(t - \frac{2k\ell}{a}\right) + \cos\omega_2\left(t - \frac{2k\ell}{a}\right) - 1\right] \quad (4.3.13)$$

$$k = m \quad \text{when} \quad \frac{2m\ell}{a} < t < \frac{2(m+1)\ell}{a}$$

$$m = 0, 1, 2, 3, \cdots.$$

We may, therefore, rewrite (4.3.11) in the form

$$\frac{\epsilon a}{v} = -\tan\frac{\omega_2\ell}{a}\sin\omega_2 t + (-1)^k\left[\tan\frac{\omega_2\ell}{a}\sin\omega_2\left(t - \frac{2k\ell}{a}\right)\right.$$

$$\left. + \cos\omega_2\left(t - \frac{2k\ell}{a}\right) - 1\right] \quad (4.3.14)$$

$$0 \leqq t \leqq \frac{\pi}{\omega_2}$$

$$k = m \text{ when } \frac{2m\ell}{a} < t < \frac{2(m+1)\ell}{a}$$

$$m = 0, 1, 2, 3 \cdots .$$

The expression (4.3.14) is simple enough so that the maximum value (ϵ_m) of the strain at the attached end can be obtained without difficulty for any ratio of the fundamental frequency ($\omega_1 = \pi a/2\ell$) of the bar to the frequency (ω_2) of the disturbing acceleration. The amplification factor

$$A_m = \left|\frac{\epsilon_m}{\epsilon_0}\right| = \frac{|\epsilon_m| E}{v\omega_2\rho\ell} = \frac{2\omega_1 a}{\pi\omega_2 v}|\epsilon_m|, \tag{4.3.15}$$

may then be calculated. The results of these calculations are plotted in Fig. 4.3.2. The important feature of this curve is that the amplification factor is everywhere less than the corresponding amplification factor for the one-degree-of-freedom system (Fig. 3.2.2, $\beta_1 = 0$). *Hence the assumption of lumped parameters is on the side of safety as regards amplification factor.*

It is interesting to observe that the curve of A_m vs. ω_1/ω_2, for this case, is a straight line between $\omega_1/\omega_2 = 0$ and $\omega_1/\omega_2 = 1$. This arises from the fact that, for $\omega_1/\omega_2 \leqq 1$, equation (4.3.14) reduces to

$$\frac{\epsilon a}{v} = \cos \omega_2 t - 1, \qquad \left(\frac{\omega_1}{\omega_2} \leqq 1\right). \tag{4.3.16}$$

Hence, when the duration of shock is less than the half period of the fundamental mode of vibration, the maximum value of strain occurs at the end of impact and is equal to twice the ratio of the approach velocity to the velocity of wave propagation in the bar.

The whole solution of the problem is not yet completed; for, although it is fairly evident from the fact that there is at least one maximum in the interval $0 \leqq t \leqq \pi/\omega_2$ for all values of ω_1/ω_2, it must be verified that the maximum strain (and, therefore, the amplification factor) is never greater after $t = \pi/\omega_2$ than before. Defining a new time coordinate

$$t' = t - \frac{\pi}{\omega_2}, \tag{4.3.17}$$

we have, for the initial and boundary conditions of equation (4.3.4) for $t \leqq \pi/\omega_2$,

$$[u]_{t'=0} = \frac{8v\ell}{\pi^2 a} \sum_{n=1,3,5\cdots}^{\infty} \frac{\sin \dfrac{na\pi^2}{2\omega_2 \ell} \sin \dfrac{n\pi x}{2\ell}}{n^2\left[\left(\dfrac{n\pi a}{2\omega_2 \ell}\right)^2 - 1\right]} \tag{4.3.18}$$

$$\left[\frac{\partial u}{\partial t}\right]_{t'=0} = \frac{v \cos \dfrac{\omega_2}{a}(\ell - x)}{\cos \dfrac{\omega_2 \ell}{a}} + \frac{4v}{\pi} \sum_{n=1,3,5\cdots}^{\infty} \frac{\cos \dfrac{na\pi^2}{2\omega_2 \ell} \sin \dfrac{n\pi x}{2\ell}}{n\left[\left(\dfrac{n\pi a}{2\omega_2 \ell}\right)^2 - 1\right]} \tag{4.3.19}$$

$$[u]_{x=0} = vt', \tag{4.3.20}$$

$$\left[\frac{\partial u}{\partial x}\right]_{x=l} = 0. \tag{4.3.21}$$

The first and second conditions state that the displacement and velocity of every point in the bar must be the same at the beginning of the second interval as at the end of the first interval; the expressions in (4.3.18) and (4.3.19) are obtained from (4.3.10). The third condition prescribes the constant velocity of departure from the floor of the mass m_2 and, therefore, of the end of the bar attached to it. The last condition states, again, that the strain at the free end of the bar is zero.

It may be verified that a solution of (4.3.4) satisfying conditions (4.3.18) to (4.3.21) is

$$u = vt' + \sum_{n=1,3,5\cdots}^{\infty} C_n \sin \frac{n\pi x}{\ell} \sin\left(\frac{n\pi a t'}{2\ell} + \gamma_n\right) \tag{4.3.22}$$

$$(t' \gtrless 0,\ t \gtrless \pi/\omega_2),$$

where

$$C_n \sin \gamma_n = \frac{8v\ell \sin \dfrac{na\pi^2}{2\omega_2 \ell}}{\pi^2 an^2\left[\left(\dfrac{n\pi a}{2\omega_2 \ell}\right)^2 - 1\right]} \tag{4.3.23}$$

$$C_n \cos \gamma_n = \frac{8v\ell\left(1 + \cos \dfrac{na\pi^2}{2\omega_2 \ell}\right)}{\pi^2 an^2\left[\left(\dfrac{n\pi a}{2\omega_2 \ell}\right)^2 - 1\right]} \tag{4.3.24}$$

$$\frac{n\pi a}{2\omega_2 \ell} \neq 1.$$

Hence, the strain at the attached end of the bar is

$$\epsilon = \left[\frac{\partial u}{\partial x}\right]_{x=0} = \frac{4v}{\pi a} \sum_{n=1,3,5\cdots}^{\infty} \frac{\sin \dfrac{n\pi a t}{2\ell}}{n\left[\left(\dfrac{n\pi a}{2\omega_2 \ell}\right)^2 - 1\right]} + \frac{4v}{\pi a} \sum_{n=1,3,5\cdots}^{\infty} \frac{\sin \dfrac{n\pi a t'}{2\ell}}{n\left[\left(\dfrac{n\pi a}{2\omega_2 \ell}\right)^2 - 1\right]}. \tag{4.3.25}$$

The two series may be summed, as before, with the result

$$\frac{\epsilon a}{v} = (-1)^k \left[\tan \frac{\omega_2 \ell}{a} \sin \omega_2\left(t - \frac{2k\ell}{a}\right) + \cos \omega_2\left(t - \frac{2k\ell}{a}\right) - 1\right]$$
$$+ (-1)^{k'} \left[\tan \frac{\omega_2 \ell}{a} \sin \omega_2\left(t' - \frac{2k'\ell}{a}\right) + \cos \omega_2\left(t' - \frac{2k'\ell}{a}\right) - 1\right] \tag{4.3.26}$$

$$t \gtrless \pi/\omega_2\,, \qquad t' = t - \pi/\omega_2$$

$$k = m \quad \text{when} \quad \frac{2m\ell}{a} < t < \frac{2(m+1)\ell}{a},$$

$$k' = m' \quad \text{when} \quad \frac{2m'\ell}{a} < t' < \frac{2(m'+1)\ell}{a}$$

$$m = 0, 1, 2, 3 \cdots \qquad m' = 0, 1, 2, 3 \cdots .$$

Once more, the expression for the strain at the attached end of the bar is in a form suitable for rapid calculation and it can be shown the ϵ in equation (4.3.26) for $t \gtrless \pi/\omega_2$ is never greater than the ϵ in equation (4.3.14) for $0 \leqslant t \leqq \pi/\omega_2$ for the same ω_1/ω_2. Hence, Fig. 4.3.2 and the conclusions following equations (4.3.15) and (4.3.16) need not be modified.

NOTATIONS

A	Cross sectional area of a bar element of the packaged article. Also, a constant of integration.
A_0	Amplification factor when the reference acceleration is G_0. Ratio of maximum dynamic response to the response to a slowly applied acceleration of magnitude $G_0 g$.
A_m	Amplification factor when the reference acceleration is G_m. Ratio of maximum dynamic response to the response to a slowly applied acceleration of magnitude $G_m g$.
A_n	In Section 1.15, the sum of all the trapezoidal areas from $x_2 = 0$ to $x_2 = (x_2)_n$. Also, in Section 4.2, the coefficient of the nth term of a series.
ΔA_n	The area of a trapezoid with altitude $\Delta(x_2)_n$ and sides P_{n-1} and P_n.
a	x_0/l in the tension spring package. Also, in Part IV, the velocity of propagation of longitudinal waves.

B	A parameter of cushioning with cubic elasticity defined in equation (1.5.3). Also, a constant of integration.
B_n	Coefficient in the n^{th} term of a series.
b	f/l in the tension spring package.
C	A constant of integration.
C_n	Coefficient of the n^{th} term of a series.
c	A constant defined in equation (1.7.11)
c_1	Damping coefficient of an element of a packaged article.
c_2	Damping coefficient of linear cushioning.
cn	The elliptic cosine function.
d_0	Hypothetical displacement that would result if initial spring rate were maintained.
d_b	Maximum possible displacement of packaged article in cushioning with tangent elasticity.
d_m	Maximum displacement of packaged article.
d_m'	Value of d_m when $k_0 = k_0'$.
d_s	Displacement of bi-linear cushioning at which the spring rate changes from k_0 to k_b.
E	Modulus of elasticity.
e	In the tension spring package the stretch of a spring when the displacement is d_m.
exp ( )	$e^{(\ )}$, where e is the Naperian base 2.718$\cdots$
F	In section 2.7, a frictional force.
F_m	In the tension spring package, the maximum force on a spring.
f	In the tension spring package, the difference between l and the distance between hooks of an unstretched spring.
f_1	Frequency of vibration of an element of the packaged article.
f_2	Frequency of vibration of the packaged article on its cushioning.
G_0	Hypothetical maximum acceleration (in number of times g) that would result if initial spring rate were maintained.
G_e	A_mG_m or A_0G_0, i.e. the slowly applied acceleration (in number of times g) that will produce the same maximum response as a transient acceleration of maximum value G_m or G_0.
G_F	Maximum acceleration (in number of times g) in cushioning with friction and spring rate k_F.
G_m	Absolute value of maximum acceleration of packaged article in units of "number of times gravitational acceleration."
G_m'	Value of G_m when $k_0 = k_0'$.

G_n	In section 1.15, the maximum acceleration (in number of times g) experienced by the suspended mass when dropped from a height h_n. In Part IV, the maximum acceleration (in number of times g) of the n^{th} mode of vibration.
G_r	Maximum acceleration (in number of times g) after rebound.
G_s	Safe value of G_c.
g	Gravitational acceleration.
h	Height of drop.
h_n	In Section 1.15, the height of fall that will cause the cushioning to displace an amount $(x_2)_n$.
K	In the tension spring package, the initial spring rate of the suspension. In Section 2.8, the complete elliptic integral of the first kind.
K_1, K_2, K_3	The initial spring rates in the three mutually perpendicular directions normal to the faces of the package frame.
k	In the tension spring package, the spring rate of a spring. In Section 2.8, the modulus of an elliptic integral.
k, k'	In Section 4.3, 0, 1, 2, 3, $\cdots$.
k_0	Initial spring rate of non-linear cushioning.
k_0'	Optimum value of initial spring rate k_0.
k_1	Spring rate of lumped elasticity of element of packaged article.
k_2	Spring rate of linear cushioning.
k_b	Spring rate of bilinear cushioning after bottoming.
k_p	Spring rate defined in equation (2.7.7).
L	Constant defined in equation (1.8.2).
l	In the tension spring, the projection of l_i on a horizontal plane. In Section 4.2, length of cushioning. In Section 4.3, length of element of packaged article.
l_i	In the tension spring package, the distance between the two support points of a spring when the suspended article is in the equilibrium position.
M	Constant defined in equation (1.8.4), equal to G_m/G_0.
m	Reduced mass defined in equation (2.4.5).
m, m'	In Section 4.3, 0, 1, 2, 3, $\cdots$.
m_1	Lumped mass of element of packaged article.
m_2	Lumped mass of packaged article.
m_3	Lumped mass of outer container.
m_c	Mass of cushioning.
N	M^2.

n	0, 1, 2, 3, $\cdots$.
P	Force transmitted through cushioning.
P_0	Asymptotic value of force transmissible through cushioning with hyperbolic tangent elasticity.
P_m	Maximum force exerted on packaged article by cushioning.
P_n	In Section 1.15, the load that produces displacement $(x_2)_n$.
R	Force between package and floor.
r	Coefficient of cubic term in load-displacement function for cushioning with cubic elasticity.
s, t, u	The direction cosines of the acceleration direction with respect to the normals to the faces of the package frame.
sn	The elliptic sine function.
T_2	The period of vibration of the packaged article on its cushioning.
t	Time coordinate.
t'	$t - \frac{\pi}{\omega_2}$
t_0	Time of first contact of package with floor.
t_m	Time at which maximum displacement or acceleration occurs.
t_r	Time at which package leaves floor on rebound.
t_s	Time at which the displacement reaches d_s.
u	Displacement in x direction.
v	Approach velocity.
W_2	Weight of packaged article.
W_3	Weight of outer container.
x	$x_1 - x_2$; relative displacement of m_1 with respect to m_2.
$\dot{x}$	$\dot{x}_1 - \dot{x}_2$.
$\ddot{x}$	$\ddot{x}_1 - \ddot{x}_2$.
x'	Relative displacement of m_1 with respect to m_2 at time t'.
x_0	In the tension spring package, the perpendicular distance from an inner spring support point to the nearest plane, perpendicular to the displacement direction and containing four outer spring support points.
x_1	Displacement of m_1.
$\dot{x}_1$	Velocity of m_1.
$\ddot{x}_1$	Acceleration of m_1.
x_2	Displacement of m_2.
$\dot{x}_2$	Velocity of m_2.

$\ddot{x}_2$	Acceleration of m_2.
x_{max}	Maximum value of x.
$(x_2)_n$	In Section 1.15, the displacement associated with the n^{th} point.
x_{st}	The value x would have if the acceleration reached its maximum value in a very long time.
$(\Delta x_2)_n$	In Section 1.15, equals $(x_2)_n - (x_2)_{n-1}$.
y	$x_2 - x_1$.
z	x_2/l (tension spring package).
$\alpha, \gamma, \delta, \zeta, \eta$	Phase angles.
β_1	Fraction of critical damping of an element of the packaged article.
β_2	Fraction of critical damping of package cushioning.
γ_n	Phase angle of n^{th} term of series (equation (4.3.22)).
ϵ	Strain at attached end of element under transient conditions.
ϵ_0	Strain at attached end of element under non-transient conditions.
ϵ_m	Maximum strain at attached end of element under transient conditions.
θ	Angle between the displacement direction and the acceleration direction.
π	3.14159$\cdots$.
ρ	Density (mass per unit of volume)
τ_0	Pulse duration of a half-sine-wave acceleration.
τ_2	Pulse duration associated with non-linear cushioning.
τ_B	Duration of bottoming of cushioning with bi-linear elasticity.
τ_P	Time required to reach peak value of a triangular acceleration pulse.
ω	Radian frequency defined in equation (2.4.6).
ω_1	Radian frequency of vibration of an element of the packaged article.
ω_1'	Radian frequency of vibration of damped element of packaged article.
ω_2	Radian frequency of vibration of the packaged article on its cushioning.
ω_2'	Radian frequency of vibration of the packaged article on damped cushioning.
ω_b	A frequency defined in equation (2.10.10).
ω_c	A frequency defined in equation (2.8.8).
ω_n	Radian frequency of nth mode.

Abstracts of Technical Articles by Bell System Authors

Dimensional Stability of Plastics.[1] ROBERT BURNS. Because of inherent insulating properties, rigid plastics play an important part in the design and manufacture of precision electrical apparatus. Almost invariably, practical design considerations require that the plastics have reasonable structural possibilities since it is rarely practicable to disassociate completely electrical and structural functions.

This paper discusses one of the important factors in the successful use of plastics in precision devices, namely, dimensional stability. Since plastics are organic compounds, one must be prepared to accept a degree of instability not usually encountered in metals. The measurement of this property is therefore of prime importance to the user of plastics since the data provide a basis for design adjustment which frequently is the difference between failure and success.

The various types of dimensional change are reviewed. Data illustrating the separate effects of humidity, drying, and cycling procedures are submitted. The influence of fabricating processes such as compression or injection molding, and sheeting, is included.

Some Numerical Methods for Locating Roots of Polynomials.[2] THORNTON C. FRY. It is the purpose of this paper to discuss the location of the roots of polynomials of high degree, with particular reference to the case of complex roots. This is a problem with which the Laboratories has been much concerned in recent years because of the fact that the problem arises rather frequently in the design of electrical networks. Attention is not given to strictly theoretical methods, such as the exact solution by elliptic or automorphic functions: nor to the development of roots in series or in continued fractions, though such methods exist and one at least—development of the coefficients of a quadratic factor—is of great value in improving the accuracy of roots once they are known with reasonable approximation.

Instead, the paper deals with just two categories of solutions: one, the solution of the equations by a succession of rational operations, having for their purpose the dispersion of the roots; the other, a method depending on Cauchy's theorem regarding the number of roots within a closed contour.

Thermistor Technics.[3] J. C. JOHNSON. This paper is confined to a study of how the three basic types of thermistors, namely, externally-heated or ambient temperature type, the directly-heated type, and also the indirectly-

[1] *A.S.T.M. Bulletin*, May 1945.
[2] *Quarterly Applied Mathematics*, July 1945.
[3] *Electronic Industries*, August 1945.

heated type, are used in simple feedback amplifiers as regulation and control devices to effect the economies inherent in an entirely electrical system by eliminating such mechanical devices as motor-driven condensers, sliding contacts and rotary switches.

Dynamic Measurements on Electromagnetic Devices.[4] E. L. NORTON. A method is presented by which measurements of flux may be made at any desired time during the operate cycle of an electromagnet. Apparatus is described which operates the magnet cyclically at an accurately held rate, and provides a means for measuring flux either by the use of a search coil or by the operating winding of the magnet itself. When using a search coil, it is connected to a direct-current milliammeter at the time in the cycle at which the value of the flux is desired and disconnected at the end of the cycle or just before the magnet is energized for the next pulse. If proper precautions are taken, the steady reading of the instrument is an accurate measure of the difference in the flux in the coil between the time it is connected to the meter and the time it is removed, or, since the latter is zero except for residual flux, the reading is a direct measure of flux.

The same apparatus may be used for the measurement of instantaneous current by the addition of an air core mutual inductance, and its use is extended to the measurement of armature position and velocity by the addition of a photoelectric cell and the proper amplifiers.

A form of vacuum tube filter is described which effectively filters the pulses from the indicating instrument without affecting the accuracy of the measurements.

Coaxial Cables and Television Transmission.[5] HAROLD S. OSBORNE. Communication techniques and facilities useful to the entertainment industry have evolved naturally from the Telephone Companies' main objective—the transmission of speech. The development of carrier systems for long-distance transmission and technical features involved in the latest carrier medium—the coaxial cable—are reviewed. The television transmission capabilities of this medium, both now and what may be expected shortly after the war, are mentioned. The extensive system of such cables planned for the next five years, supplemented by radio relay systems to the extent that these prove themselves as a part of a communications network, will provide an excellent beginning for a nation-wide television transmission network. Planned primarily to meet telephone requirements, this network of cables will be suitable to meet the transmission needs of the television industry.

The Performance and Measurement of Mixers in Terms of Linear-Network Theory.[6] L. C. PETERSON AND F. B. LLEWELLYN. This paper discusses

[4] *Elec. Engg., Transactions Section*, April 1945.
[5] *Jour. S.M.P.E.*, June 1945.
[6] *Proc. I.R.E.*, July 1945.

the properties of mixers in terms of linear-network theory. In Part I the network equations are derived from the fundamental properties of nonlinear resistive elements. Part II contains a résumé of the appropriate formulas of linear-network theory. In Part III the network theory is applied, first to the case of simple nonlinear resistances, and next to the more general case where the nonlinear resistance is embedded in a network of parasitic resistive and reactive passive-impedance elements. In Part IV application of the previous results is made to the measurement of performance properties. The "impedance" and the "incremental" methods of measuring loss are contrasted, and it is shown that the actual loss is given by the incremental method when certain special precautions are taken, while the impedance method is in itself incomplete.

A Figure of Merit for Electron-Concentrating Systems.[7] J. R. PIERCE. Electron-concentrating systems are subject to certain limitations because of the thermal velocities of electrons leaving the cathode. A figure of merit is proposed for measuring the goodness of a device in this respect. This figure of merit is the ratio of the area of the aperture which, in an ideal system with the same important parameters as the actual system, would pass a given fraction of the cathode current to the area of the aperture which in the actual system does pass this fraction of the cathode current. Expressions are given for evaluating this figure of merit.

A 60-Kilowatt High-Frequency Transoceanic-Radiotelephone Amplifier.[8] C. F. P. ROSE. Here is described a high-frequency radio amplifier recently developed for the transoceanic-telephone facilities of the Bell System at Lawrenceville, New Jersey. In general, the amplifier is capable of delivering 60 kilowatts of peak envelope power when excited from a 2-kilowatt radio-frequency source. It is designed to operate as a "class B" amplifier for transmitting either single-channel double-sideband or twin-channel single-sideband types of transmission. Features are described which permit rapid frequency-changing technique from any preassigned frequency to another lying anywhere within the spectrum of 4.5 to 22 megacycles.

Some Notes on the Design of Electron Guns.[9] A. L. SAMUEL. A method is outlined for the design of electron guns based on the simple theory first published by J. R. Pierce. This method assumes that the electrons are moving in a beam according to a known solution of the space-charge equation, and requires that electrodes exterior to the region of space charge be shaped so as to match the boundary conditions at the edge of the beam. An electrolytic tank method is used to obtain solutions for cases which are not amenable to direct calculation. Attention is given to some of the

[7] *Proc. I.R.E.*, July 1945.
[8] *Proc. I.R.E.*, October 1945.
[9] *Proc. I.R.E.*, April 1945.

complications ignored by the simple theory and to some of the practical difficulties which are encountered in constructing guns according to these principles. An experimental check on the theory is described, together with some information as to the actual current distribution in a beam produced by a gun based on this design procedure.

Microwave Radiation from the Sun.[10] G. C. SOUTHWORTH. During the summer months of 1942 and 1943, a small but measurable amount of microwave radiation was observed coming from the sun. This appeared as random noise in the outputs of sensitive receivers designed to work at wavelengths between one and ten centimeters. Over a considerable portion of the range, the energy was of the same order of magnitude as that predicted by black-body radiation theory.

Attempts were made to determine the effect of the earth's atmosphere on this radiation. Measurements made near sunrise or sunset, when the path through the earth's atmosphere was relatively long, differed only slightly from those made at noon. This suggested that any absorption that may have been present was small. In this connection it is of interest that small temperature differences could be noted between points below the horizon and the sky immediately above. This also suggested that the earth's atmosphere was relatively transparent.

In another kind of measurement the parabolic receiver was centered on the sun and its output was observed as the sun's disc moved out of the aperture of the receiver. The directional pattern so obtained indicated that at the shorter wave-lengths the sun's apparent diameter was considerably larger than that measured by ordinary optical means. This suggested that there may have been some refraction or perhaps scattering by the earth's atmosphere.

Resistive Attenuators, Pads and Networks—An Analysis of their Applications in Mixer and Fader Systems (Part Eight of a Series).[11] PAUL B. WRIGHT. In last month's discussion, the series-connected fader and the parallel-connected fader systems were considered, together with an analysis of their performance expressed both algebraically and in terms of the hyperbolic functions of a real variable. In this installment, the series-parallel-connected fader system discussion is continued and equations describing the complete behavior of this type network system are developed. This is followed by further analytical work dealing with the parallel-series-connected fader and mixer system and several lesser known systems which are quite useful to use. These are the *multiple bridge* and the *lattice network systems* which may be utilized to advantage for some applications. All of

[10] *Jour. Franklin Institute*, April 1945.

[11] Communications, September 1945. (*Preceding parts of this Series appeared in earlier issues of Communications.*)

the equations which are derived are shown in the algebraical, hyperbolical and symbolical forms. The key chart which was presented earlier in this series may be used to great advantage when checking the definitions of the symbols used which are not specifically defined in the text. This procedure also may be directly applied to the hyperbolic equations shown. It is of course necessary to take into account that, in general, subscripts are used in most of the equations in the text while the key chart does not have any subscripts. This does not, however, alter the fundamental forms nor their definitions in terms of the propagation function, theta. To avoid the necessity for extensive interpolation of the hyperbolic function tables to find the correct numerical values for the various functions used throughout the text, a series of tables providing all of the functions required is presented.

Contributors to this Issue

RAYMOND D. MINDLIN, B.A., Columbia University, 1928; B.S., 1931; C.E., 1932; Ph.D., 1936. Assistant 1932–38, Instructor 1938–40, Assistant Professor 1940–45, Associate Professor 1945–, Department of Civil Engineering, Columbia University. Consultant, Section T, National Defense Research Committee (later Office of Scientific Research and Development), 1940–45, on the development of the rugged radio proximity fuze and on mathematical problems in fire control. Consultant, Bell Telephone Laboratories, 1943–44, Member of the Technical Staff 1944–45, Consultant 1945–. Dr. Mindlin has been concerned with the fields of mathematical and experimental mechanics.

J. R. PIERCE, B.S. in Electrical Engineering, California Institute of Technology, 1933; Ph.D., 1936. Bell Telephone Laboratories, 1936–. Engaged in study of vacuum tubes.

A. L. SAMUEL, A.B., College of Emporia (Kansas), 1923; S.B. and S.M. in Electrical Engineering, Massachusetts Institute of Technology, 1926. Additional graduate work at M.I.T. and at Columbia University. Instructor in Electrical Engineering, M.I.T., 1926–28. Mr. Samuel joined the Technical Staff of the Bell Telephone Laboratories in 1928, where he has been engaged in electronic research and development. Since 1931, his principal interest has been in the development of vacuum tubes for use at ultra-high frequencies.